

For Reference

NOT TO BE TAKEN FROM THIS ROOM

Ex LIBRIS
UNIVERSITATIS
ALBERTAEISIS



THE UNIVERSITY OF ALBERTA

A KINETIC APPROACH TO PEROXIDASE-CATALYZED REACTIONS



BY

MEREDITH L. COTTON

A THESIS

SUBMITTED TO THE FACULTY OF GRADUATE STUDIES AND RESEARCH
IN PARTIAL FULFILMENT OF THE REQUIREMENTS FOR THE DEGREE

OF

DOCTOR OF PHILOSOPHY

DEPARTMENT OF CHEMISTRY

EDMONTON, ALBERTA

SPRING, 1973

ABSTRACT

In order to investigate the nature of compounds I and II of horseradish peroxidase, the kinetics of the horseradish peroxidase catalyzed ferrocyanide oxidation were studied using stopped-flow and steady-state methods. With the stopped-flow technique, the pH dependence of the apparent second-order rate constant for ferrocyanide oxidation by compound I prepared from ethyl hydroperoxide and m-chloroperbenzoic acid was interpreted in terms of a single ground-state dissociation constant having a pK_a of 5.3. This was identical to the result obtained previously for hydrogen peroxide. The second-order rate constant for the ferrocyanide-compound II reaction also showed the same pH dependence for the three oxidizing substrates. The reaction was interpreted in terms of two ground-state acid dissociation constants having pK_a values of 8.5 and < 2. The same dependence on pH suggested structurally identical active sites for both compounds I and II prepared from the three different oxidizing substrates.

The effect of cyanide on the steady-state oxidation of ferrocyanide catalyzed by horseradish peroxidase was studied at pH values 9.00, 7.10 and 5.00. An inhibition was observed which could be explained by the binding of cyanide only to the native enzyme. This indicated that a species, likely a hydroxyl group, was bound at the sixth coordination position of the iron in both compounds I and

II. Equations were derived from which the rate of attainment of the steady-state could be computed.

The kinetics of aromatic amine oxidation catalyzed by horseradish peroxidase was investigated as a function of pH at 25° and ionic strength 0.11. p-Aminobenzoic acid was used as a substrate to reduce compounds I and II. In reactions with both these intermediates deviations from a first-order relationship in the enzyme were explained in terms of a free radical interaction of product with the enzyme. Observed deviations from first-order in substrate were explained by a mechanism involving an enzyme-substrate complex which reacted with an additional molecule of substrate but at a slower rate. The log rate-pH relationships similar to those obtained for ferrocyanide suggested similar proton-transfer mechanisms for both reducing substrates. The reduction of compound II by p-aminobenzoic acid appeared to be influenced by two ionizable groups on the enzyme affecting the electronic environment of the heme. The lack of influence of substrate ionizable groups on the rate indicated that the reaction in the acid region of pH was diffusion-controlled. The reduction of compound I by p-aminobenzoic acid was characterized by the influence of two ground-state ionizations only one of which could be assigned unequivocally to the enzyme. The dependence of the dissociation constant for the enzyme-substrate complex on pH indicated a

preferential binding of p-aminobenzoic acid's completely protonated state. The reaction mechanism for both intermediates was discussed in terms of transition-state theory.

ACKNOWLEDGEMENTS

I am indebted to my research director, Professor H.B. Dunford, for his many helpful suggestions and advice, to my fellow graduate students and Dr. J.E. Critchlow for their co-operation and helpful discussions, and to my wife, Lesley, without whose understanding my research would not have been possible.

CONTENTS

	Page
Abstract	i
Acknowledgements	iv
Contents	v
List of Tables	ix
List of Figures	xii
Chapter I: Introduction, A Survey.....	1
1.1 Peroxidases.....	2
Historical Note.....	2
Occurrence and Characteristics of Peroxidases.....	3
1.2 Physical Properties of HRP.....	13
Optical Spectrum.....	13
The Structure of Native HRP.....	13
Nature of the Axial Ligands.....	15
Structural Modification Studies.....	15
The Electronic Configuration of Heme Iron in HRP and its Complexes.....	19
Heterogeneity of Native HRP.....	23
Structure of the HRP Protein Moiety.....	29
1.3 Peroxidatic Activity of HRP Catalysis.....	32
Nature of the Oxidizing Substrate and the Properties of HRP Compounds.....	34

	Page
Nature of the Reducing Substrate and Products of Reaction.....	41
Modification of Peroxidatic Activity.....	47
Kinetic Studies.....	52
 Chapter 2: The Ferrocyanide Peroxidation	
Catalyzed by Horseradish Peroxidase and the	
Nature of the Enzyme's Active Site.....	57
2.1 Introduction.....	57
2.2 Experimental.....	59
Materials.....	59
Kinetic Experiments.....	62
2.3 Results.....	65
Kinetics of the HRP-II-Ferrocyanide Reaction.....	66
Kinetics of the HRP-I-Ferrocyanide Reaction.....	96
2.4 Discussion.....	103
 Chapter 3: Aromatic Amine Peroxidation Catalyzed	
by Horseradish Peroxidase.....	106
3.1 Introduction.....	106
3.2 Experimental.....	108
Materials.....	108
Stopped-Flow Experiments.....	109
The pK_a Values for PABA.....	112

	Page
Binding to Native HRP.....	113
Steady-State Experiments.....	114
3.3 Results.....	114
The pK_a Values for PABA.....	114
The Order of Reaction with Respect to HRP-II.....	115
The Order of Reaction with Respect to Substrate.....	129
Spectrophotometric Evidence for an Enzyme- Substrate Interaction.....	149
Dependence of the Kinetic Parameters on pH.....	168
The Steady-State Reaction.....	186
3.4 Discussion.....	188
Chapter 4: The Kinetic Effect of Cyanide	
Inhibition on the Steady-State Peroxidation Catalyzed by Horseradish Peroxidase.....	196
4.1 Introduction.....	196
4.2 Experimental.....	197
Materials.....	197
Steady-State Kinetic Studies.....	197
Spectral Measurements.....	198
4.3 Results.....	200
Steady-State Kinetic Studies.....	200
Spectral Measurements.....	214

	Page
4.4 Discussion.....	215
References.....	218
Appendix 1: The Analysis of Stopped-Flow Kinetic Data.....	233
Appendix 2: Derivation of Expressions for the Steady-State HRP Catalyzed Ferrocyanide Oxidation in the Presence of Cyanide.....	237
Appendix 3: The Derivation of an Expression for the Dependence of Absorbance on pH for two Spectrophotometrically Observable pK_a Values.....	248
Appendix 4: Concerning the Observed Deviations from First-Order Kinetics for the Aromatic Amine, p-Aminobenzoic Acid.....	250
Appendix 5: Concerning the Characterization of HRP.....	253

LIST OF TABLES

Table	Page
1.1 The Magnetic Properties of Native HRP and its Complexes.....	20
1.2 The Amino Acid Composition of HRP Isoenzymes.....	26
1.3 The Catalytic Properties of HRP Isoenzymes in o-Dianisidine Oxidation.....	27
1.4 Reducing Substrates for the HRP-Catalyzed Peroxidatic Reaction and the Apparent Rate Constants for HRP-II Reduction.....	43
2.1 The Second-Order Rate Constants Determined for the HRP-II-Ferrocyanide Reaction.....	69
2.2 The Second-Order Rate Constants for the HRP-II-Ferrocyanide Reaction Determined from Steady-State Kinetics.....	73
2.3 The Parameters Obtained from a Nonlinear Least-Squares Analysis for the HRP-II- Ferrocyanide Reaction.....	87
2.4 The Second-Order Rate Constant Determined for the HRP-I-Ferrocyanide Reaction.....	97
2.5 The Parameters Obtained from a Nonlinear Least-Squares Analysis for the HRP-I- Ferrocyanide Reaction.....	101
3.1 The Second-Order Rate Constants Determined for the HRP-II-PABA Reaction.....	138

Table	Page
3.2 Parameters from the Nonlinear Least-Squares Analysis of the Dependence of the Pseudo-First-Order Rate Constant on PABA Concentration for the HRP-II-PABA Reaction at pH < 5.....	140
3.3 The Second-Order Rate Constants Determined for the HRP-I-PABA Reaction.....	143
3.4 Parameters from the Nonlinear Least-Squares Analysis of the Dependence of the Psuedo-First-Order Rate Constant on PABA Concentration for the HRP-I-PABA Reaction at pH < 5.....	145
3.5 Parameters Obtained from the Binding of PABA and Related Substrates to HRP.....	157
3.6 Parameters Obtained from a Nonlinear Least-Squares Analysis for HRP-II Reduction by PABA.....	171
3.7 Parameters Obtained from a Nonlinear Least-Squares Analysis for HRP-I Reduction by PABA.....	181
3.8 Parameters Obtained from a Nonlinear Least-Squares Analysis of the $\log 1/K_M$ vs. pH.....	185

Table	Page
4.1 A Table Relating Parameters from the General and Specific Steady-State Equations.....	204
4.2 Slopes and Intercepts of the Double Reciprocal Plots of $[HRP]_o/v$ vs. $1/[Fe(CN)_6^{-4}]_o$ as a Function of $[CN]_o$	207
4.3 The slope of $[HRP]_o [Fe(CN)_6^{-4}]_o/v$ vs. $[CN]_o$ at Three pH Values.....	210
4.4 The Calculated and Observed Changes in Absorbances at Several Wavelengths in the Soret Region for Mixtures of HRP and HRP-II with and without Cyanide Present....	216

LIST OF FIGURES

Figure	Page
1.1 Structure of Ferriprotoporphyrin IX.....	12
1.2 The Interrelation of HRP and its Intermediate Compounds.....	33
1.3 Soret Spectra of HRP and its Intermediate Compounds HRP-I and HRP-II.....	36
2.1 The Dependence of the HRP-I-Ferrocyanide Reaction on Ferrocyanide Concentration.....	67
2.2 The Dependence of the HRP-II-Ferrocyanide Reaction on Ferrocyanide Concentration.....	68
2.3 Semilogarithmic Plots of the Apparent Second-Order Rate Constants <i>vs.</i> pH for the HRP-I-Ferrocyanide and HRP-II-Ferrocyanide Reactions.....	72
2.4 Plot of $[HRP]_O/v$ <i>vs.</i> $1/[Fe(CN)_6^{4-}]_O$ at Four pH Values Obtained by Steady-State Kinetics.....	75
2.5 Semilogarithmic Plot of k_{3app} Determined by Steady-State Kinetics <i>vs.</i> pH for the HRP-II-Ferrocyanide Reaction.....	79
2.6 Plot of $\log k_{3app}$ <i>vs.</i> pH for the HRP-II- Ferrocyanide Reaction Shown Schematically..	83
2.7 Schematic Representation of the Active Site of HRP-II and the Electron-Transfer Process with p-Cresol.....	92

Figure	Page
2.8 Plot of $\log k_{3app}$ vs. pH for the HRP-II-Ferrocyanide Reaction Showing, Schematically, the Possibility of Two Overlapping Mechanisms Each Involving a Single Ionization.....	95
2.9 Plot of $\log k_{2app}$ vs. pH Shown Schematically for the HRP-I-Ferrocyanide Reaction.....	100
3.1 Plot of Absorbance vs. pH for PABA at 10^{-4} M in Buffered Solutions of Total Ionic Strength 0.11.....	116
3.2 Semilogarithmic Plot of the Voltage Change Against Time for the HRP-II Reduction by PABA at a pH Value of 5.17.....	117
3.3 Semilogarithmic Plot of Absorbance Change at 425 nm Against Time for the HRP-II-PABA Reaction.....	119
3.4 Semilogarithmic Plot of the Calculated Absorbance Change vs. Time for the Observed Deviation from Linearity in the Initial Portion of the Fig. 3.3.....	121
3.5 Plot of the k_{obs} vs. [PABA] for the First-Order Initial Reaction Proposed for Typical Kinetic Responses Such as Fig. 3.3.....	122
3.6 Plot of the k_{obs} vs. [PABA] for the Final Linear Portion of the Reaction Trace Typified by Fig. 3.3.....	123

Figure	Page
3.7 Semilogarithmic Plot of the Voltage Change vs. Time for the HRP-II Reduction by PABA at 3×10^{-3} M.....	125
3.8 Plot of the Pseudo-First-Order Rate Constant Against the PABA Concentration at a pH of 6.15.....	131
3.9 A Plot of the Observed Pseudo-First-Order Rate Constant Against PABA Concentration For HRP-II Reduction at a pH Value of 4.17.....	132
3.10 Lineweaver-Burk Plot of the Data of Fig. 3.9.....	135
3.11 Semilogarithmic Plot of $1/K_M$ for the HRP-I and HRP-II Reactions with PABA, as well as the Rate Constant for the HRP-I-PABA Reaction k_{2app} and the Rate Constant for the HRP-II-PABA Reaction, k_{3app} against pH....	146
3.12 The Difference Spectrum of the Native Enzyme in the Presence of 7.5×10^{-3} M PABA Relative to HRP.....	151
3.13 The Difference Spectra of the Native Enzyme in the Presence of Aniline and Acetic Acid- Acetate Buffer Relative to HRP.....	154

Figure	Page
3.14 Plot of the Changing Absorbance Difference Against the Contribution of Acetate Buffer to the Constant Total Ionic Strength.....	156
3.15 The Difference Spectrum of HRP in the Presence of 7.5×10^{-3} M Benzoic Acid Relative to HRP.....	160
3.16 Plot of the Changing Absorbance Difference Against Substrate Concentration for Benzoic Acid, PABA and Aniline.....	161
3.17 The Changing Absorbance Difference Observed Plotted Against its Value Calculated from Equation 3.46 as a Test for Competitive Binding of Benzoic Acid and Aniline.....	164
3.18 The Changing Absorbance Difference Plotted Against its Calculated Value as a Test for Competitive Binding of PABA and p-Cresol.....	166
3.19 The Changing Absorbance Difference Observed Plotted Against its Calculated Value (Equation 3.47) as a Test for Uncompetitive Binding.....	167
3.20 Semilogarithmic Plot of k_{4app} for the HRP-II- PABA Complex Reacting with a Second Molecule of PABA Against pH.....	173

Figure	Page
3.21 Schematic Representation of $\log k_{2\text{app}}$ <i>vs.</i> pH for PABA Oxidation by HRP-I.....	180
4.1 The HRP Reaction Cycle Showing the Possibility of Cyanide Binding to all Forms of HRP.....	202
4.2 The Double Reciprocal Plots of $[HRP]_o/v$ <i>vs.</i> $1/[Fe(CN)_6^{4-}]_o$ at pH 5.00 with $[CN]_o$ Varying from 0 to 7.5×10^{-4} M.....	206
4.3 The Slopes of $[HRP]_o/v$ <i>vs.</i> $1/[Fe(CN)_6^{4-}]_o$ Plotted as a Function of Cyanide Concentrations of pH 9.00.....	209
4.4 The Initial Velocity Plotted Against $[HRP]_o$ at pH = 5.00.....	213

CHAPTER 1

INTRODUCTION, A SURVEY

An attempt has been made in this chapter, subdivided for the convenience of the reader, to review the extensive literature of horseradish peroxidase. Following a brief historical note, several well known peroxidases are discussed to emphasize some of their basic similarities and differences.

A discussion of the physical properties of horseradish peroxidase centers about the enzyme's active site, critical to the enzyme's kinetic response. The electronic nature of the prosthetic group, ferriprotoporphyrin IX, as manifest in optical spectra as well as ESR and magnetic susceptibility studies is described. Speculation dealing with the iron's two axial ligands is mentioned. Investigations demonstrating the influence of groups on the porphyrin ring are described. The isoenzymes isolated from crude extracts and the structure of the enzyme's protein moiety are discussed in detail.

To provide a background for later chapters the peroxidatic activity of horseradish peroxidase, the nature of its enzymatic intermediates and the types of compounds able to function as oxidants and reductants are described. Inhibition and activation of the enzyme are mentioned. Finally, kinetic studies over a wide range of pH, which demonstrate the proton transfer mechanisms participating

in the peroxidatic reaction, are considered.

1.1 Peroxidases

Historical Note:

Peroxidases are enzymes catalyzing the oxidation of a variety of organic and inorganic compounds by hydrogen peroxide or related compounds. Widespread in plant materials, peroxidases have been implicated with the control of plant growth (Galston *et al.*, 1956) and the participation in coupled oxidations (Keilin and Mann, 1955). The interest in these enzymes has largely centered about the mechanism of their reactions in an attempt to demonstrate their function and determine reasons for their presence in living tissues.

Peroxidase activity was first reported when a fresh horseradish root was observed to turn guaiacum an intense blue colour (Planche, 1810). Much later, certain substances occurring in plant tissues were observed to catalyze the oxidation of organic compounds in dilute hydrogen peroxide solutions (Schonbein, 1855). By the turn of the century horseradish peroxidase had been isolated and shown to catalyze reactions involving phenols and aromatic amines (Bach and Chodat, 1903). It was discovered also that ethyl hydrogen peroxide could replace hydrogen peroxide as the oxidizing agent. The purification of horseradish peroxidase (Willstatter, 1923) and the determination of its activity (Willstatter, 1932) was followed by a demonstration that a proportional

relationship existed between peroxidase activity and the absorption of the enzyme preparation in the Soret spectral region (Kuhn *et al.*, 1931). Soret spectral bands were known to be typical of iron prophyrrins indicating that horseradish peroxidase was a hematin compound, a fact that was confirmed later (Keilin and Mann, 1937). The cleavage and resynthesis of the peroxidase showed, subsequently, that ferripropo-porphyrin IX (Fig. 1.1) is the prosthetic group. (Swedin and Theorell, 1940; Theorell *et al.*, 1942).

In 1939 the oxidase function of the horseradish peroxidase - Mn⁺² - dihydroxyfumaric acid system was described (Theorell and Swedin, 1939). By 1942 horseradish peroxidase became the fourth hemoprotein to be crystallized, succeeding hemoglobin, myoglobin and catalase (Theorell *et al.*, 1942). Participation of peroxidases in some hydroxylations was discovered by Mason *et al.* (1957). Dolin (1957), discovered a metal-free peroxidase in *Streptococcus faecalis* and identified it as a flavoprotein.

Occurrence and Characteristics of Peroxidases:

Peroxidases occur in most higher plants as well as bacteria and fungi. They are also found in animals at most levels of evolutionary development. In many plants the peroxidase content is greatest in the root system (Wachholder, 1942). However, there are variations in content depending upon the season and the specimen's maturity. As well, peroxidases located in different tissues of the plant may have

different properties, making it difficult to generalize concerning the distribution of peroxidatic activity within plants. The roots of horseradishes are particularly rich in the enzyme for unknown reasons (Sumner and Howell, 1936). As a result, this has become a convenient source of the much studied horseradish peroxidase (EC 1.11.17; donor: H_2O_2 oxidoreductase) referred to hereafter as HRP. Before considering HRP in detail, a brief discussion of several other known peroxidases will serve to outline the diverse character of this group of enzymes performing a similar function.

Chloroperoxidase, although having many chemical and physical properties in common with HRP, has pronounced catalatic properties (the ability to decompose hydrogen peroxide) as well as the unique ability to catalyze the oxidation of chloride ions. Upon isolation and crystallization from the mould *Caldariomyces fumago* (Morris and Hager, 1965), the prosthetic group was shown to be ferri-protoporphyrin IX. The minimal molecular weight was 40,200 based on heme content and 42,000 based on hydrodynamic measurements. This enzyme is a glycoprotein with the carbohydrate moiety contributing 25% to 30% to its total molecular weight. The protein moiety is rich in four amino acids: aspartic acid, glutamic acid, serine and proline. These residues constitute 45% of the total amino acid content. The native enzyme has an absorption maximum at 403 nm. ($\epsilon = 7.5 \times 10^4 M^{-1} cm^{-1}$) similar to HRP. The biological

function of chloroperoxidase is believed to be related to the oxidation of chloride ion in the biosynthesis of the fungal metabolite *Caldariomycin* (2,2-dichloro-1,2-cyclopentanediol).

Another hemoprotein known to contain a single prosthetic group (ferriprotoporphyrin IX) is cytochrome c peroxidase. Its molecular weight of 34,100 is somewhat lower than other peroxidases because of the absence of a carbohydrate moiety (Yonetani, 1970). Although first isolated from baker's yeast in 1940 (Altschul *et al.*, 1940), it was not until 1965 that a highly purified preparation was obtained (Yonetani and Ray, 1965) and the enzyme crystallized (Yonetani *et al.*, 1966). Its specific activity toward ferrocyanocytocrome c is exceedingly high when compared with other reducing agents. Apparently, this specificity is integrally involved with the formation of a definite complex with both oxidized and reduced forms of cytochrome c. The interaction between the two macromolecules may be electrostatic since they are acidic and basic proteins (Yonetani, 1970).

Iodide oxidation is almost ubiquitous to hemoproteins. The biosynthesis of the growth hormone, thyroxine, occurs through the oxidation of iodide catalyzed by a peroxidase isolated from mammalian thyroid glands (Hosoya, 1968). Thyroid peroxidase has also been implicated in the iodination of tyrosine residues of thyroglobulin (Taurog, 1970). Just recently it has been shown that the enzyme exhibits specificity

in the iodination of tyrosine residues in a peptide linkage, which suggests specific interaction of the protein with the peptide substrate (Krinsky and Fruton, 1971). Thyroid peroxidase, isolated in a relatively pure form (molecular weight 62,000) exhibits spectral characteristics typical of heme-proteins (Taurog, 1960). However, because the spectral details are somewhat different from HRP, it would appear that the prosthetic group is more tightly bound or, possibly not ferriprotoporphyrin IX. Nevertheless, the heme may be extracted with 0.2 N HCl-acetone indicating that it is not covalently bound to the protein moiety.

A green hemoprotein, myeloperoxidase, was isolated from the white blood cells found in pus (Agner, 1941), and was subsequently crystallized (Schultz, *et al.*, 1957; Agner, 1958). The molecular weight was determined as 149,000 (Agner, 1941) with an iron content corresponding to two prosthetic groups. The carbohydrate moiety was shown to be absent. The Soret spectrum exhibits two distinct maxima in the absorption pattern. Apparently one of the porphyrins was extracted readily with acetic acid -ether whereas the second was more tightly bound. Neither group has been positively identified. The enzyme is capable of activating chlorine, apparently to hypochlorite. Since the two prosthetic groups of myeloperoxidase are unique, this may be a prerequisite to formation of the chloride compound (Paul, 1963).

Bovine lactoperoxidase, readily purified from cow's

milk, has been the most extensively studied animal peroxidase. This glycoprotein has a molecular weight of 75,000-80,000 with a single heme group (Rombouts *et al.*, 1967). The prosthetic group has not been unequivocally identified because of the difficulty in extracting it from the protein moiety with organic solvents. However, it has been suggested that the prosthetic group may be a derivative of mesoheme IX, with the heme-protein linkage occurring through an ester bond (Hultquist and Morrison, 1963). The prosthetic group is not ferriprotoporphyrin IX, the different hemes of lactoperoxidase and HRP manifesting themselves in the different absorbances characteristic of the native enzymes and their complexes. Despite these differences, the catalytic properties of lactoperoxidase-catalyzed oxidation of iodide (Maguire and Dunford, 1972a) and p-cresol (Maguire and Dunford, 1972b) bear a striking resemblance to the HRP-catalyzed oxidation of these compounds (Roman *et al.*, 1971; Critchlow and Dunford, 1972a).

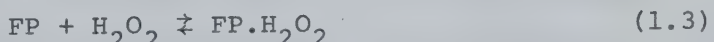
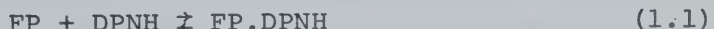
Japanese-radish and turnip peroxidase, both isolated from plant roots, are two enzymes which have the same prosthetic group as HRP. Recently, the Japanese-radish peroxidase crude extract has been reported to consist of eighteen isoenzymes (Morita *et al.*, 1970). Isoenzymes, usually characterized by different molecular forms of the protein moiety, will be discussed in considerable detail for HRP later in this chapter. An abundance of an acidic isoenzyme, designated by these workers as No. 3, was found. This was

in contrast to the preponderance of a neutral species in HRP crude extracts. The molecular weight of isoenzyme No. 3 was reported as 45,000 (Morita *et al.*, 1971) whereas a second basic isoenzyme which was readily crystallized was found to have a molecular weight of 30,000. Some of the difference in the molecular weight reflected a smaller carbohydrate moiety. Turnip peroxidase has been shown to contain five isoenzymes (Mazza *et al.*, 1968) which show marked differences in their spectral characteristics, unlike HRP isoenzymes. Recently, an investigation of the most basic and most acidic isoenzyme has indicated differences in the environment of the heme iron (Ricard *et al.*, 1972).

A number of peroxidases which are not hemoproteins are known to exist in living tissues. One of these is glutathione peroxidase first reported by Mills (1957) and later shown to be present in a wide variety of tissues (Mills, 1960). Originally isolated from bovine erythrocytes, this enzyme was shown not to be inhibited by azide or cyanide (Mills, 1959). The enzyme is heat labile and plays a primary role in protecting hemoglobin from oxidative degradation in both catalase-rich and catalase-deficient erythrocytes (Cohen and Hockstein, 1963). Recent kinetic studies confirm that the main metabolic pathway of hydrogen peroxide destruction at low concentration (10^{-6} M) is the enzymatic oxidation of glutathione by glutathione peroxidase (Flohe *et al.*, 1969). The sulphhydryl compound is oxidized to the corresponding di-

sulphide. The enzyme shows a radically different reducing substrate specificity when compared with hemoproteins. For example, pyrogallol, guaiacol, or toluidine will not serve as hydrogen donors (Mills, 1959). As well, this peroxidase oxidation has a maximum activity at pH 8 with no observable activity below pH 6. This behaviour, together with its insensitivity to conventional inhibitors of heme-proteins, is characteristic of flavoproteins.

Another flavoprotein with peroxidase activity was isolated from the bacterium *Streptococcus faecolis* and purified (Dolin, 1957). The enzyme has a minimum molecular weight of 120,000, contains flavin adenine dinucleotide (FAD) as a prosthetic group with no heme or metal ion. Unlike hemoproteins, the enzyme shows a high degree of substrate specificity with diphosphopyridine nucleotide (DPNH) the only known physiological reductant. Kinetic investigations suggest the formation of a ternary complex with a possible mechanism (Dolin, 1961):



where FP represents the native flavoprotein, FP.DPNH, FP.H₂O₂, FP.DPNH.H₂O₂ the three possible intermediate complexes and DPN⁺ the oxidized form of diphosphopyridine nucleotide.

Peroxidatic activity has been observed also with other hemoproteins such as hemoglobin, myoglobin and catalase but their function as peroxidases are inefficient in comparison with true peroxidases. Catalase catalyzes the decomposition of hydrogen peroxide to oxygen and water. Catalase and peroxidase are related enzymes insofar as they are both capable of promoting hydrogen peroxide oxidation by mechanisms which involve similar enzymatic intermediates.

Model systems consisting of metal ions in aqueous solution (Barb *et al.*, 1949; 1951a; 1951b; Baxendale, 1952; Kremer and Stein, 1959, Haggett *et al.*, 1960; Kremer, 1962; 1963), hemin (Kremer, 1965; 1967; Gatt and Kremer, 1968; Brown *et al.*, 1968; Brown and Jones, 1968) and various chelated cations (Wang, 1970; Sigel, 1969) have been investigated. Frequently, catalytic efficiencies of such systems were found to be orders of magnitude less than true peroxidases, and, at least in some cases, the oxidation products were found to be different (Saunders *et al.*, 1964). This would suggest reaction mechanisms for model systems that are different than for peroxidases. Jones *et al.* (1959) proposed a mechanism for the decomposition of hydrogen peroxide catalyzed by ferric salts involving the replacement of water molecules in the hydration shell of the cation forming ferric-peroxy complexes. Later, spectrophotometric evidence for complexes of the type $[Fe(H_2O)_5(H_2O_2)]^{+3}$ was presented (Haggett *et al.*, 1960). Studying the hemin-catalyzed

oxidation of ascorbic acid, Kremer (1967) proposed that the reaction proceeded through two enzymatic intermediates in an analogous fashion to the HRP-catalyzed reaction. However, in this investigation no consideration was given the autoxidation of hemin. Brown *et al.* (1968) showed the hemin-catalyzed reaction cannot be studied easily since the latter was oxidized by hydrogen peroxide to a spectroscopically well defined, catalytically active species designated as hemin (A). A study over the pH range 6.5 - 13.2 suggested that hemin (A) and hematin (A) functioned as independent catalytic entities (Brown and Jones, 1968). Recently, spectrophotometric evidence for a peroxidatic deuterhemin-peroxide complex similar to the HRP intermediate compound I has been reported (Portsmouth and Beale, 1971). These workers and others (Kurozumi *et al.*, 1961) have accounted for slower reaction rates of model peroxidase systems in terms of the rate of formation of this enzymatic intermediate. The rate at which this intermediate reacts with reducing agents is affected to a lesser extent.

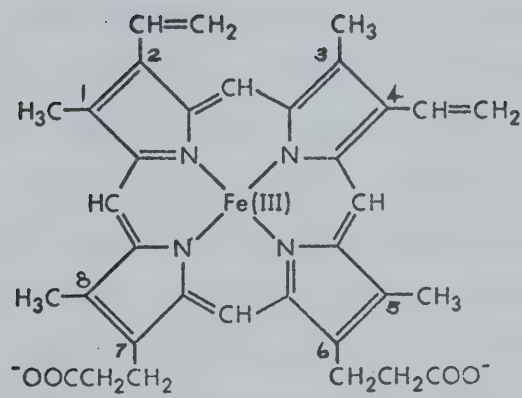


Fig. 1.1: Structure of Ferriprotoporphyrin IX.

1.2 Physical Properties of HRP

Optical Spectrum:

Hemoproteins are most frequently characterized by their ultraviolet and visible spectra. The interpretation of spectra for several hemoproteins has been reviewed by Smith and Williams (1969). Metalloporphyrin spectra exhibit three distinct bands resulting from $\pi \rightarrow \pi^*$ transitions in the conjugated ring system. Two of these bands appear in the visible spectral region (molar absorptivity $\sim 10^5 \text{ M}^{-1}\text{cm}^{-1}$). Heme proteins present a more complex spectrum with several additional visible spectral bands probably resulting from charge transfer. The band in the Soret has been used in this work, as in most other investigations involving hemoproteins, as a monitor of concentration. The change in the maximum absorption in this spectral region also has been used to distinguish between the various enzymatic species of HRP and complexes which it forms. The intensity of this band permits one to follow the rate of appearance or disappearance of the HRP intermediates conveniently in very dilute solutions ($\sim 10^{-6} \text{ M}$).

The Structure of Native HRP:

Native HRP consists of a protein moiety to which is bound the prosthetic group, ferriprotoporphyrin IX (Fig. 1.1). The enzyme's molecular weight is 42,000. A carbohydrate moiety associated with the protein structure constitutes 18.4% of this total weight. Although the protein

consists of nearly 300 amino acid residues, many having ionizable groups, one need only consider the enzyme's active site in order to explain most gross kinetic effects. It is generally accepted that the paramagnetic iron is located at this active site. The reasons for this belief are many. Transition metals are easily interconverted between their oxidized and reduced forms. All metals of the first transition series are known to catalyze oxidations in solution (Bateman, 1954; Waters, 1958). In addition to the peroxidatic activity observed for iron salts and hematin in dilute aqueous solution, the respiratory hemoproteins myoglobin and hemoglobin, that have the same prosthetic group as HRP, are known to bind oxygen. In a similar manner to HRP, this process can be retarded by classic anionic inhibitors such as fluoride, cyanide and azide. The corresponding change in the visible spectrum attributed to the binding of these species to heme can be observed. Hence, because of its prime catalytic importance, the configuration of the iron and its immediate environment have been investigated extensively.

The paramagnetic iron is octahedrally co-ordinated with the four equatorial positions occupied by pyrrole nitrogens (Fig. 1.1). These four ligands are conventionally numbered one through four. The axial ligands are numbered: five for the donor group which is associated with the protein, and six for the site accessible to the aqueous medium believed to be occupied by a weakly co-ordinated water molecule. The

structure of metmyoglobin is known to a resolution of 1.4 \AA° . In this enzyme the iron atom is located $0.3 - 0.5 \text{ \AA}^{\circ}$ on one side of the planar porphyrin ring equidistant from the four nitrogen atoms (Watson, 1968). The ESR studies of Blumberg *et al.* (1968) have indicated a lack of axial symmetry about the co-ordinated iron in HRP. Recent investigations of the native enzyme and the protein moiety after removal of the prosthetic group (apoenzyme) demonstrate major structural differences between the two proteins far beyond those reasonably expected from conformational change (Phelps *et al.*, 1971). Although it has long been thought that the ease with which the heme may be reversibly detached from the apoenzyme is good evidence to indicate that the heme is not covalently bound to the protein, the titration data of Phelps *et al.* would suggest that the protein-heme interaction, nevertheless, may be sufficiently strong to distort the protein backbone and the structure of the heme group.

Nature of the Axial Ligands:

The manner in which the prosthetic group in HRP is attached to the protein is not known with certainty. It is generally accepted that the fifth co-ordination site is occupied by an amino acid residue of the polypeptide chain. In the case of myoglobin, which has spectral and magnetic properties similar to those of HRP, it has a histidine residue at the fifth position and a water molecule at the sixth co-ordination position. However, it has been suggested that

the different chemical behaviour of these two hemoproteins may be related to the nature of the bound species at the iron's axial co-ordination sites. Brill (1966) has suggested that there are only a limited number of possibilities for the ligand at the fifth position of the heme iron in HRP: a carboxylate anion, a histidyl imidazole, an amino group, a tyrosyl phenolate, or a sulphydryl group of cysteine. The last possibility may be excluded since all cysteine groups present in HRP partake in disulphide bridges (Welinder *et al.*, 1972).

On the basis of titration data, Theorell (1943) first suggested that a carboxyl group was co-ordinated to the heme iron. Investigations of mixed ferriprotoporphyrin IX complexes in aqueous solution indicated that nitrogenous ligands are more effective in enhancing the peroxidatic activity than oxygenated ligands (Tokjo *et al.*, 1962). Nakamura *et al.* (1963) observed a maximum peroxidatic activity with a mixed ligand system at the axial positions, namely, histidine and guanidine. This suggested that histidine may occupy the fifth position in HRP. By way of a trans effect, this would necessarily imply a weakly co-ordinated ligand in the sixth position. Since lower rates of peroxidation were associated with a much slower rate at which peroxide interacted with the heme, this trans effect would account for the rapid interaction of peroxide at the sixth position to form the HRP intermediate compounds. Smith and Williams (1969) have similarly concluded that

histidine and water are the axial ligands in HRP by comparing its visible spectrum with myoglobin and hemoglobin. Using difference spectroscopy below 250 nm. the same conclusion has been reached (Brill and Sandberg, 1968).

Structural Modification Studies:

Myoglobin, having the same prosthetic group and a visible spectrum similar to that of HRP has often been used as a model to describe the molecular structure surrounding the heme of HRP. In myoglobin the porphyrin ring is held in a crevice of the protein with the vinyl groups buried in a hydrophobic interior, the iron co-ordinated in the fifth position with an imidazole side-chain, and the propionic acid groups weakly bound to basic amino acids near the protein's outer perimeter (Kendrew, 1962).

That the side-chains of the heme group are fundamental to the heme-protein association and to the catalytic activity of HRP has been demonstrated by investigations involving modified heme groups. Many years ago Theorell (1941) demonstrated the reversible cleavage of HRP into ferriproto-porphyrin IX and the apoenzyme. Later, it was shown that recombination of the apoenzyme with protoporphyrin IX (no chelated iron atom present) could be accomplished and that ferriprotoporphyrin IX and protoporphyrin IX compete for the same site on the protein (Maehley, 1961). Apparently, heme side-chain interactions play a primary role in binding to the protein. Furthermore, it has been well established that the propionic acid residues at positions six and seven

of the porphyrin ring (Fig. 1.1) are essential to the enzymatic activity of HRP (Theorell *et al.*, 1942; Paul, 1958; Paul, 1959). The esterification of these acid groups greatly reduces the affinity of the protein for the heme (Maehly, 1961; Tamura *et al.*, 1972). The monomethyl ester's activity was 20% of that of the native enzyme's, and the dimethyl ester was inactive (Tamura *et al.*, 1972). Substitution of the vinyl groups in the two and four ring positions in some cases caused a decrease in activity but the effects could be described as minor, never rendering the modified system enzymatically inactive (Paul, 1959).

Further evidence exists that would suggest that the heme side-chains play a very specific role in the peroxidatic mechanism. The monomethyl ester of ferriproto-porphyrin IX upon recombination with the apoenzyme reacted in a normal fashion with cyanide, fluoride and carbon monoxide to form well-defined complexes. Intermediate compounds of HRP were readily formed from hydroperoxides. However, in the case of the dimethyl ester, neither ligand binding nor intermediate compound formation were observed suggesting that the ionizable carboxyl group at positions six or seven was mandatory for ligand binding and peroxidatic activity (Tamura *et al.*, 1972). Substitution of the vinyl groups for acetyl groups depressed the enzyme's activity, but the rate at which peroxide reacted with the modified enzyme to form the intermediate compounds was not affected. The rate

at which compound II reduction occurred accounted in total for the observed decrease in the overall reaction rate (Chance, 1960). (See Fig. 1.2 for reaction cycle).

The Electronic Configuration of Heme Iron in HRP and its Complexes:

ESR, magnetic susceptibility and visible spectroscopy have been used to probe the paramagnetic iron's electronic configuration in hemoproteins. Magnetic moments have been measured for native HRP and its complexes (see Table 1.1). Generally, the ESR signals obtained have agreed with earlier conclusions regarding the number of unpaired electrons (Peisach *et al.*, 1968). A thermal equilibrium between high and low spin states of ferric hemoproteins was originally suggested by Theorell and Ehrenberg (1951). This implies that the iron porphyrin has an electron pairing energy such that at very low temperatures the low spin state will predominate but will be converted to the high spin state with increasing temperature as the electron pairing energy is overcome. To pursue this point further, temperature dependent studies of paramagnetic susceptibilities of hemoproteins using a sensitive torsion balance demonstrated that the Curie Law was not obeyed (Iizuka *et al.*, 1968; Iizuka and Kotani, 1968, 1969a, 1969b). This phenomenon was explained by thermal mixing of high and low spin states. The ESR signal of Japanese-radish peroxidase was found to be characteristic of high and low spin states

Table 1.1: The Magnetic Properties of Native HRP and its
Complexes

	Magnetic Moment (Bohr Magnetons)	ESR Signature (77°K)
HRP	5.5 ^a	High Spin ^{b,c}
HRP-OH	2.7 ^a	Low Spin ^{b,d}
HRP-CN	2.7 ^a	Low Spin ^{b,c}
HRP-F	5.9 ^a	High Spin ^c
HRP-N ₃	-	High Spin ^e

^aKeilin and Hartree (1951)

^bPeisach *et al.* (1968)

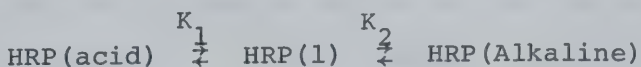
^cTamura (1971a)

^dTamura and Hori (1972)

^eTamura (1971b).

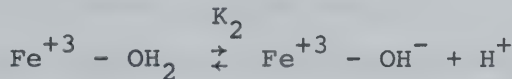
at liquid nitrogen temperatures (Morita and Mason, 1965) as was cytochrome-c peroxidase (Yonetani and Ehrenberg, 1967). A similar thermal equilibrium was used to explain the temperature dependence of magnetic susceptibilities of the HRP-azide complex (Tamura, 1971a). Investigations from liquid nitrogen to room temperature indicated that the HRP-CN complex was a pure low spin complex and HRP-F was a pure high spin complex. The native enzyme, however, appeared to consist of a pH dependent mixture of three distinct molecular forms, only two of which were, in turn, thermal equilibrium mixtures of high and low spin states (Tamura, 1971b).

An ESR study at liquid hydrogen and liquid helium temperatures was completed over a range of pH for two isoenzymes of HRP, the acid and neutral forms (Tamura and Hori, 1972). Isoenzymes and the heterogeneity of HRP are discussed in detail below. The results obtained were consistent with the existence of the three pH dependent components of each isoenzyme where interconversion could be accounted for in terms of ionizations of single acid groups:



The pK's for the neutral isoenzyme were $pK_1 = 9$ and $pK_2 = 11$ whereas for the acid isoenzyme the values were $pK_1 = 6.5$ and $pK_2 = 9$. It was suggested that there were two enzymatic components in acidic solution, HRP (Acid) and HRP(1), each of which appear thermally equilibrated between the two spin

states. In the alkaline pH region only one component, HRP (Alkaline), appeared to exist in a pure low spin state over the temperature range 1.4 - 293°K. The optical absorption spectra were in good agreement with these conclusions (Tamura and Hori, 1972). From optical spectra the pK_2 , indicative of the transition from HRP(1) to HRP(Alkaline), is observed at room temperature. This transition has been simply explained by the deprotonation of a water molecule co-ordinated at the heme iron's sixth position:



This equilibrium has been investigated by optical spectroscopy (Keilin and Hartree, 1951; Ellis and Dunford, 1969), magnetic susceptibility (Theorell, 1942) and ESR measurements (Morita and Mason, 1965; Blumberg *et al.*, 1968). However, the transition from HRP(Acid) to HRP(1) is not observed optically at room temperature. This is explained readily because of the similarity of the two high spin forms of HRP(Acid) and HRP(1) predominating at room temperature. The transition from HRP(1) to HRP(Alkaline) is observed because of the change in spin state which must occur at room temperature.

The pK_2 was observed to be 8.9 for HRP (neutral isoenzyme) reconstituted from the monomethyl ester of ferri-protoporphyrin IX, but 10 - 11 for HRP reconstituted with hemes containing different substituents at positions two and

four of the ring (Tamura *et al.*, 1972). These latter values for pK_2 were not very different from that of the native enzyme. Therefore, these results would suggest that the propionic acid ionization is integrally involved in the transition HRP(1) - HRP(Aalkaline). Interestingly enough, this is the same conclusion arrived at for intermediate compound formation and complex formation. By comparison with metmyoglobin and methemoglobin one might conclude that the pK_1 is a result of ionization of histidine at the heme iron's fifth co-ordination position in HRP (George *et al.*, 1961). This discussion will be pursued further in a later chapter concerning a well-defined pK_a observed for the HRP intermediate compound II in the alkaline region of pH.

Heterogeneity of Native HRP:

The presence of more than one component in HRP was first reported by Theorell (1942). Of the two species separated electrophoretically, the second peroxidatically active component was called paraperoxidase. These two enzymatic species were identical in composition except that paraperoxidase lacked the carbohydrate moiety (Theorell and Akeson, 1943). The paraperoxidase was found to denature much more readily at extremes of pH and in unbuffered solutions at room temperature. This would suggest that the carbohydrate serves to stabilize the tertiary structure of HRP.

Later, further enzyme heterogeneity was established.

Several components, called isoenzymes, were isolated from the crude HRP extract. Generally, each isoenzyme of a crude enzyme preparation has the same enzymatic specificity but possesses different molecular forms of the protein and, in some cases, exhibits different activity. Isoenzymes generally differ in their primary amino acid sequence, but recent success in demonstrating the interconversion of the multiple enzyme forms of chicken mitochondria malate dihydrogenase (Kitto *et al.*, 1966) would suggest that some isoenzymes also may differ only in their conformational forms. As many as twenty different isoenzymes have been reported for HRP using thin layer isoelectric focusing (Delincée and Radola, 1970). Although the authors argue that this isoelectric focusing technique provides a higher degree of resolution than other investigations, these workers have not been able to characterize the reported isoenzymes. As a result the possibility of enzyme fragmentation or protein aggregation cannot be ruled out in these experiments.

From a crude ammonium sulphate suspension of HRP Shannon *et al.* (1966) have isolated and purified seven isoenzymes, A₁, A₂, A₃ and B,C,D,E, by column chromatography. Each isoenzyme was characterized with regard to electrophoretic mobility, sedimentation coefficient, RZ value (ratio of the absorbance of the Soret maximum to that at 280 nm.), chromatographic behaviour, amino acid composition (Table 1.2) and carbohydrate analysis. No interconversion among these iso-

enzymes was detected and the two most abundant isoenzymes B and C were crystallized. The HRP heterogeneity was found to affect the catalytic properties (Kay *et al.*, 1967). As is apparent from Table 1.3, these isoenzymes of HRP can be classified into two distinct groups based upon their peroxidatic activity, A1, A2 and A3 comprising one group and B, C, D and E comprising the other group. Strickland *et al.* (1968) have investigated the isoenzymes A1 and C and the corresponding apoenzymes using circular dichroism in the visible-ultraviolet spectral regions. Their results and the tryptic mapping experiments of Chen (1968) have demonstrated that these isoenzymes may be further classified into three groups based primarily upon their amino acid composition which in turn is reflected in their different conformational forms and electrophoretic response: an anionic group A1 and A2, a second anionic group A3 and a third cationic group B, C, D, E.

Paul and Stigbrand (1970) have isolated four isoenzymes from an HRP extract by column chromatography: a highly acidic HRP(I), a neutral species HRP(III) and two basic fractions HRP(V) and HRP(VI). These homogeneous fractions were characterized by gel and disc electrophoresis as well as by isoelectric focusing. Their isoelectric points well reflected the amino acid composition. Possibly there are only three isoenzymes isolated in this case since HRP(VI) was essentially identical to HRP(III) except that a fragment

Table 1.2: The Amino Acid Composition
of HRP Isoenzymes (Residues-Mole⁻¹)

Amino Acid	B ^a	C ^a	HRP(III) ^b	Mann ^c
Lysine	6	6	6	6
Histidine	3	3	3	3
Arginine	22	21	18	20
Aspartic Acid	54	50	47	47
Threonine	27	23	25	25
Serine	23	22	26	26
Glutamic Acid	20	19	21	20
Proline	17	17	17	17
Glycine	18	15	17	17
Alanine	25	23	22	23
Half-Cystine	4	4	-	8
Valine	18	17	16	18
Methionine	3	3	4	4
Isoleucine	13	13	13	12
Leucine	39	36	34	35
Tyrosine	5	5	6	6
Phenylalanine	24	23	20	20

^aShannon *et al.* (1966)

^bPaul and Stigbrand (1970)

^cWelinder *et al.* (1972)

Table 1.3: The Catalytic Properties of Horseradish
Peroxidase Isoenzymes in o-Dianisidine Oxidation

Isoenzyme	pH Optimum	Azide Required For 50% Inhibition (10^{-3} M)	H_2O_2 Required For 50% Inhibition (10^{-3} M)
A1	5.8	7.7	75
A2	5.6	9.8	75
A3	5.6	2.0	25
B	5.0	0.8	2.3
C	5.0	0.7	2.2
D	5.0	0.9	2.1
E	5.0	0.7	2.3

of forty amino acids was absent in the former. From a comparison of the electrophoretic response and the relative amounts of arginine and methionine in the amino acid analyses (Table 1.2), isoenzyme HRP(III) may be identified with B and C, and HRP(I) associated with A1, A2 and A3. However, there appears to be nothing corresponding to HRP(V). Therefore, there is agreement that an acidic and a neutral isoenzyme are present in HRP preparations but results are not as well defined for the basic enzymatic forms. The fractions B and C show little difference in their amino acid composition but C has a carbohydrate moiety about 20% smaller than B. For this reason Paul and Stigbrand (1970) have suggested that B may have been formed from C under the rather severe acid conditions used in elution of these fractions from the CM-cellulose column. Although the inconsistencies among these workers may be attributed to variations in the composition of the crude extract dependent upon environmental conditions of the plant, there is no conclusive evidence to indicate that this is, in fact, the case.

It has been shown that both isoenzymes HRP(III) (Paul and Stigbrand, 1970) and B, C (Shannon *et al.*, 1966) account for about 50 % of the total enzymatic activity in the crude extract. Several commercial samples of HRP have been investigated using the techniques of Shannon *et al.* (1966) and Paul (1958). No acidic isoenzymes were detected (Kasinsky and Hackett, 1968). Welinder *et al.* (1972) have

isolated an electrophoretically pure component corresponding to HRP(III) from HRP purchased from Mann Research Laboratories, and show that the tryptic peptide maps of electrophoretically pure HRP from Worthington Biochemical Corporation to have no significant differences from the Mann product. Using gel isoelectric focusing (pH = 8 - 10) the two bands observed in the sample were attributed to differences in the carbohydrate moiety and not the primary amino acid sequence. Phelps and Antonini (1969) have isolated HRP(III) as the major component from HRP obtained from Boehringer-Mannheim. Similar results have been reported from this laboratory (Roman, 1972). Kinetic results obtained using both the second grade and electrophoretically purified HRP from Boehringer-Mannheim have shown no significant differences. At no time could the observed kinetics be interpreted in terms of HRP heterogeneity. Therefore, it would appear that this commercial source of HRP, used for all investigations described in this thesis, contains a large preponderance of the isoenzyme HRP(III) with kinetically undetectable amounts of the acid form HRP(I). A further discussion on this point will be postponed until Chapter 3.

Structure of the HRP Protein Moiety:

As mentioned previously, attempts to define the protein's primary structure in the form of amino acid analysis have shown the major differences among the HRP isoenzymes to be attributable to different amino acid composition.

Recently, amino acid sequence studies of HRP(III) (Welinder *et al.*, 1972) have defined complete sequences for 21 tryptic peptides accounting for 203 of the approximately 300 amino acid residues. Eight sites for carbohydrate attachment were identified of which seven appear to involve asparagine. Four disulphide bonds were identified, and an N-terminal pyrrolidone carboxyl group suggested.

Investigations of protein structure by optical rotatory dispersion (ORD) and circular dichroism (CD) have made major contributions to the measurement of the presence and extent of secondary structure. The phenomenon of ORD occurs when a medium containing assymetric molecular forms transmits the two circularly polarized components of an incident beam of plane-polarized light unequally. The result is an emerging ray of plane-polarized light rotated with respect to the incident ray. In the case of CD the two circularly polarized components of the incident ray are absorbed unequally giving rise to an elliptically polarized emergent beam. The two effects are intimately related. ORD is a dispersive phenomenon whereas CD is an absorptive phenomenon, observable only in the frequency intervals where optical absorption occurs. As a result, CD spectra may be interpreted with far less ambiguity.

In proteins, the optical activity is not necessarily an additive function of the various amino acid optical activities comprising the polypeptide chain. More specifically,

the α -helix shows a very marked extra dextrarotatory power because of its own particular conformational asymmetry. The depth of the ORD trough at 233 nm has been shown to be conformation dependent and its depth has been used as a measure of the protein's α -helical content (Simmons *et al.*, 1961). An ORD investigation of HRP indicated an α -helical content of 43% which was reduced significantly upon splitting the heme from the protein (Ellis and Dunford, 1968a). However, no gross conformational changes could be attributed to complex formation (i.e. HRP-CN, HRP-F and HRP-OH).

The protein's conformational characteristics were investigated for the two isoenzymes HRP(I) and HRP(III) by CD (Strickland *et al.*, 1968). The results suggested very similar active sites with only minor conformational differences in protein structure. The α -helical content for each was estimated at 40%. Upon formation of the HRP intermediates, a minor change in the CD spectrum at 282 nm was attributed to the reorientation of one or two aromatic amino acids. Otherwise, the similar spectral pattern suggested the same secondary structure in the native enzyme and its intermediate compounds. A comparison of the CD and absorption spectra of ferrimyoglobin, ferri-HRP, and the corresponding cyanide complexes suggested that the conformation of the protein moiety surrounding the heme in ferri-HRP was significantly different from that of ferrimyoglobin (Willick *et al.*, 1969). The dramatic reduction in the heme-associated

optical activity upon HRP reduction from the ferri to the ferro form indicated that HRP undergoes a local conformational change with respect to the heme upon its change in oxidation state (Willick *et al.*).

1.3 Peroxidatic Activity of HRP

Catalysis:

HRP catalyzes the peroxidation of aromatic amines, phenols and a variety of inorganic reducing agents. The reaction proceeds by way of a number of intermediate steps distinguished by the formation of unstable intermediate compounds with profoundly different spectroscopic properties. These reaction steps are represented diagrammatically in Fig. 1.2. As may be surmised from the diagram, the peroxidatic reaction involves primarily the two intermediates HRP-I and HRP-II. Kinetic experiments have confirmed that HRP-I precedes HRP-II and have demonstrated that HRP-II was formed only from HRP-I (Chance, 1949a). George (1952) showed by means of titrations with ferrocyanide, ferrous sulphate, and ferrocytocchrome-c that HRP-II reduction to HRP involved a one-electron transfer. Chance (1952a) found a similar one-electron transfer when HRP-I was reduced to HRP-II. For many years it was believed that HRP-I could be converted only to HRP-II (Chance, 1949a) but recent investigations have shown that HRP-I may be reduced directly to HRP in a two-electron transfer process with some inorganic reducing substrates (Roman and Dunford, 1972a, 1973).

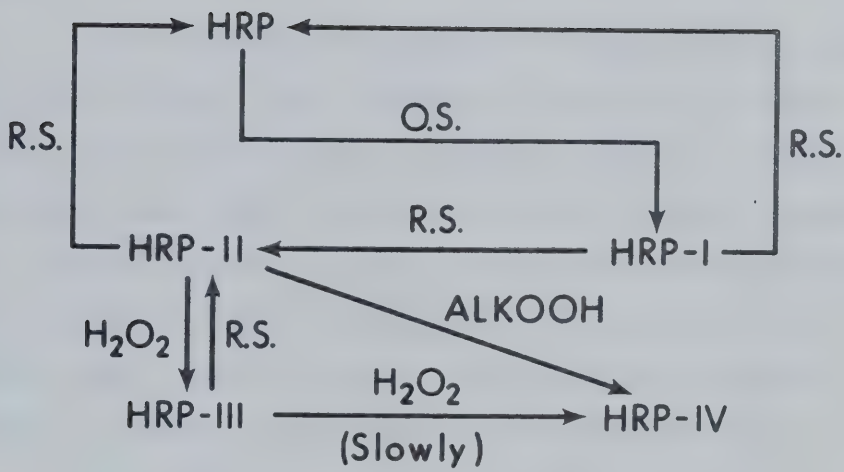


Fig. 1.2: The Interrelation of HRP and its Intermediate Compounds. R.S. = Reducing Substrates; O.S. = Oxidizing Substrate; ALKOOH = alkyl hydroperoxide.

Although HRP-I and HRP-II may function as rate-determining enzyme-substrate complexes, neither is a Michaelis-Menten complex in the original sense. Both contribute to the overall mechanism in a bimolecular step.

Nature of the Oxidizing Substrate and the Properties of HRP Compounds:

Long before any intermediate compounds were known (Keilin and Hartree, 1937; Theorell, 1941), early investigations indicated that alkyl hydroperoxides could function as oxidizing substrates in HRP-catalyzed reactions (Boeseken, 1930). Inactivity with dialkyl peroxides demonstrated that the OOH structure was an essential characteristic of the oxidizing agent (Elliot, 1932). In addition to dialkyl peroxides, no reaction was observed for secondary and tertiary alkyl hydroperoxides. This observation was confirmed for tert-butyl hydroperoxide, cumene hydroperoxide and p-methane hydroperoxide (Cotton, unpublished results). The acyl hydroperoxides were also acceptable oxidizing substrates (Boeseken, 1930) as well as many inorganic non-peroxidic oxidants: HOCl, HOBr, NaClO₂, ClO₂, KBrO₃, KIO₄, O₃ and K₂S₂O₈ + Ag⁺ (George, 1953). Recently, Markland (1971) has shown that hydroxymethylhydroperoxide is also an oxidizing substrate for HRP although it was believed for many years not to be.

Chance (1949c) obtained the Soret spectra of HRP-I and HRP-II formed from H₂O₂ and its monosubstituted

alkyl analogs. Accurate spectra for these intermediate compounds have been determined recently (Fig. 1.3) (Critchlow and Dunford, 1972b, Roman, 1972). Because Chance observed these spectra to be independent of oxidizing agents which he used, he concluded that each compound must involve the same type of iron-peroxide bond. He suggested an enzyme-substrate complex HRP-OOR as a possible structure for HRP-I (Chance, 1949c). George examined the spectra of HRP-I and HRP-II prepared from various inorganic oxidizing agents and obtained similar spectral results to those of Chance in each case (George, 1953a). Therefore, he proposed that HRP compounds formed from these different oxidizing substrates must have a common structure. Rather than an enzyme-substrate complex, he suggested that a more acceptable structure for HRP-I might be a higher oxidation state of the prosthetic group. However, later experimental evidence (Fergusson, 1956) indicated that formation of HRP-I from at least some inorganic oxidants may be preceded by hydrogen peroxide formation which then formed the HRP "complex".

Another interpretation, based primarily upon spectral studies in the visible and Soret regions (Brill and Williams, 1961) proposed that HRP-I prepared from ethyl hydroperoxide was an equilibrium mixture of two compounds, one containing the alkyl fragment at the active site. Magnetic susceptibility measurements indicated that HRP-I may be comprised of iron in its pentavalent state (three unpaired

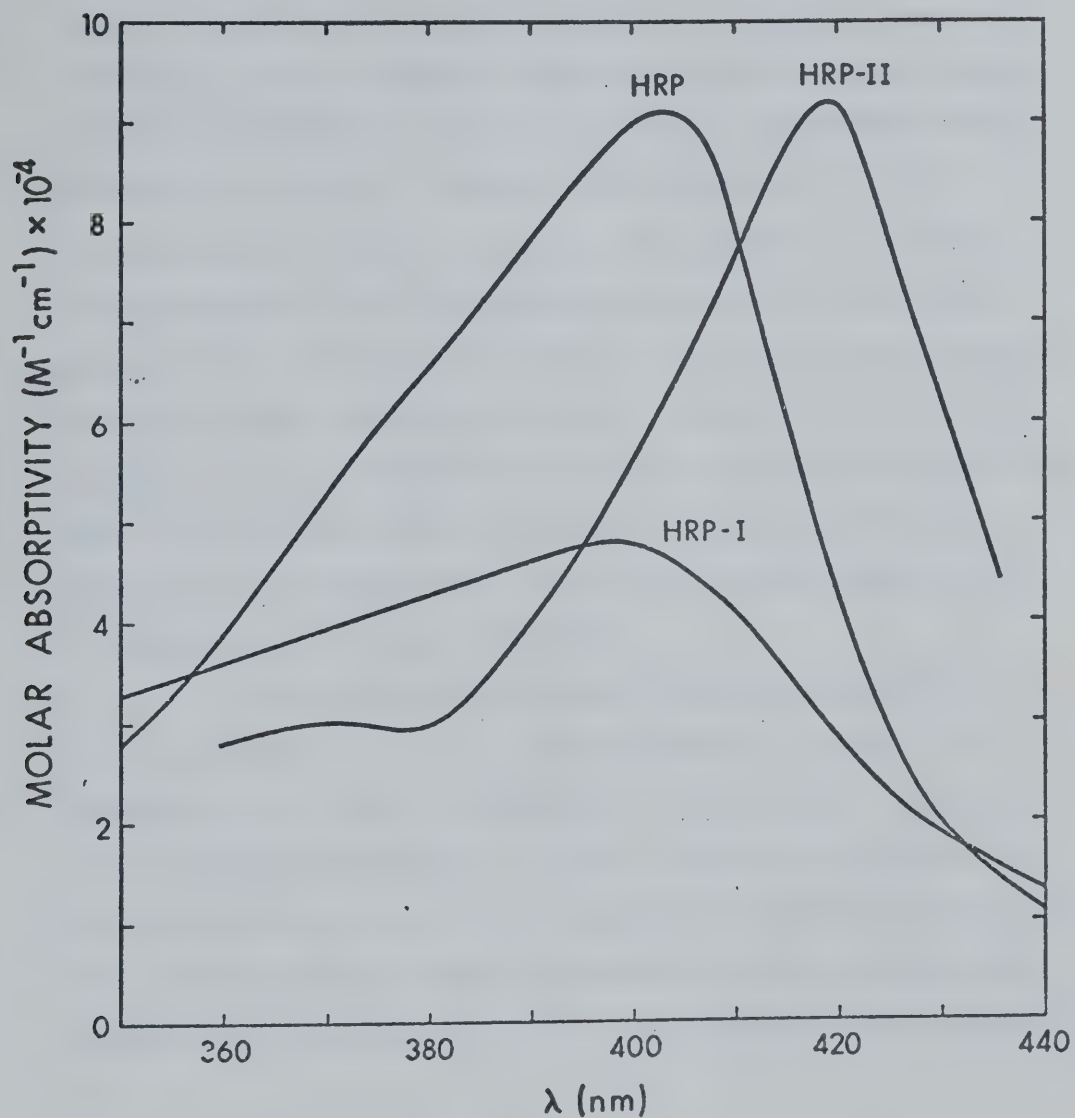
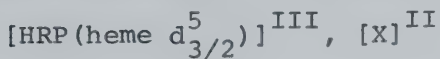


Fig. 1.3: Soret Spectra of HRP and its Intermediate Compounds HRP-I and HRP-II.

electrons) and HRP-II may contain iron in its quadrivalent low spin state (two unpaired electrons) (Theorell and Ehrenberg, 1952). However, because of the transient nature of these intermediate compounds accurate measurements are difficult to obtain. Probably these experiments need to be repeated using the steady-state approach to insure a preponderance of one intermediate species at a known concentration. Nevertheless, using the magnetic susceptibility and the visible spectrum for HRP-II, Brill (1966) has concluded that this intermediate must have the ferryl structure. This structure was first proposed by George (1953b) and consists of a quadrivalent iron with a single oxygen atom coordinated at the sixth position.

The information obtained from low temperature optical spectra (15 - 77°K) and ESR spectra (1.4°K) led Peisach *et al.* (1968) to propose a structure for the active site of HRP-I and HRP-II. A ferric complex for HRP-I was postulated with two oxidizing equivalents temporarily stored at a methine bridge carbon or pyrrole α -carbon of the porphyrin ring represented by X in the structural representation:



The expression in parenthesis indicates the spin multiplicity of the heme. The axial ligands provide a very weak component to the ligand field. Therefore, HRP-I for-

mation was envisioned as simply the two electron removal from HRP by the oxidant with no permanent complex formation. For HRP-II a ferrous low spin electronic configuration of the heme was suggested with an oxygen-containing ligand where the two oxidizing equivalents of the species resided:



Support for such a proposal was obtained by Noble and Gibson (1969) who demonstrated that the ferroperoxidase underwent a single electron transfer upon oxidation with hydrogen peroxide to form HRP-II. These structures predict similar active sites for HRP-I formed from hydrogen peroxide and alkyl hydroperoxides but possible structural differences for HRP-II prepared from different oxidizing substrates. From evidence presented in Chapter 4 concerning the effect of cyanide on the steady-state HRP-ferrocyanide oxidation, this structural model for HRP-I is an improbable one.

Recently, π -cation radicals of metalloporphyrins have been shown to be stable and have visible spectra similar to that of HRP-I but not HRP-II (Dolphin *et al.*, 1971). This has led to the currently popular view that HRP-I formation involves the transfer of one electron from the iron atom and one from the porphyrin π -orbitals. The reduction of HRP-I to HRP-II must then involve electron transfer to the porphyrin leaving a quadrivalent iron complex. This is

in agreement with the conclusion from Mossbauer spectroscopy that the electronic configuration of the iron in these two intermediates is the same (Moss, 1969). Further support for these proposals has been obtained by preparing stable one-electron oxidation products of ferric porphyrins. These systems are best characterized as being electron deficient at the metal atom rather than in the porphyrin π system (Felton *et al.*, 1971).

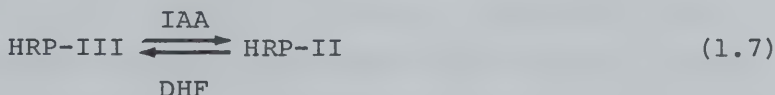
Hager *et al.* (1972) suggest a definite chemical composition for compound I of chloroperoxidase. Their O^{18} labelling studies demonstrated that at least one oxygen from the acyl hydroperoxide, m-chloroperbenzoic acid, was incorporated into compound I upon its formation and that no solvent exchange occurred. Both Hager *et al.* (1972) for chloroperoxidase and Schonbaum and Lo (1972) for HRP have shown that m-chlorobenzoate and p-nitrobenzoate, respectively, are the products on compound formation. This provides convincing evidence for an HRP-I formation step involving O-O bond cleavage (rather than C-O bond cleavage) incorporating one oxygen atom into compound I. The kinetic study discussed in Chapter 2 (Cotton and Dunford, 1973) provides quantitative evidence for the similarity of the active site of HRP-I and HRP-II formed from different oxidizing substrates over the accessible range of pH. Recent investigations demonstrating the apparent inaccessibility of cyanide ion to the active site of these intermediate compounds indicate a tightly

bound ligand at the iron's sixth coordination position (Cotton *et al.*, 1973). These results present a reasonable model for the active site of HRP-I and HRP-II discussed in a later chapter.

Much less information has been obtained concerning the intermediate compounds HRP-III and HRP-IV. The intermediate HRP-III is formed not only from HRP-II in the presence of excess hydrogen peroxide but also upon addition of dihydroxyfumarate in aerobic solutions, necessarily implicating HRP-III in the oxidase reaction (Mason, 1957). This intermediate compound reacts readily with reducing agents to give the native enzymatic form. An oxyperoxidase structure like oxymyoglobin or oxyhemoglobin was originally suggested by George (1956) (Fe^{+2}O_2) and was confirmed later by observing the direct formation of HRP-III from ferro-peroxidase and oxygen (Yamazaki, 1965; Wittenberg *et al.*, 1967). Apparently, HRP-III does not play an important role in the peroxidatic reaction.

Using a mixture of dimethylformamide and aqueous buffer (volume ratio 70:30), Douzou *et al.* (1970) successfully prepared intermediate compounds of HRP at temperatures from -15°C to -65°C in liquid solution. This allowed the preparation of stable solutions of the HRP intermediates for spectral investigations (Douzou *et al.*, 1971). The fast reactions were conveniently studied by classical spectro-

photometric methods using this technique of thermally controlled rates (Douzou, 1971a). Isolation of HRP-III at -40°C to -65°C permitted the study of its reactions in an aerobic system (Douzou, 1971b). In the presence of indoleacetic acid (IAA) and dihydroxyfumarate (DHF) cyclic conversion between HRP-II and HRP-III was successfully induced and followed spectrophotometrically on a Cary 14 at -30°C.



A spectroscopically distinct HRP-IV is formed from HRP-II or HRP-III upon addition of large excesses of peroxide. Recent investigations in the near infrared (Bagger and Williams, 1971) have demonstrated that HRP-IV may be formed by way of another unstable but, nevertheless, spectrally distinct intermediate formed from HRP-II called P-940. However, HRP-IV formation results in the simultaneous destruction of the enzyme and its biological significance seems doubtful.

Nature of the Reducing Substrate and Products of Reaction:

While HRP shows a specific preference for organic peroxides containing the -OOH group, its reducing substrate specificity is not as clearly defined. In fact, it is difficult to point to any specific group on the reducing agent for which peroxidases are specific. This is rather surprising and difficult to rationalize considering that catalase, a

hemoprotein having many structural and mechanistic features in common with peroxidase, oxidizes only primary and secondary alcohols or their related structures (Chance, 1949b). For HRP, organic reducing substrates fall into essentially three categories: phenols, aromatic amines, and endiols; but there are a number of exceptions including many inorganic reducing substrates (Table 1.4).

The rate of HRP-I reduction, generally, is at least an order of magnitude faster than that for HRP-II reduction at neutral pH. Less information concerning the rate of HRP-I reduction is available because, quite frequently, this reaction is very fast, and it is impossible to monitor by classical or stopped-flow kinetic techniques (Critchlow and Dunford, 1972a). Because HRP-II reduction is often the slowest, and, therefore, the rate-limiting step in the peroxidatic cycle, steady-state kinetics can be used only to determine experimentally the rate constant for this reaction step. It should be emphasized that the rate constants tabulated in Table 1.4 may serve only as a very crude comparison of reducing substrate dependent reaction rates. These constants are pH dependent and valid conclusions concerning the dependence of structure on reaction rate are difficult to attempt until this pH dependence is better understood.

The products isolated from HRP-catalyzed reaction

Table 1.4: Reducing Substrates for the HRP-Catalyzed Peroxidatic Reaction and the Apparent Rate Constants for HRP-II Reduction at 25 - 30°C.

Type of Reducing Substrate	Reducing Substrate	$k_{3, app}$ ($M^{-1} s^{-1}$)	pH
Phenols	p-Hydroxydiphenyl ^a	$\sim 8 \times 10^7$	7
	Hydroquinone ^a	3×10^6	7
	Hydroquinone Monomethyl Ether ^a	2×10^6	7
	Catechol ^a	2×10^6	7
	Resorcinol ^a	3×10^5	7
	p-Cresol ^b	1×10^6	7
Amines	o-Phenylenediamine ^a	$\sim 5 \times 10^7$	7
	m-Phenylenediamine ^a	1×10^6	7
	Aniline ^a	7×10^4	7
	p-Aminobenzoic Acid ^a	1×10^3	7
	p-Aminobenzoic Acid ^c	5×10^2	7
Endiols	Reductone ^a	$\sim 1 \times 10^6$	4.2
	Dihydroxymaleic Acid ^a	$\sim 1 \times 10^4$	7
	Ascorbic Acid ^a	2×10^4	4.7
Miscellaneous	Uric Acid ^a	$\sim 2 \times 10^4$	7
	Leucomalachite Green ^a	3×10^5	4.7

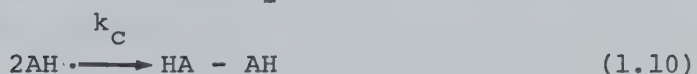
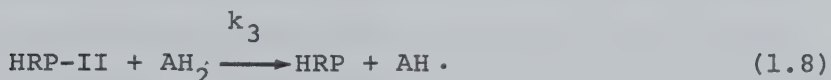
(Table continued on next page)

Table 1.4 continued

Ferrocyanide ^d	1.8×10^4	7
DPNH ^a	$\sim 3 \times 10^3$	7
Sulfite ^e	1×10^2	7
Iodide ^f	1.2×10	7
Nitrite ^a	1.7×10	7

^aChance (1951)^bCritchlow and Dunford (1972a)^cChapter 3, this thesis^dCotton and Dunford (1973)^eRoman and Dunford (1973)^fRoman *et al.* (1971)

mixtures indicate that free radicals often are intermediates. The initial steps for an organic reducing substrate AH_2 , where a single electron transfer is involved in the peroxidatic reaction are:



Yamazaki *et al.* (1960) have identified free radical formation in the oxidation of ascorbic acid, hydroquinone and dihydroxyfumaric acid by ESR. They estimated the intermediate steady-state concentrations in their flow system to be 5 - 20 times greater than the initial enzyme concentration. They could obtain no evidence for interaction of enzyme and the free radicals. The technique used was likely sensitive to the preferential oxidation of the free radical by either HRP-I or HRP-II but it is doubtful whether the change in free radical concentration for an equimolar free radical - enzyme interaction would be observable at the HRP concentration used (10^{-8} - 10^{-7} M) under steady-state conditions.

Considerable effort has been expended in the

isolation and characterization of reaction products. This work has been extensively reviewed (Saunders *et al.*, 1964; Mason, 1957). From a mechanistic point of view such an approach provides information concerning the nature of the initial free radical generating reaction. A comparison of products derived from the action of Fenton's reagent and HRP demonstrates the specificity created by the presence of the protein moiety and porphyrin ring. In the case of mesidine oxidation, the peroxidase gives a single product, 2,6-dimethylbenzoquinone-4-(2',4',6'-trimethyl) anil (Chapman and Saunders, 1941) whereas the ferrous salts give an ill-defined dark mass of multiple reaction products.

An understanding of the products resulting from the oxidation of a given substrate can allow the selection of a suitable reducing substrate to simplify the steady-state reaction. In order to obtain kinetically meaningful data readily from the steady-state it is essential that a region exist in the absorption spectrum in which the reducing substrate absorbs or in which products, related to the initial reaction step either directly or by way of very fast reaction steps, absorb. If several observable products are formed consecutively at similar rates, the steady-state system is not easily interpreted. As a result, activity tests usually utilize reducing substrates that yield a predominant product. Examples of such substrates are pyrogallol and mesidine. Hydroquinone is known to form

the free radical semiquinone structure (Yamazaki, 1960) which then forms quinone. Guiacol forms a single substituted biphenyl product through a coupling reaction. Both of these last two substrates were used in a steady-state kinetic study with lactoperoxidase (Maguire *et al.*, 1971). Vanillin (Baumgartner, 1966) and tyrosine (Morrison, 1972) give rise to a single biphenyl product allowing a reasonably facile investigation of the kinetics in the steady state. This was not the case for the nonsubstituted or p-disubstituted aromatic substrates. For p-cresol several reaction products have been isolated and attempts to study the steady-state system failed (Critchlow and Dunford, 1972a). Similarly, a variety of reaction products have been isolated from the oxidation of aniline, p-toluidine, p-anisidine, and p-chloroaniline. A successful steady-state investigation of ferrocyanide oxidation yielding the single product, ferricyanide, is discussed in both chapters 2 and 4. In Chapter 3 mention is made of the unsuccessful attempt to study p-aminobenzoic acid by the steady-state technique.

Modification of Peroxidatic Activity:

Enzymes frequently show inhibition or activation in the presence of metabolites which are substrates, precursors or products in the metabolic pathway. Quite frequently, these processes are particularly important in maintaining the concentrations of species at acceptable physiological levels. This regulation or control of

metabolic activity may be mediated by changes in the enzyme's conformation or by changes in the electronic environment of the active site. Usually, such phenomena may be explained by binding of the activator or inhibitor to a binding site that is not the active site. If this binding site is located near the active site then inhibition may arise from steric interference. Possibly, with the addition of suitably oriented reactive groups located on the bound species, the transition state may be attained with greater or lesser facility depending upon the interaction of this bound species (near the active site) and the reacting substrate.

Somewhat related to this last case is the hypothesis of nonproductive binding. If a good specific substrate exists with one or more binding groups complementary to binding sites on the enzyme (thus, allowing the substrate to be located in a particularly advantageous position for reaction) then, conceivably, a poor substrate could exist in which one or more binding sites are missing, or the steric orientation of the enzyme-substrate reactive center is unfavourable to the attainment of the transition state. Therefore, complex formation, although apparently enzymatically unproductive for one substrate, may be the major catalytic pathway for another related substrate. Little evidence exists for a productive HRP complex with a reducing substrate but, recent kinetic results would suggest that the

HRP-p-cresol complex is unproductive (Critchlow and Dunford, 1972a). Such complex formation may be a good indication that a reducing substrate may exist which forms a very efficient productive complex with the enzyme. The rate given for compounds such as p-hydroxydiphenyl for HRP-II reduction (see Table 1.4) would indicate that the reaction for such substrates may be approaching the diffusion-controlled limit. In addition, such complex formation may be an initial indication that a control mechanism serves to regulate the enzyme's activity *in vivo*.

A decade ago, Fridovich (1963) found that ammonia, pyridine, imidazole and hydrazine, although not functioning as electron donors in the peroxidatic reaction, activated the HRP-catalyzed oxidation of dianisidine above pH 7. Because competitive activation was observed for ammonia and pyridine, a single activating site was presumed to exist with which these nitrogenous ligands may interact rapidly and reversibly. Since these compounds are known for their ability to ligate to hemin iron (Nakamura *et al.*, 1963), as are hydroxide and cyanide which Fridovich found to compete with them, it was suggested that the binding site may be one side of the iron porphyrin possibly involving the ligand at the iron's fifth co-ordination position.

Andrejew *et al.* (1959) demonstrated that isoniazid (Isonicotinyl Hydrazine) and hydrazine competitively inhibited HRP in the acid region of pH. Apparently, compounds

of the structure $H_2N-NH-R$ cause irreversible inhibition whereas those of the form H_2N-O-R function as reversible inhibitors for HRP (Hidaka *et al.*, 1971). Hidaka and Udenfriend (1970) have also shown that iproniazid (Isopropyl isonicotinyl Hydrazine) reacts stoichiometrically and covalently in a 1:1 ratio with the enzyme. The apoenzyme retained 80% of the radioactivity that was retained by the native enzyme upon treatment with ^{14}C -iproniazid. They have attributed this phenomenon to a hydrazine reactive group such as a carbonyl or thiol located on the apoenzyme near the active site.

Ricard *et al.* (1968) reported a difference spectrum for the interaction of β -indolebutyric acid with HRP. Addition of the acid to the native enzyme caused a small spectral shift with a marked enhancement occurring in the 400 - 440 nm region. These results were explained by a reversible binding of the acid to HRP. A difference spectrum for the β -indolebutyric acid-hemin system was also obtained. This spectral shift was remarkably similar to the acid-HRP interaction. The interaction of indoleacrylic acid with HRP also showed a difference spectrum with an enhanced absorption in the 400 - 440 spectral region (Gasper *et al.*, 1972). Since there was no evidence for complex formation with the apoenzyme, a heme-binding site was suggested. Therefore, considering results obtained for these acids and the hydrazines, there would appear to be at least two binding sites at the active center of the native enzyme,

one associated with the heme group and the other on the protein. A spectral shift similar to that for β -indolebutyric acid has been reported upon the addition of acetic anhydride to native HRP (Schonbaum *et al.*, 1971). Although little evidence exists to suggest that acids alter the activity, these workers have reported a 50% inhibition with acetic anhydride which they attributed to acetylation of a histidine residue near the active site. Volkov *et al.* (1971) have reported recently that glutamic acid may alter the activity of the thyroid gland. Possibly, this observation is implicated with the activity of thyroid peroxidase.

As has been mentioned earlier, Critchlow and Dunford (1972a) have interpreted the kinetics of the HRP-catalyzed oxidation of p-cresol in terms of an inactive complex formed in the alkaline region of pH. At pH values above 10, this complex appeared to react at a reduced rate with a second molecule of p-cresol giving rise to an additional second order reaction. Difference spectra obtained for the interaction of p-cresol with the native enzyme were attributed to binding (Critchlow and Dunford, 1972a). However, the difference spectra for the p-cresol-HRP and the β -indolebutyric acid-HRP interactions in the 440 - 400 nm region are significantly different.

The kinetics of the oxidation of p-aminobenzoic acid has been investigated and interpreted in terms of substrate inhibition due to reversible binding to the enzyme.

These results will be discussed in detail in Chapter 3.

Kinetic Studies:

Enzyme kinetics seeks to define the mechanism by which an enzyme catalyzes biological reactions. It attempts to describe biochemical functions in detail, and, indirectly, to establish the structural nature of an enzyme's active site. Since one of the fundamental characteristics of any enzyme is its unique ability to promote efficiently a specific reaction, kinetics is a powerful tool for investigating its function and structure.

Two basic kinetic approaches exist in this field. Originally enzymatic reactions were studied in the steady state. Using small concentrations of the enzyme, quite frequently only obtainable in minute quantities through tedious purification procedures, experimentalists were able to slow the over-all reaction and study its kinetics by classical techniques (see Appendix 2). By systematic variations of the reactant and product concentrations, one is able to deduce a considerable amount about the mechanism (Cleland, 1963). However, if the mechanism is complicated by several enzyme intermediates, which is frequently the case, unambiguous interpretation of the steady-state kinetics can be very difficult. Many of the kinetic parameters cannot be evaluated quantitatively either because they are associated with reaction steps much faster than the rate-controlling step or because they are not separable as in-

dividual constants. The second approach involves observing a single turnover of the enzyme or, preferably, a single reaction step. This necessarily requires, in most cases, a fast reaction kinetic method. The stopped-flow technique is particularly amenable to the HRP-catalyzed reactions. The kinetics can be conveniently simplified by studying each reaction step separately. This is possible only because the HRP intermediates, although unstable, nevertheless, can be prepared immediately prior to an experiment with a half-life of about fifteen minutes. The rates of HRP-I and HRP-II reduction with an excess of reducing substrate are within the time regime of the stopped-flow method (half-life $\approx 0.005 - 0.1$ seconds). Under these pseudo-first-order conditions the need to know the slowly decaying initial concentration of the HRP intermediate is avoided. The large change in the Soret molar absorptivities upon reduction of the enzyme intermediates allows one to observe the rate of disappearance of these species spectrophotometrically. Therefore, in the kinetic investigations that follow, the HRP-catalyzed oxidations were studied primarily by the stopped-flow technique. Whenever possible, the stopped-flow data were complemented by the steady-state method. The latter approach proved a particular asset in the cyanide binding study to the HRP intermediates.

Early reports indicated that the reduction of HRP-I and HRP-II with reducing substrates were both pH

dependent (Getchell and Walton, 1931; Balls and Hale, 1934; Wilder, 1962) and pH independent (Chance, 1952b). Kinetic investigations of the binding of fluoride (Dunford and Alberty, 1967) and cyanide (Ellis and Dunford, 1968b) indicated the presence of ionizable groups at the active site of HRP. A study of the ferrocyanide oxidation over the range of pH 3 - 11 showed that the rate of HRP-I reduction varied over two orders of magnitude and HRP-II reduction five orders of magnitude (Hasinoff and Dunford, 1970). The log rate-pH profiles were interpreted in terms of a single ionization at 5.3 for HRP-I and three ionizations at 3.4, 5.2 and 8.6 for HRP-II. The kinetics of several inorganic reducing substrates have been investigated (Roman *et al.*, 1971; Roman and Dunford, 1972a; 1973). For HRP-I reduction a single ionization ($pK_a = 4.6$) was postulated to account quantitatively for the observed pH-rate profile with iodide whereas with sulphite two ionizations at 5.1 and 3.3 were indicated. For HRP-II reduction by iodide no ionizations were observed over the accessible range of pH (2.7 - 9.1). With sulphite the pH dependence in the region 2.4 - 6.9 was interpreted in terms of a single ionization at 3.9. In the reduction of both intermediates the log rate-pH profile was interpreted in terms of a sulphite ionization at 6.9.

Critchlow and Dunford (1972a), studying the oxidation of p-cresol by HRP-II, found a well-defined enzyme pK_a at 8.6. Two further enzyme ionizations at 2.2 and 5.7

were indicated. The substrate $pK_a = 10.4$ was also observed. As discussed previously, the existence of an HRP-II-p-cresol complex was demonstrated. Since the dissociation constant for the complex and the second-order rate constant for HRP-II reduction do not depend on any common ionizing group of the enzyme, it was argued that the complex was unproductive. p-Cresol was shown to react only in its unionized form over the experimental range of pH. This fact was demonstrated by showing that the calculated concentration of the anion was so small that for the observed rate, the second-order rate constant would have to be larger than the diffusion-controlled limit. This would suggest that electrostatic arguments could not explain the degree of complexity of the log rate-pH profile for this phenol oxidation. An attempt was made to correlate the log rate-pH profiles, observed isotope effects and over-all rate constants of the ferrocyanide, iodide and p-cresol oxidations with HRP-II in terms of a mechanism involving intramolecular general acid catalysis (Crutchlow and Dunford, 1972b) which gives way to a specific acid catalysis in sufficiently acidic solutions. The slower the over-all rate of reaction the higher the pH at which specific acid catalysis begins to compete successfully.

This thesis, then, is part of a continuing program to elucidate the mechanism and structure of HRP. The ferrocyanide oxidation has been used as a convenient system to probe the nature of the enzyme's active site. Aromatic

amines are one major class of reducing substrates. As a result, p-aminobenzoic acid was chosen as a convenient representative species to explore the kinetic response and to obtain more information with which to augment and expand upon existing mechanistic ideas.

CHAPTER 2

THE FERROCYANIDE PEROXIDATION CATALYZED BY HORSERADISH
PEROXIDASE AND THE NATURE OF THE ENZYME'S ACTIVE SITE2.1 Introduction

It has been proposed by many that a peroxide fragment must be retained at the active site (Chance, 1949; Brill and Williams, 1961; Hollenberg and Hager, 1972; Peisach *et al.*, 1968) when HRP intermediate compounds are formed. Spectral investigations in the Soret spectral region of HRP-I and HRP-II suggested that the HRP compounds formed with different oxidizing agents contain the same type of iron-peroxide bond (Chance, 1949), or simply contain a prosthetic group in a higher oxidation state (George, 1959). However, it has been shown that the chlorinating compound formed from HRP and NaClO₂ is spectrally identical to HRP-I (Hollenberg and Hager, 1972). Since HRP-I is not a chlorinating agent, spectral evidence alone is not a sufficient criterion for a proposed structure of the active site.

Although many techniques have been applied to the study of the HRP intermediate compounds (Moss *et al.*, 1969; Peisach *et al.*, 1968; Brill and Sandberg, 1968; Ellis and Dunford, 1968; Willick *et al.*, 1969), the kinetic method, in principle, provides one of the better sources of information concerning the nature of the active site. The rather complex dependence of reaction rates upon pH ob-

served for different reducing substrates in HRP-catalyzed reactions are indicative of proton-transfer processes which affect the rate-determining step. These proton transfers involve ionizable groups present on the enzyme or reducing substrate. Formation of HRP compounds with hydroperoxides may result in structural changes if the organic fragment is retained at, or near, the active site of the enzyme. This fragment could conceivably interfere with, or block, one or more proton transfers that have been shown to occur during the reduction of HRP-I and HRP-II prepared from hydrogen peroxide. A distinctly different pH dependence would then emerge. Therefore, in order to investigate these possibilities which may have remained undetected by experimental approaches less sensitive to such alterations, two organic hydroperoxides, ethyl hydroperoxide and *m*-chloroperbenzoic acid, were chosen to study the peroxidase-catalyzed ferrocyanide oxidation. The ferrocyanide oxidation was chosen because a previous investigation utilizing hydrogen peroxide to prepare HRP-I and HRP-II had demonstrated three protonations over the accessible range of pH for HRP-II reduction and at least one for HRP-I reduction, (Hasinoff and Dunford, 1970). A shift in the observed pK_a 's or their disappearance would show that the structure of the active site was dependent upon the structure of the oxidizing substrate.

2.2 Experimental

Materials:

Horseradish peroxidase was obtained from Boehringer-Mannheim as a highly purified ammonium sulphate suspension. Prior to use, the suspension was dialyzed and filtered through a Millipore filter of 8 micron pore size. Using the spectrophotometric purity criterion, the final enzyme preparation had a P.N. of not less than 3.0. The purity number (P.N.) is the ratio of the absorbance at the Soret maximum of 403 nm to the absorbance at 280 nm. The enzyme was characterized and its concentration determined spectrophotometrically as is described in considerable detail in Appendix 5.

Water, distilled from alkaline potassium permanganate followed by double redistillation from glass, was used in the preparation of all solutions. A constant ionic strength (μ) of 0.11 was maintained in all reaction mixtures with 0.01 contributed by the buffer and the remainder by Fisher reagent grade potassium nitrate and potassium ferrocyanide. Ferrocyanide stock solutions were prepared immediately prior to use under diffuse lighting and stored in the dark.

The ethyl hydroperoxide was obtained from Polysciences Inc. as a 10% aqueous solution. A polarographic analysis of the reagent in dilute alkaline lithium sulphate solution detected no hydrogen peroxide (Bruschweiler and

Minkoff, 1955). The presence of other possible oxidizing agents known to form compounds with HRP was not observed by NMR. A 5×10^{-4} M aqueous solution of the alkyl hydroperoxide was stored at 5°C and its concentration was analyzed periodically by spectrophotometry utilizing the HRP-catalyzed oxidation of iodide to triiodide. This analytical technique was developed from a method for the analysis of hydrogen peroxide using molybdate as a catalyst (Ovenston and Rees, 1950; Ramette and Sandford, 1965). Molybdate is a poor catalyst for alkyl hydroperoxides and the rate of formation of triiodide is too slow to be analytically useful. In the newly developed method, a solution consisting of 0.05 M sodium iodide and 10^{-8} M HRP was prepared in an acetate buffer of pH 3.8 and ionic strength 0.01. A 2 ml aliquot was pipetted into a cuvette and the absorbance change observed upon the addition of 50 μ l of the hydroperoxide solution. The amount of triiodide formed was determined quantitatively by measuring its absorbance at 353 nm on the Cary-14 spectrophotometer using a molar absorptivity of $2.55 \times 10^4 \text{ M}^{-1} \text{ cm}^{-1}$ (Ramette and Sandford, 1965). The solutions of hydrogen peroxide used to prepare the HRP compounds were also stored and analyzed in a similar manner.

An independent analysis of hydrogen peroxide present in the ethyl hydroperoxide solutions made use of the difference in the relative rates with which hydro-

peroxides and hydrogen peroxide react with iodide (Johnson and Siddiqi, 1970). In the presence of 0.005% by weight ammonium molybdate the hydrogen peroxide oxidation was very rapid and occurred within the time required to mix the solutions in the cuvette. Comparing this dead-time reaction with the total change in absorption when HRP was added, showed that less than 2% hydrogen peroxide was present in the ethyl hydroperoxide.

Technical grade *m*-chloroperbenzoic acid was obtained from the Aldrich Chemical Company. A 10% solution of this acyl hydroperoxide was made up in acetone and stored at -10°C. Stock solutions of about 4×10^{-4} M were prepared prior to each day's experimental work by adding 0.1 ml acetone solution to 100 ml distilled water. The concentration of the acyl hydroperoxide was determined by the spectrophotometric method described above for ethyl hydroperoxide. However, because *m*-chloroperbenzoic acid rapidly and spontaneously oxidizes iodide, no HRP was required to catalyze the reaction. Hydrogen peroxide oxidation of iodide is very slow in the absence of a suitable catalyst. Therefore, spontaneous oxidation was used in the determination of the acyl hydroperoxide concentration and addition of HRP facilitated the determination of the total concentration of oxidizable material (hydroperoxide + hydrogen peroxide concentration). It was estimated by this means that slow hydrolysis (Swern, 1971) or contamin-

ation of the acyl hydroperoxide resulted in <5% of the total peroxide as hydrogen peroxide in the stock solutions 8 - 10 hours after preparation.

Kinetic Experiments:

Investigations were carried out using a stopped-flow apparatus thermostatted at 25°C. Details of the instrument are described elsewhere (Ellis, 1968, Hasinoff, 1970). The experimental traces were monitored on a 564B Tektronix storage oscilloscope, and the stopped-flow data were recorded as an amplified photomultiplier voltage print-out digitized at 30 equally spaced intervals of time. In a typical experiment, HRP-I was prepared by adding 0.8 molar equivalents of the hydroperoxide to a 2×10^{-6} M unbuffered aqueous solution of the native enzyme. The HRP-II was prepared by adding 0.4 molar equivalents of p-cresol to HRP-I based on the original native HRP concentration. The absence of HRP-I was checked periodically by observing the absorbance at 411 nm, the wavelength at which HRP and HRP-II are isosbestic. The absence of a change in the absorbance at 411 nm as HRP-II decays to HRP demonstrates the absence of HRP-I. In a kinetic study of HRP-II reduction, the presence of HRP-I in the enzyme preparation is not a critical factor provided that the rate of HRP-I reduction is sufficiently fast to permit essentially complete time separation of the two reactions. This, in fact, was the case for the ferrocyanide oxidation. The potassium

ferrocyanide solution was prepared separately and, with the exception of the HRP-II studies at low pH to be discussed in more detail shortly, contained the buffer, potassium nitrate and about 10^{-9} M HRP. The latter component removed small amounts of oxidizing impurities and prevented anomalous formation of HRP intermediates in the initial time interval which would have interfered with the observed exponential decay of their concentrations. The other syringe contained the HRP compound. Its final concentration in the instrument's observation chamber was about 5×10^{-7} M with not less than a 10 molar excess of the ferrocyanide. The reactions were followed by observing the increase in absorbance at 411 nm for HRP-I reduction and the decrease in absorbance at 425 nm for HRP-II reduction. Not only did the change in absorbance at 411 nm have a reasonably large change in the molar absorptivity upon conversion of HRP-I to HRP-II, but also the interference from HRP-II reduction was minimized since this latter reaction was not observable at sufficiently narrow slit widths (~0.3 mm). At 425 nm the change in molar absorptivity upon reduction of HRP-II was a maximum and close to the wavelength at which HRP-I and HRP are isosbestic. The observed first order rate constants were calculated in the manner described in Appendix 1. An average rate constant and standard deviation were determined from 8 - 12 experimental exponential traces.

The kinetics of the HRP-II-ferrocyanide reaction

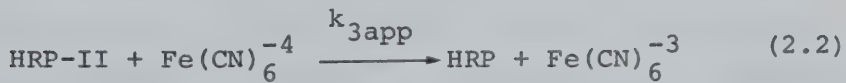
also was investigated at pH values between 9 and 10 using the Cary 14 spectrophotometer with the cell compartments thermostatted at 25°C. In these experiments 2 ml of 2.0×10^{-6} M HRP, containing the buffer and potassium nitrate, were pipetted from a constant temperature bath into a cuvette. HRP-II was prepared by the appropriate addition of hydroperoxide and p-cresol. Then, at least a 20 molar excess of ferrocyanide was quickly added. First order rate constants were calculated from the resulting spectrophotometer traces in a manner analogous to that used for the stopped-flow data.

The Cary-14 spectrophotometer also was used to study the steady-state kinetics over the range of pH 5 - 3.2. The reaction was followed by measuring the absorbance of ferrocyanide at 420 nm. The molar absorptivity at this wavelength was found to be $1030 \text{ M}^{-1} \text{ cm}^{-1}$, in good agreement with previously published results (Hasinoff and Dunford, 1970; Birk, 1969). Ferrocyanide and sufficient water to make a total volume of 2.2 ml were added with Hamilton microliter syringes to a cuvette containing 2 ml of buffer, potassium nitrate and HRP. The reaction was initiated by rapidly mixing the peroxide with the cuvette's contents using a Teflon plumper on which microliter quantities of the oxidizing substrate were deposited. The initial velocity of the reaction was computed at the extrapolated zero time by measuring the slope of the absorbance-time

trace. Initial HRP concentrations were in the range (1 - 2) $\times 10^{-8}$ M and initial peroxide concentrations (5 - 20) $\times 10^{-5}$ M. A detailed discussion of the steady-state method is given in Appendix 2.

2.3 Results

The formation of HRP-I results from the addition of oxidizing agent to the native enzyme. HRP-II is prepared by addition of suitable quantities of p-cresol as discussed previously. The established equations for the ferrocyanide oxidation with the two intermediates are (George, 1952; Chance, 1952):



With excess ferrocyanide, the reaction becomes pseudo-first order and the differential rate expressions in each case are:

$$-\frac{d[\text{HRP-I}]}{dt} = k_{2\text{obs}} [\text{HRP-I}] \quad (2.3)$$

$$-\frac{d[\text{HRP-II}]}{dt} = k_{3\text{obs}} [\text{HRP-II}] \quad (2.4)$$

$$\text{where: } k_{2\text{obs}} = k_{2\text{app}} [\text{Fe}(\text{CN})_6^{-4}] \quad (2.5)$$

$$k_{3\text{obs}} = k_{3\text{app}} [\text{Fe}(\text{CN})_6^{-4}] \quad (2.6)$$

Eqs. 2.3 and 2.4 were confirmed for both the alkyl and acyl hydroperoxides as oxidizing substrates by obtaining linear plots of $\log \Delta v$ vs. time for reaction traces of many different pH values (Δv = voltage change which may be related to absorbance change ΔA). The linear correlations of $k_{2\text{obs}}$ and $k_{3\text{obs}}$ with ferrocyanide concentrations were verified by studying the reaction rates at different ferrocyanide concentrations, using HRP-I or HRP-II prepared with ethyl hydroperoxide or m-chloroperbenzoic acid. The data from several experiments are shown in Fig. 2.1 for HRP-I and Fig. 2.2 for HRP-II. Similar studies were performed at a number of other pH values on the stopped-flow apparatus for HRP-I, and on both the stopped-flow apparatus and spectrophotometer for HRP-II. Each stopped-flow study of k_{obs} as a function of $[\text{Fe}(\text{CN})_6]^{-4}$ represented 5 - 9 different concentrations of ferrocyanide over an order of magnitude range and the analysis of 50 - 90 Δv vs. time traces.

Kinetics of the HRP-II-ferrocyanide reaction:

Values for $k_{3\text{app}}$ were determined by the stopped-flow technique over the pH range 4 - 10.6. At high pH, $k_{3\text{app}}$ values were determined on the Cary 14 spectrophotometer also. The data are presented in Table 2.1 and Fig. 2.3. The result of the steady-state studies of the HRP-catalyzed ferrocyanide reaction in the acid pH region, with ethyl hydroperoxide and hydrogen peroxide as oxidizing substrates, are presented in Table 2.2. The steady-state

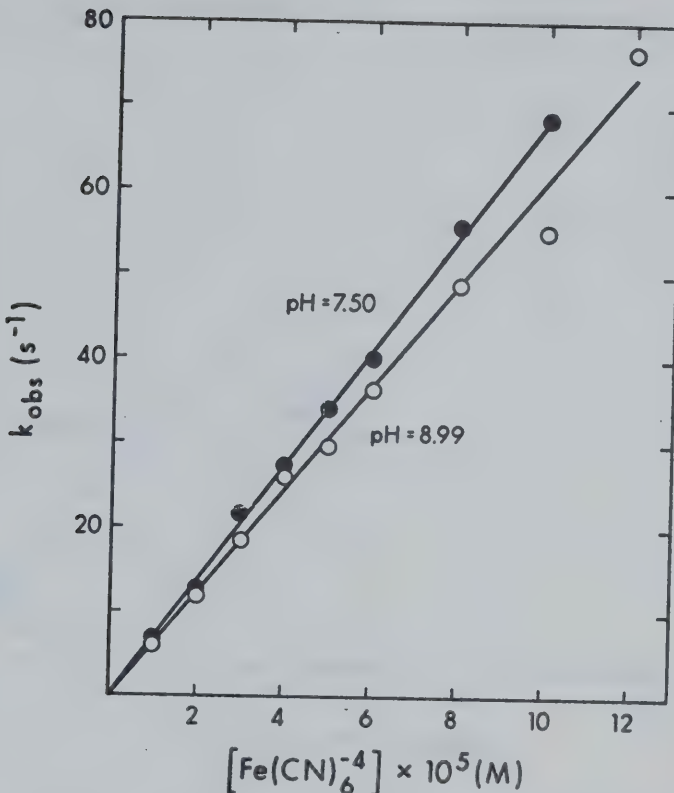


Fig. 2.1: Two studies of the dependence of the HRP-I-ferrocyanide reaction on ferrocyanide concentration. At the two pH values indicated, $k_{2\text{obs}}$ is plotted against $[\text{Fe}(\text{CN})_6]^{-4}$. The linear correlations were determined from a weighted linear least squares analysis. Within the experimental errors, the intercepts were zero. The rate constants determined from the slopes are: pH = 8.99, $k_{2\text{app}} = (6.1 \pm 0.3) \times 10^5 \text{ M}^{-1} \text{ s}^{-1}$; pH = 7.50, $k_{2\text{app}} = (6.8 \pm 0.3) \times 10^5 \text{ M}^{-1} \text{ s}^{-1}$.

Key: O, HRP-I prepared from ethyl hydroperoxide; ●, HRP-I prepared from m-chloroperbenzoic acid.

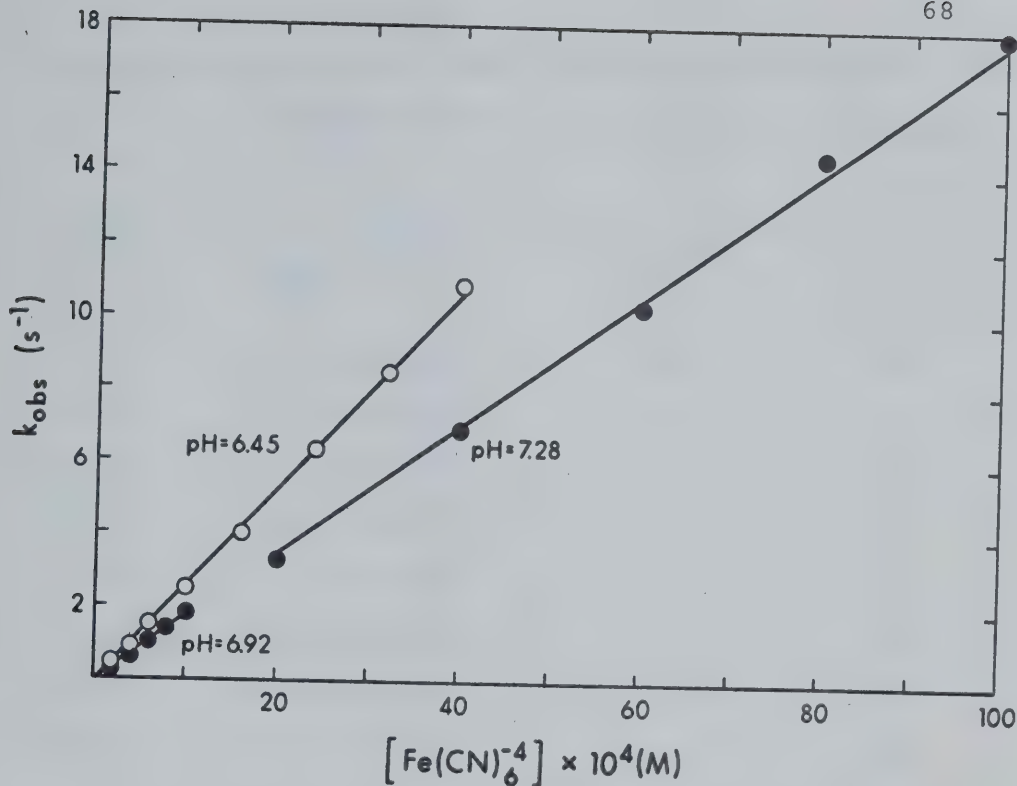


Fig. 2.2: Three studies of the dependence of the HRP-II-ferrocyanide reaction on ferrocyanide concentration. Plots of $k_{3\text{obs}}$ vs. $[\text{Fe}(\text{CN})_6^{4-}]$ are shown with correlations determined from a weighted linear least-squares analysis at the pH values indicated. In each case the intercept is zero within experimental error. At the different pH values the rate constants determined from the slopes are: pH = 6.45, $k_{3\text{app}} = (2.7 \pm 0.1) \times 10^4 \text{ M}^{-1} \text{ s}^{-1}$; pH = 6.92, $k_{3\text{app}} = (1.8 \pm 0.1) \times 10^4 \text{ M}^{-1} \text{ s}^{-1}$; pH = 7.28, $k_{3\text{app}} = (1.8 \pm 0.1) \times 10^4 \text{ M}^{-1} \text{ s}^{-1}$.

Key: O, HRP-II prepared from ethyl hydroperoxide; ●, HRP-II prepared from m-chloroperbenzoic acid.

Table 2.1: The second order rate constants determined for the HRP-II-Ferrocyanide reaction at 25° and $\mu = 0.11$.

pH ^a	k_{3app} ($M^{-1}s^{-1}$) ^b	Buffer ^c	Oxidizing Substrate ^d
4.01	$(2.0 \pm 0.2) \times 10^6$	CT	M
4.20	$(1.1 \pm 0.1) \times 10^6$	CT	E
4.38 ^e	$(8.3 \pm 0.6) \times 10^5$	A	E
4.39	$(7.8 \pm 1.4) \times 10^5$	A	H
4.60 ^e	$(4.9 \pm 0.2) \times 10^5$	A	M
4.78	$(3.0 \pm 0.3) \times 10^5$	A	H
4.78 ^e	$(3.3 \pm 0.1) \times 10^5$	A	E
4.98	$(2.1 \pm 0.4) \times 10^5$	A	M
5.16	$(1.5 \pm 0.1) \times 10^5$	A	M
5.16	$(1.4 \pm 0.1) \times 10^5$	A	H
5.40	$(9.8 \pm 0.3) \times 10^4$	A	M
5.77	$(5.9 \pm 0.4) \times 10^4$	P	E
5.89	$(5.0 \pm 0.5) \times 10^4$	P	E
5.94	$(4.3 \pm 0.1) \times 10^4$	P	H
5.96 ^e	$(4.4 \pm 0.1) \times 10^4$	P	E
6.12	$(3.7 \pm 0.2) \times 10^4$	P	E
6.25	$(3.0 \pm 0.1) \times 10^4$	P	E
6.45 ^e	$(2.7 \pm 0.1) \times 10^4$	CA	E
6.61	$(2.2 \pm 0.1) \times 10^4$	P	M

(Table continued on next page)

Table 2.1 continued

pH ^a	$k_{3app} (M^{-1}s^{-1})^b$	Buffer ^c	Oxidizing Substrate ^d
6.92 ^e	$(1.8 \pm 0.1) \times 10^4$	P	M
7.06	$(1.8 \pm 0.4) \times 10^4$	P	E
7.13	$(1.7 \pm 0.1) \times 10^4$	P	M
7.28 ^e	$(1.8 \pm 0.1) \times 10^4$	P	M
7.50	$(1.4 \pm 0.1) \times 10^4$	T	M
7.73	$(1.5 \pm 0.2) \times 10^4$	P	E
7.95	$(1.1 \pm 0.1) \times 10^4$	T	M
8.57	$(7.2 \pm 0.9) \times 10^3$	T	E
9.00 ^f	$(3.4 \pm 0.5) \times 10^3$	T	E
9.37	$(2.2 \pm 0.2) \times 10^3$	C	M
9.51 ^e	$(2.1 \pm 0.1) \times 10^3$	GN	E
9.87 ^f	$(6.7 \pm 0.3) \times 10^2$	C	E
9.94 ^f	$(5.8 \pm 0.3) \times 10^2$	C	E
10.56	$(1.6 \pm 0.1) \times 10^2$	C	M

^aErrors on pH values estimated at 0.02.

^bErrors on rate constants represent twice the standard deviation calculated from experiments performed at a given pH.

(Table continued on next page)

Table 2.1 continued

^cBuffer abbreviations: A, acetic acid-sodium hydroxide; CA, cacodylic acid-sodium hydroxide; P, potassium dihydrogen phosphate-sodium hydroxide; T, tris-nitric acid; C, sodium bicarbonate-sodium hydroxide; CT, citric acid-sodium hydroxide; GN, glycine-sodium hydroxide.

^dOxidizing substrate abbreviations: E, ethyl hydroperoxide, M, m-chloroperbenzoic acid; H, hydrogen peroxide.

^eStudy of the dependence of $k_{3\text{obs}}$ on $[\text{Fe}(\text{CN})_6]^{-4}$ from which $k_{3\text{app}}$ was calculated from the slope of a linear least-squares analysis.

^fStudy of $k_{3\text{obs}}$ vs. $[\text{Fe}(\text{CN})_6]^{-4}$ performed on the Cary 14 spectrophotometer.

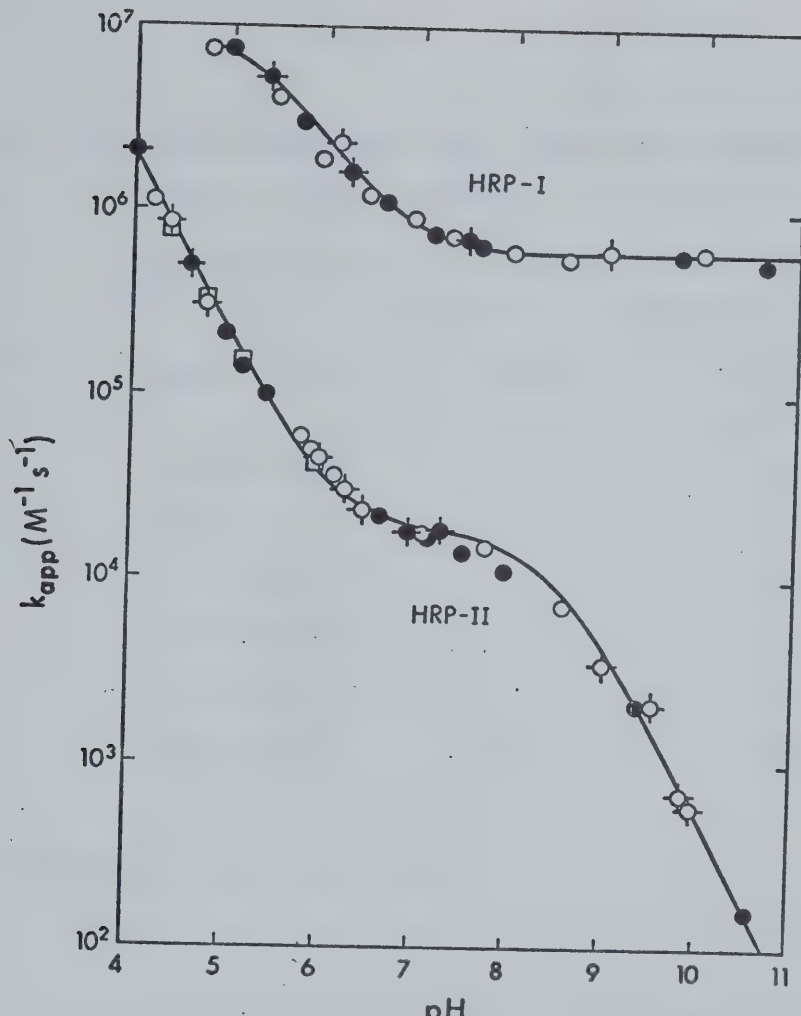


Fig. 2.3: Semilogarithmic plots of the apparent second order rate constants *vs.* pH for the HRP-I-ferrocyanide and HRP-II-ferrocyanide reactions. The correlations appearing as solid curves were obtained from the non-linear least-squares analysis of the data. The error limits, to be found in Tables I and IV, were omitted for clarity. Different oxidizing substrates were used in the preparation of the HRP compounds. Key: \square , hydrogen peroxide; \circ , ethyl hydroperoxide; \bullet , m-chloroperbenzoic acid, \diamond , \star , study of the dependence of k_{obs} on $[Fe(CN)_6]^{4-}$

Table 2.2: The second order rate constants for the HRP-II-Ferrocyanide reaction determined from steady-state kinetics at 25° and $\mu = 0.11$

pH ^a	$k_{3app} (M^{-1}s^{-1})^b$	Buffer ^c	Oxidizing Substrate ^d
3.27	$(6.9 \pm 1.4) \times 10^6$	CT	H
3.63	$(3.6 \pm 0.3) \times 10^6$	CT	E
3.85	$(2.0 \pm 0.2) \times 10^6$	CT	H
4.23	$(8.3 \pm 0.8) \times 10^5$	CT	H
4.60	$(4.9 \pm 0.3) \times 10^5$	A	E
5.01	$(1.9 \pm 0.2) \times 10^5$	A	H

^{a,b,c,d}The same as in Table 2.1

data obtained at four pH values are shown in Fig. 2.4. The steady-state determinations are in good agreement with those published previously (Hasinoff and Dunford, 1970; Critchlow and Dunford, 1972). The apparent second-order rate constants (k_{3app}, s) determined by this method are consistently about 20% lower than those obtained by studying the HRP-II-ferrocyanide reaction in isolation from the other reactions involved in the steady-state cycle, that is, by stopped-flow kinetics. Since the rate constants obtained from the steady state are dependent upon the total concentration of HRP whereas the stopped-flow results are not, this discrepancy may be due to uncertainty in the value of the molar absorptivity of HRP at 403 nm (Keilin and Hartree, 1951). Values for the molar absorptivity published more recently (Shannon *et al.*, 1966; Paul and Stigbrand, 1970) indicate that the value of Keilin and Hartree (1951) at 403 nm is too small. In addition to introducing error in measurement of the rate constant using the steady-state method, an imprecise value for the molar absorptivity of HRP may lead to the use of incorrect amounts of oxidizing and reducing substrate in preparing the HRP intermediates. From a kinetic point of view only an excess of oxidizing substrate poses a serious problem. This invariably leads to more than one turnover of the enzyme. The native enzyme resulting from HRP-II reduction will form HRP-I if oxidizing substrate is present, and another oxidation-reduction cycle

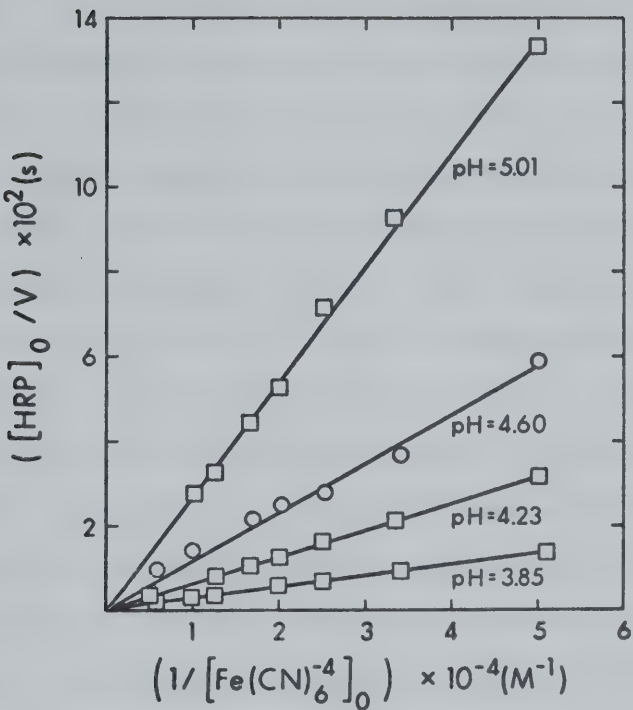


Fig. 2.4: Plot of $[H_2O_2]_0/v$ vs. $1/[Fe(CN)_6^{-4}]_0$ at four pH values obtained by steady-state kinetics. The correlations shown were determined from a linear least-squares analysis. For each set of data, pH, $[H_2O_2]_0$ or $[C_2H_5OOH]_0$, and $[HRP]_0$ were constant at the following respective values: 3.85, 5.60×10^{-4} M, 1.3×10^{-8} M; 4.23, 2.36×10^{-4} M, 1.4×10^{-8} M; 4.60, 1.91×10^{-4} M, 1.2×10^{-8} M; 5.01, 4.91×10^{-5} M, 2.2×10^{-8} M. Key: the same as for Figure 3.

will begin. This results in an observed rate constant that is too small. To prevent this complication, less than a molar equivalent of peroxide was added to allow for as much as a 20% error in determining the HRP concentration, and the absorbance at 411 nm was checked periodically to ensure no observed change due to HRP-I decay. If the molar absorptivity of $9.1 \times 10^5 \text{ M}^{-1} \text{ cm}^{-1}$ is indeed too small, then the calculated concentration of HRP is too large and the 0.8 molar equivalent peroxide added may be very close to a one molar equivalent. It was observed that small amounts of oxidizing agent in the water used to dilute the native enzyme preparation often caused small absorbance changes at 411 nm in an HRP-II preparation. This would suggest that the amount of peroxide added may be very close to the one molar equivalent limit. The situation was easily rectified by reducing the amount of peroxide and p-cresol added.

In the stopped-flow experiments a systematic deviation in reaction rates determined in successive experiments was observed in the acid region of pH. Apparently, this was due to interference from an acid-catalyzed reaction which occurred in the stopped-flow apparatus and competed for ferrocyanide. The slow decay in ferrocyanide concentration occurring in the apparatus somewhere between the driving syringes and the observation chamber resulted in a gradual decline in the observed reaction rates. An un-

changed signal amplitude indicated a reasonably stable concentration of HRP-II over this short time period. Following the initial 2 - 3 consecutive experiments, each successive trace had a progressively longer half-life and was not a duplicate of the trace immediately preceding it. An attempt to ensure fresh ferrocyanide solutions of the correct known concentration was made by thorough flushing of the instrument with the reactant solutions prior to each experiment. This resulted in reproducible data showing good first-order correlations in ferrocyanide. Interference from this competing reaction was also partially overcome by preparing HRP-II in the low pH buffer rather than making up the ferrocyanide solution in the acidic medium. Therefore, for the experiments below pH 6, the ferrocyanide solution was unbuffered prior to the final mixing of the reactants in the stopped-flow apparatus. Under these conditions, any enzyme denaturation in the acid solution was insignificant and did not affect the observed HRP-II ferrocyanide rates. Greater precision was attained at a given pH by doing many experiments at different ferrocyanide concentrations to ensure a good first-order response in ferrocyanide. Several such studies were performed at low pH. Below pH 4, this correlation was no longer linear and the investigations were terminated. Because these systematic errors were not detected in the previously reported work (Hasinoff and Dunford, 1970) the standard deviations for experiments

performed in the earlier investigation at low pH were much larger than originally estimated.

A major kinetic problem was encountered in one of the two stopped-flow apparatuses with which the ferrocyanide oxidation was investigated. Although no difficulty was observed for iodide (Roman *et al.*, 1971) or p-cresol oxidation (Critchlow and Dunford, 1972a), the reaction of HRP-II with ferrocyanide was zero order in the latter reactant. This problem was ultimately overcome by using an older, less sophisticated apparatus. A tentative explanation might be that ferrocyanide interacts with some component in the system to produce a highly reactive reducing agent which then reduces HRP-II preferentially. The same problem was encountered in the HRP-I-ferrocyanide study and in the investigation of lactoperoxidase compound II reduction by ferrocyanide (Maguire, unpublished results).

The resulting $\log k_{3\text{app}}$ *vs.* pH profile did not justify the inclusion of an acid dissociation constant with a pK_a of 5.2 as was reported previously (Hasinoff and Dunford, 1970). This was the case for HRP-II prepared from hydrogen peroxide as well as the two hydroperoxides. The steady-state data confirmed this conclusion and provided no evidence for the pK_a reported at 3.4 (Fig. 2.5). There was no evidence for any acid dissociation occurring on the enzyme or substrate over the pH range 5.0 - 3.2. Below pH 3.2 the formation of HRP-I became rate-limiting

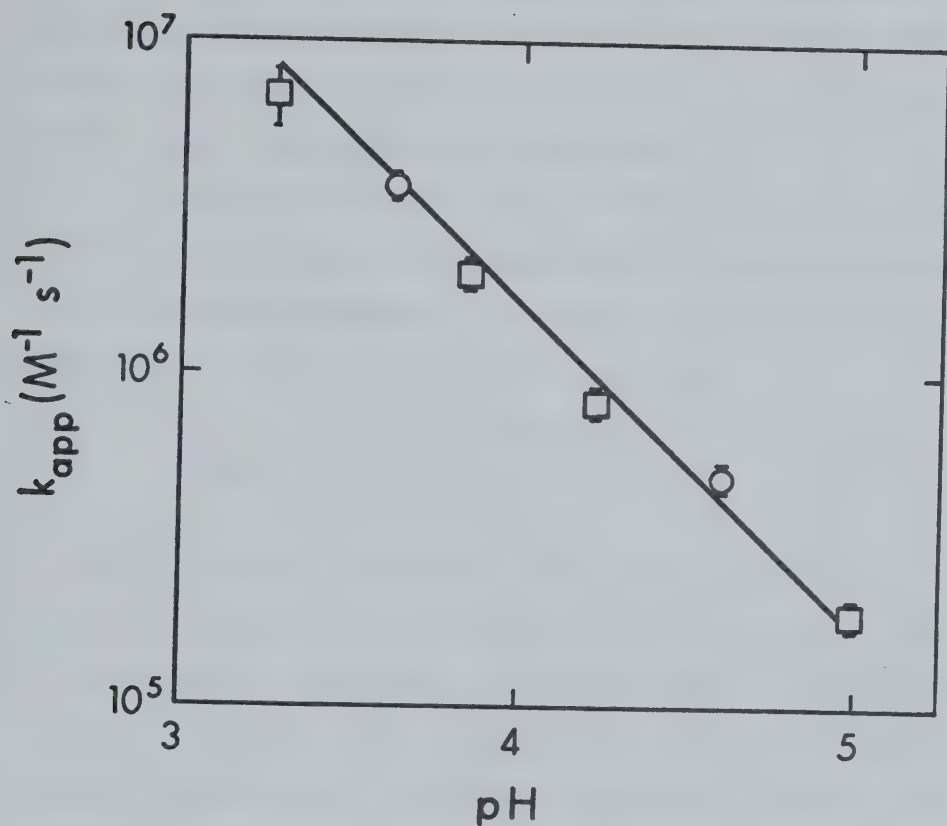


Fig. 2.5: Semilogarithmic plot of $k_{3\text{app}}$ determined by steady-state kinetics *vs.* pH for the HRP-II-ferrocyanide reaction. Error limits were estimated as the 95% confidence limit from the linear least-squares analysis at each pH. The correlation was obtained from a weighted nonlinear least-squares analysis of the data using the K_1^+ and K_2 values appearing in Table 2.3 as fixed parameters.
Key: the same as for Figure 2.3.

so that $k_{3\text{app}}$ could not be evaluated under steady-state conditions. The agreement among the rate constants using all three oxidizing substrates at high pH for HRP-II reduction with ferrocyanide is excellent.

The solid curves shown in Fig. 2.3 represent the best-fit correlations from a nonlinear least squares analysis. For the HRP-II-ferrocyanide reaction, a good fit was obtained using the phenomenological equation:

$$k_{3\text{app}} = \frac{A_1 [H^+] (1 + [H^+]/A_2)}{(1 + [H^+]/A_3)} \quad (2.1)$$

In order to assign kinetically meaningful parameters to the values determined for the variable parameters A_1 , A_2 and A_3 two different approaches have been used. One method was to attempt a prediction of a reaction scheme including all possible reactions of the various protonated forms of the enzyme and substrate. In such a scheme it was assumed that proton transfer is much faster than reactions between the enzyme and the reducing substrate. (Alberty and Bloomfield, 1968). One may derive an expression for the pH dependence of the apparent rate constant in terms of the rate constants and equilibrium dissociation constants of the proposed reaction scheme. The denominator will contain a term for each enzyme or substrate acid dissociation constant. Nonlinear analysis should permit the unambiguous determination of a quantitative value for each

equilibrium constant. In the case of k_{3app} for the HRP-II reduction, A_3 may be readily identified with the single acid dissociation assigned to the enzyme. The numerator usually consists of more complex terms and the parameters A_1 and A_2 are identified with clusters of constants, each of which cannot be determined unambiguously. An analysis of this type was performed for the alleged three acid dissociations observed for the HRP-II-ferrocyanide reaction and the single dissociation of the HRP-I-ferrocyanide reaction (Hasinoff and Dunford, 1970). These dissociation constants must necessarily refer to molecular rather than group ionizations. This is so because kinetics can observe only ionizations occurring on a molecular species but cannot distinguish the specific group at which ionization is occurring if two or more ionizable species are present. Therefore, in order for the value assigned to the specific parameters to be correct, the detailed mechanism initially assumed involving group ionization constants must first be correct. This problem has been discussed in detail by Roman (1972).

The second alternative involves transition-state theory and the assignment of inflections in the log rate-pH profile to ground-state and transition-state acid dissociation constants. The expression for the apparent rate constant's dependence on pH has the same terms in the denominator as in the first approach, but the clustered

parameters making up the terms of the numerator are now replaced by transition-state acid dissociation constants. The transition-state method has been derived elsewhere and its application to enzyme-catalyzed systems discussed in considerable detail (Critchlow and Dunford, (1972c)).

To demonstrate the application of transition-state theory to an analysis of the $\log k_{3\text{app}}$ vs. pH plot of the data, consider a hypothetical pH profile obtained if one were able to study the oxidation of ferrocyanide by HRP-II at very low and very high pH. At a sufficiently low pH all groups of the substrate and enzyme will be predominantly in their protonated forms. As a result, continuing to reduce the pH will produce infinitely small changes in the concentrations of these protonated forms and the reaction rate will appear independent of pH. Very small changes in the concentrations of the unprotonated forms at sufficiently high pH, necessarily, results in another pH independent region. If no further inflections in the curve occur in the pH regions which are not observable, except those required to satisfy these two limiting cases at the extremes of pH, the minimum pH profile will resemble Fig. 2.6. The broken line represents the assumed nature of the log rate-pH profile in the unobserved regions of pH.

The dependence of the apparent rate constant on pH may be treated in a way somewhat analogous to the depen-

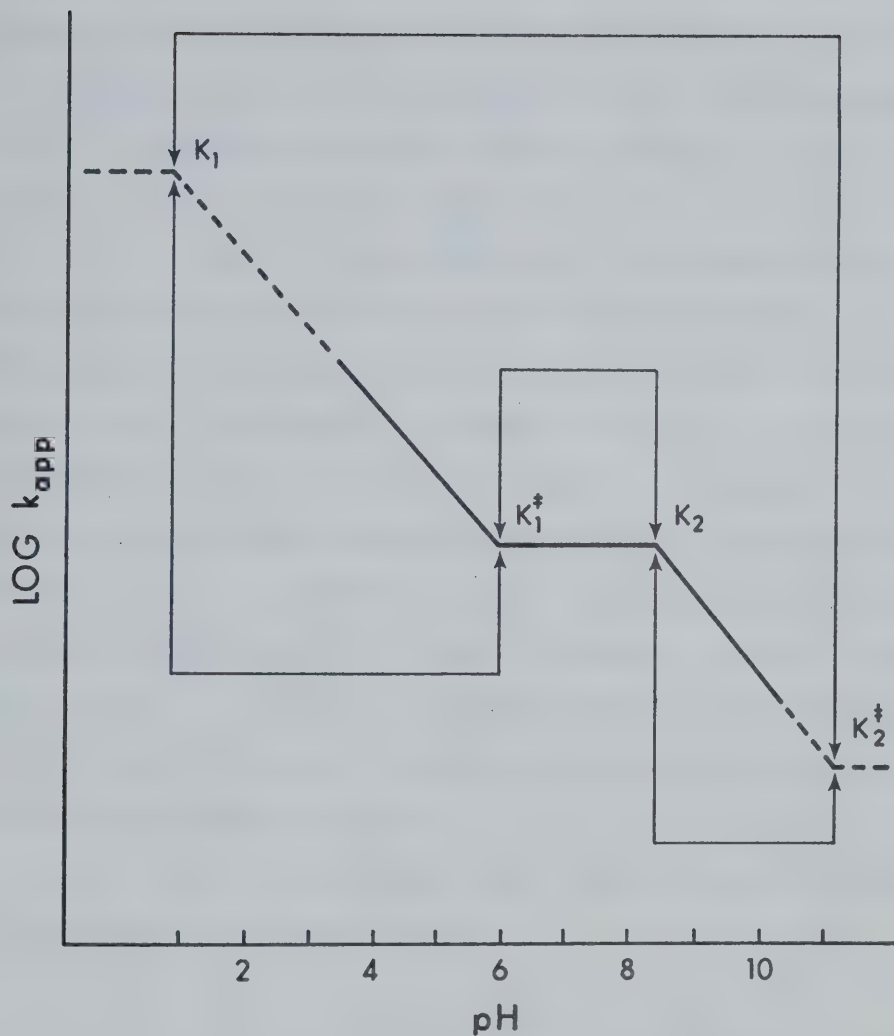


Fig. 2.6: Plot of $\log k_{3\text{app}}$ vs. pH for the HRP-II-ferrocyanide reaction shown schematically. The solid line represents the experimental curve and the broken line the unobservable hypothetical curve at the extremities of pH. The arrows shown above and below the curve represent the two possible pairing mechanisms assuming the curve may be described by a single mechanism over the entire range of pH.

dence on pH of the Michaelis-Menten association constant discussed by Dixon and Webb (1964). By a simple extension of the rules applying to the latter situation (Dixon, 1953), a unit change in slope of the curve (Fig. 2.6) may be related to either a transition-state acid dissociation constant if the change is negative or ground-state acid dissociation constant if the change is positive with decreasing pH. Beginning at highest pH in Fig. 2.6, a transition-state acid dissociation constant is implied at $\text{pH} > 11$ as the slope changes from 0 in the pH independent region to -1. A ground-state acid dissociation constant is encountered at $\text{pH} = 8.5$ with a positive change in slope from -1 to 0. This is followed by another transition state acid dissociation and, finally, by the ground-state acid dissociation implied at $\text{pH} < 2$.

The pH dependence of the apparent rate constant, then, takes the general form:

$$k = \frac{k'_3 \left(\dots \frac{K_i^{\ddagger}}{[H^+]} + 1 + \frac{[H^+]}{K_{i+1}^{\ddagger}} + \frac{[H^+]^2}{K_{i+2}^{\ddagger}} + \dots \right)}{\left(\dots \frac{K_i^E}{[H^+]} + 1 + \frac{[H^+]}{K_{i+1}^E} \dots \right) \left(\dots + \frac{K_i^S}{[H^+]} + 1 + \frac{[H^+]}{K_{i+1}^S} + \dots \right)} \quad (2.8)$$

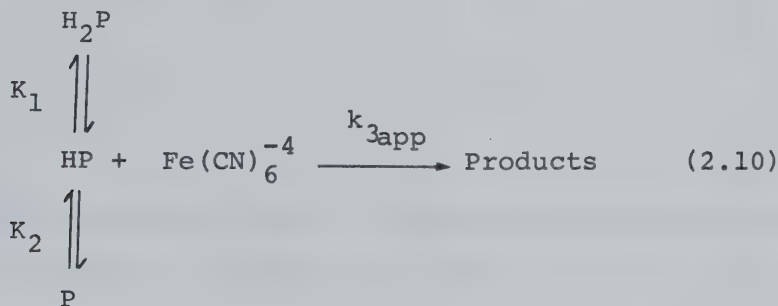
In this expression k'_3 is a pH independent rate constant, K_i^{\ddagger} the transition-state acid dissociation constant of the i th ionizable group and K_i^E , K_i^S refer to ground-state ionizations

occurring on the enzyme and substrate, respectively. For the proposed log rate-pH profile of Fig. 2.6 the transition-state approach leads to the following expression for $k_{3\text{app}}$:

$$k_{3\text{app}} = \frac{k'_3 \left(1 + \frac{[H^+]}{K_2^\ddagger} + \frac{[H^+]^2}{K_1^\ddagger K_2^\ddagger} \right)}{\left(1 + \frac{[H^+]}{K_2} + \frac{[H^+]^2}{K_1 K_2} \right)} \quad (2.9)$$

where K_2^\ddagger is the transition-state acid dissociation constant above a pH value of 11 and K_1^\ddagger the transition-state dissociation constant at neutral pH. In this case k'_3 refers to a pH-independent second-order rate constant at high pH. The two ionizable groups of the ground-state having a major kinetic effect are represented by the acid dissociation constants K_1 and K_2 . The ionization at a pK_a value of 8.5 (pK_2) has been assigned to a group on the enzyme since it cannot be associated with any of the protonated forms of ferrocyanide. The effect of this group has also been observed for the HRP-II oxidation of both p-cresol (Critchlow and Dunford, 1972a) and p-aminobenzoic acid (see Chapter 3). The assignment of the ionization associated with K_1 to a group on the enzyme is not clear from the HRP-II-ferrocyanide data alone. Several ionizations of ferrocyanide at pK_a values < 2 (Jordan and Ewing, 1962) would suggest that K_1 may be a substrate dissociation constant. However, it has been conclusively shown that an enzyme pK_a < 2 has

a major influence on the HRP-II-iodide reaction (Roman *et al.*, 1971). A similar kinetic response for p-amino-benzoic acid indicates that K_1 is very likely substrate independent; hence, it has been assigned to an enzyme ionization. The simplest mechanism which adequately describes the data is



where Fe(CN)_6^{-4} refers to all protonated and unprotonated forms of ferrocyanide and H_2P , HP and P represent the various protonated forms of the enzyme distinguishable kinetically.

The parameters estimated from the nonlinear least squares analysis (A_1 , A_2 , A_3 in Eq. 2.7) may be readily identified with the dissociation constants of Eq. 2.9. In the numerator the first term in parentheses makes a negligible contribution over the pH range 2 - 11, and may be ignored. The third term in parentheses in the denominator also makes a negligible contribution over the pH range studied since the effect of K_1 is not observed. As a result Eq. 2.9 simplifies to:

Table 2.3: The parameters obtained from a nonlinear least squares analysis for the HRP-II-Ferrocyanide reaction^a

$$k_3'/K_2^{\ddagger} = (1.8 \pm 0.1) \times 10^{11} \text{ M}^{-2}\text{s}^{-1}$$

$$K_1^{\ddagger} = (9.2 \pm 0.6) \times 10^{-7} \text{ M}$$

$$K_2 = (3.3 \pm 0.2) \times 10^{-9} \text{ M}$$

^aThe errors reported were the standard deviations obtained from the nonlinear computer analysis.

$$k_{3\text{app}} = \frac{\frac{k_3' [\text{H}^+]}{K_2^{\ddagger}} \left(1 + \frac{[\text{H}^+]}{K_1^{\ddagger}} \right)}{\left(1 + \frac{[\text{H}^+]}{K_2} \right)} \quad (2.11)$$

which is of the same form as Eq. 2.7. Results from the nonlinear least squares analysis of the data are tabulated in Table 2.3. The K_2 value reported here is in good agreement with the acid dissociation constant published earlier (Hasinoff and Dunford, 1970). The correlation of Fig. 2.5 was obtained from the steady-state data using the parameters of Table 2.3.

For a log rate-pH profile over the entire pH range including the unobservable rates at the pH extremities, such as is represented in Fig. 2.6, the number of ground-state and transition-state acid dissociations must be the same. In principle, all ionizable groups on both substrate and enzyme intermediate must be capable of protonation or deprotonation in the transition state at some hydrogen ion concentration. Each ground state ionization may then be identified with a transition state ionization. In general, pairing of the pK_a 's and pK_a^{\ddagger} 's leads to n different pairing schemes or $n!$ different mechanisms where n is the number of pK_a 's or pK_a^{\ddagger} 's in the log rate-pH profile. In a particular mechanism, if the pK_a^{\ddagger} value of a particular group is higher than the pK_a value to which it is paired then

protonation promotes the reaction. However, if the pK_a^{\ddagger} value is lower than its corresponding pK_a then deprotonation of this group promotes the reaction. The difference between the pK_a of a group in the ground state and its pK_a^{\ddagger} in the transition state is a measure of the extent to which proton transfer of this group affects the kinetics. The larger the $|pK_a - pK_a^{\ddagger}|$ the greater the sensitivity of the reaction rate to protonation. If there are one or more ionizable groups at or near the active site one may expect the reaction rates to be very sensitive to the extent of their protonation. However, for many ionizable groups of the protein well removed from the enzyme's active center, protonation may have no observable effect on the rates. Such insensitivity results when $pK_a^{\ddagger} = pK_a$. These considerations should allow one to discriminate between several possible pairing schemes and inductively arrive at the most rational mechanism.

The two possible mechanisms for the HRP-II-ferrocyanide reaction are shown as two pairing schemes, one above and the other below the curve of Fig. 2.6. First, let us consider the mechanism involving the pairing scheme in which K_1 is paired with K_2^{\ddagger} and K_2 with K_1^{\ddagger} . Such a mechanism describes an ionizable species having a $pK < 2$, the protonation of which has a very large accelerating effect on the rate ($|pK_1 - pK_2^{\ddagger}|$ is very large). Such a group probably would have to be a part of the porphyrin

ring or a group at the iron's fifth or sixth coordination position. Ionization influences the electronic configuration of the active site or aids in the bond-breaking step upon displacement of the bound species at the iron's sixth position of HRP-II. Protonation of the second ionizable group has a much smaller effect on the reaction rate. Since $pK_2 > pK_1^\ddagger$, protonation retards the reaction. Because of the apparent insensitivity of the reaction to the influence of the acid group corresponding to the latter pairing scheme it would be reasonable to assign such an ionization to a group on the protein located near the bound species at the sixth position.

Such a mechanism was postulated in an attempt to rationalize the difference in the log rate-pH profiles obtained for the HRP-II-ferrocyanide and the HRP-II-iodide reactions (Roman, 1972). In the latter case a slope of -1 was obtained with no inflections corresponding to pK_1^\ddagger or pK_2 . Roman (1972) suggested that the mechanism for the two reactions may differ only in the small effect resulting from an ionizable group on the protein lying very near the active site which influences the ferrocyanide but not the iodide oxidation. Since deprotonation of this group appears to promote the reaction, this would imply a base-catalyzed mechanism. This is in sharp contrast to the overall acid catalysis as indicated by the dominant negative unit slope in the log rate-pH profile. In order that all inflections

in the log rate-pH profile may be meaningfully assigned to dissociation constants either in the ground or transition state, a single acid-catalyzed mechanism must apply over the entire range of pH. Therefore, the effect of a neighbouring group must be by way of participation in the overall acid-catalyzed mechanism if a single mechanism is to apply. From electrostatic considerations, protonation of a neighbouring group should promote the approach of the large negative charge on the ferrocyanide anion. Inspection of Fig. 2.6 shows that a mechanism involving the pairing of K_2 and K_1^\ddagger necessarily implies that protonation of this group retards the rate by about two and one-half orders of magnitude. This is very difficult to rationalize. Again, this would suggest that such a mechanism should be discounted.

The second mechanism is a more acceptable alternative. The pairing of $K_1 - K_1^\ddagger$ and $K_2 - K_2^\ddagger$ implies that the reaction is influenced by two protonations both of which promote the reaction. This is essentially the mechanism proposed by Critchlow and Dunford (1972) discussed in considerable detail elsewhere. They view the acid-catalyzed reduction of HRP-II as occurring through a rate-determining electron-transfer step involving the displacement of a group occupying the iron's sixth co-ordination position as is shown schematically in Fig. 2.7. The transfer of a

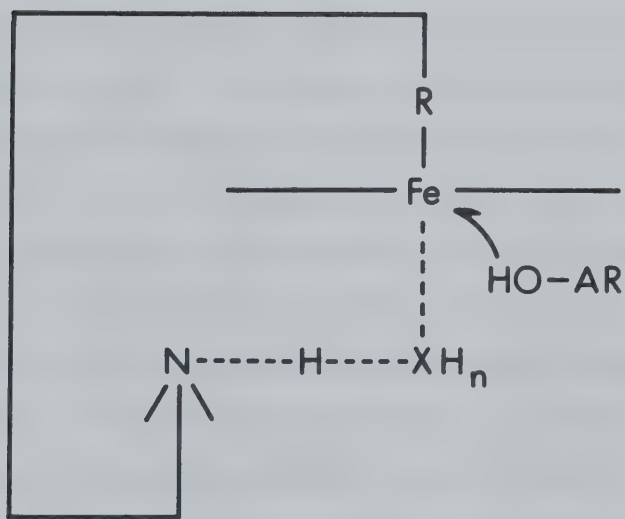


Fig. 2.7: The proposed mechanism for reaction of HRP-II with p-cresol shown schematically.

proton to this species, likely a hydroxyl group, may occur by two different processes. In an alkaline medium where hydrogen ion concentration is low, protonation occurs mainly through the participation of a neighbouring group. Protonation of the group at the sixth position, then, is a result of intramolecular proton transfer from the neighbouring distal group to the group about to be displaced. As the pH decreases in the alkaline medium, more and more of the distal group's acid form will be present to participate in the proton transfer process. The rate of HRP-II reduction shows an increase with decreasing pH until the distal group having a pK_a of 8.6 is completely in its acid form. At pH values below the pK_a of this group the log rate-pH profile exhibits a pH independent region. However, with a further decrease in pH, a second proton transfer process becomes significant. The group at the sixth position is capable of being protonated by hydrogen ions from the acid medium. Therefore, the rate of reaction is no longer pH independent and a unit negative slope develops in the acid pH region of the log rate-pH profile as the pH decreases further.

Although several ionizable groups may be present which are potentially capable of influencing the electronic configuration of the porphyrin ring, it is very reasonable to postulate that a nucleophilic displacement of the bound species at the iron's sixth position is sensitive to pro-

tonation of the species being displaced. Protonation greatly enhances its ability to function as a leaving group in much the same fashion as protonation of a hydroxyl group in the acid-catalyzed esterification of primary alcohols. The mechanism as proposed by Critchlow and Dunford (1972), necessarily implies a strategically situated ionizable group having a pK_a of 8.6 in the environment of the active site. There is little evidence, to date, for the existence of this distal species in the vicinity of the active site.

Both of these mechanisms described by the pairing schemes of Fig. 2.6 assume that the effect of pH on the reaction rate may be described by one mechanism affecting the rate-determining step over the entire range of pH. Of course, this may or may not be the case. Consideration of Fig. 2.6 might suggest a third alternative involving two independent acid-catalyzed mechanisms. An attempt to depict two possible overlapping mechanisms is shown in Fig. 2.8. The pK_1^{\ddagger} is now not kinetically observable. The negative change in slope occurring at pH = 6 is a result of the change in mechanism and is not interpreted in terms of a transition-state acid dissociation. As with the second mechanism described above, this scheme implies that two ionizations affect the reaction rate, both promoting the reaction upon protonation. The critical difference between the second and third proposal is that the rate-determining

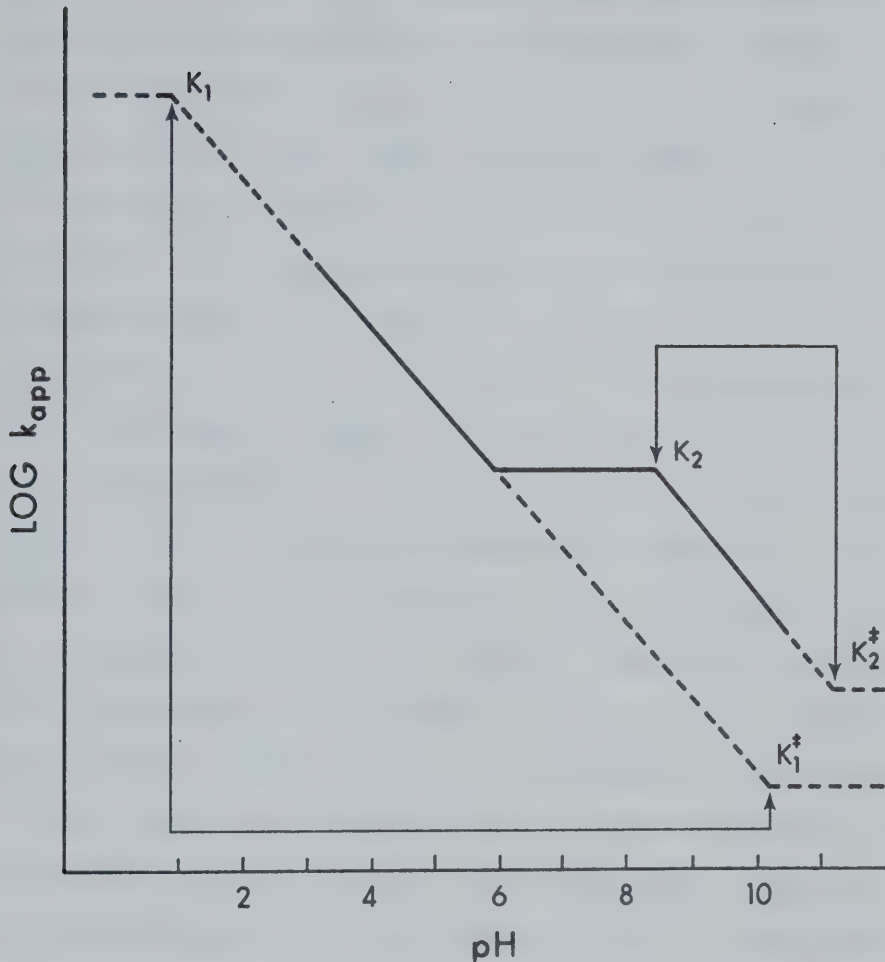


Fig. 2.8: Plot of $\log k_{\text{app}}$ vs. pH for the HRP-II-ferro-cyanide reaction showing, schematically, the possibility of two overlapping mechanisms each involving a single ionization. The solid line represents the experimental curve, whereas the broken line represents the unobservable hypothetical portions. The only possible pairing mechanism for each ionization is shown by arrows.

step is influenced by protonation of a single group in the former case rather than by two independent ionizations. If two independent ionizable groups are to influence the rate-determining step, then they most likely will affect the electronic structure of the heme. Such groups may be identified with an ionization at the sixth position, an ionizable group on the heme, or, possibly, one located on the residue at the fifth position. If two such groups exist, the ensuing change in the electronic configuration upon their ionization should be observable in the native enzyme as well as its two intermediate compounds. Until recently, only one such ionization had been known for the native enzyme of $pK_a = 11$. However, temperature dependent E.S.R. investigations of Tamura and Hori (1972) provide rather strong evidence for two ionizations. The reduction of HRP-II with p-aminobenzoic acid, also, is probably best described in terms of such a dual mechanism. However, a detailed discussion of this mechanism will be postponed until the kinetics of p-aminobenzoic acid oxidation is considered in Chapter 3.

Kinetics of HRP-I Ferrocyanide Reaction:

Values for the k_{2app} calculated from Eq. 2.5 are tabulated in Table 2.4 and plotted in Fig. 2.3 for both oxidizing substrates. Problems encountered in the study of HRP-I in the acid region of pH were similar to those discussed for HRP-II. The fast rates of the HRP-I-

Table 2.4: The second order rate constant determined for the HRP-I-Ferrocyanide reaction at 25° and $\mu = 0.11$

pH ^a	$k_{2app} (M^{-1}s^{-1})^b$	Buffer ^c	Oxidizing Substrate ^d
4.78	$(7.3 \pm 2.2) \times 10^6$	A	E
4.97	$(7.5 \pm 1.4) \times 10^6$	A	M
5.38 ^e	$(5.3 \pm 0.3) \times 10^6$	CA	M
5.48	$(4.1 \pm 0.8) \times 10^6$	A	E
5.73	$(3.0 \pm 0.4) \times 10^6$	A	M
5.94	$(1.9 \pm 0.4) \times 10^6$	P	E
6.12 ^e	$(2.3 \pm 0.1) \times 10^6$	P	E
6.23 ^e	$(1.6 \pm 0.1) \times 10^6$	P	M
6.43	$(1.2 \pm 0.1) \times 10^6$	CA	E
6.61	$(1.1 \pm 0.1) \times 10^6$	P	M
6.93	$(9.1 \pm 0.1) \times 10^5$	P	E
7.14	$(7.5 \pm 0.8) \times 10^5$	P	M
7.34	$(7.5 \pm 1.2) \times 10^5$	P	E
7.50 ^e	$(6.8 \pm 0.3) \times 10^5$	T	M
7.62	$(6.3 \pm 1.2) \times 10^5$	P	M
7.98	$(6.1 \pm 0.6) \times 10^5$	T	E
8.57	$(5.5 \pm 1.4) \times 10^5$	T	E
8.99 ^e	$(6.1 \pm 0.3) \times 10^5$	T	E
9.75	$(5.9 \pm 0.9) \times 10^5$	C	M

(Table continued on next page)

Table 2.4 continued

pH ^a	$k_{2\text{app}} (\text{M}^{-1}\text{s}^{-1})^{\text{b}}$	Buffer ^c	Oxidizing Substrate ^d
9.98	$(6.0 \pm 0.6) \times 10^5$	T	E
10.63	$(3.3 \pm 0.6) \times 10^5$	C	M

^{a,b,c,d}The same as in Table 2.1

^eStudy of $k_{2\text{obs}}$ vs. $[\text{Fe}(\text{CN})_6^{4-}]$ from which $k_{2\text{app}}$ was calculated from the slope of a linear least-squares analysis.

ferrocyanide reaction made tests of Eqs. 2.3 and 2.5 very difficult at low pH. As a result, the data obtained below pH = 5 have large experimental errors and the pH profile could not be defined readily below pH = 4.8 using the stopped-flow technique. The steady-state method is not amenable to an estimate of the $k_{2\text{app}}$ because $k_{2\text{app}}$ is at least an order of magnitude faster than $k_{3\text{app}}$, the rate constant for the rate-controlling step.

The HRP-I-ferrocyanide reaction kinetics may be best considered in terms of transition-state theory in a manner completely analogous to the HRP-II-ferrocyanide reaction. The simplest hypothetical log rate-pH profile is sketched in Fig. 2.9 with the dotted areas designating the unobservable extremities of pH. The one possible pairing mechanism for this proposed pH profile is also shown. This mechanism involves a single enzyme ground-state ionization having a dissociation constant K_3 and a transition-state dissociation constant K_3^\ddagger . Protonation of this group promotes the reaction as in the case of HRP-II reduction; one may calculate $k_{2\text{app}}$ from the relationship:

$$k_{2\text{app}} = \frac{k'_2 ([\text{H}^+]/K_3^\ddagger + 1)}{([\text{H}^+]/K_3 + 1)} \quad (2.12)$$

In this expression k'_2 is the pH independent limiting second order rate constant at high pH. Results from the nonlinear least-squares analysis of the data are given in Table 2.5.

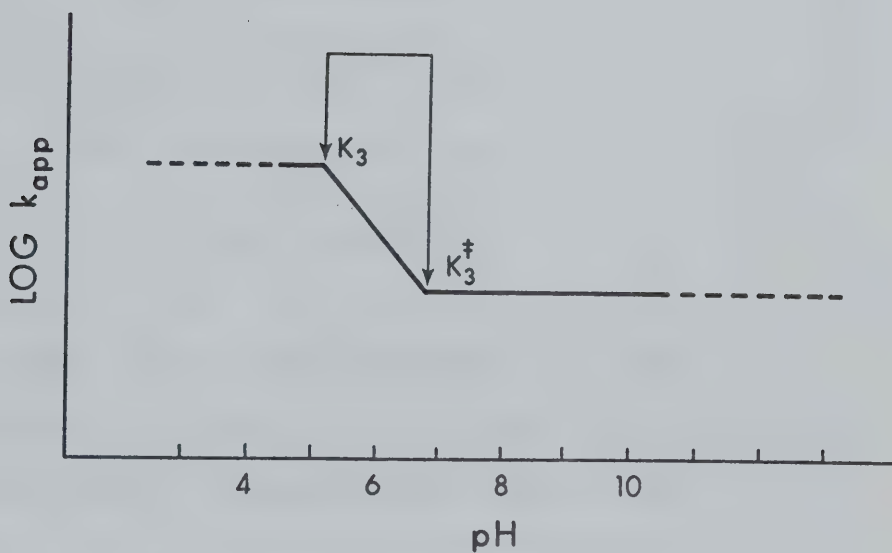


Fig. 2.9: Plot of $\log k_{2\text{app}}$ vs. pH shown schematically for the HRP-I-ferrocyanide reaction. The solid line represents the experimental curve, whereas the broken line represents the unobservable hypothetical curve at extremities of pH. The only possible pairing mechanism is also shown.

Table 2.5: The parameters obtained from nonlinear least-squares analysis for the HRP-I-ferrocyanide reaction^a

$$k_2' = (6.0 \pm 0.2) \times 10^5 \text{ M}^{-1}\text{s}^{-1}$$

$$K_3^\ddagger = (2.5 \pm 0.2) \times 10^{-7} \text{ M}$$

$$K_3 = (4.2 \pm 0.8) \times 10^{-6} \text{ M}$$

$$k_2'^b = (6.0 \pm 0.2) \times 10^5 \text{ M}^{-1}\text{s}^{-1}$$

$$K_3^{\ddagger b} = (4.0 \pm 0.6) \times 10^{-7} \text{ M}$$

$$K_3^b = (4.9 \pm 1.6) \times 10^{-6} \text{ M}$$

^aThe errors reported were estimated as in Table 2.3

^bFrom previously reported data for HRP-II prepared from hydrogen peroxide (Hasinoff and Dunford, 1970).

For purposes of comparison the data reported earlier for the HRP-I reaction prepared from hydrogen peroxide (Hasinoff and Dunford, 1970) were reanalyzed in terms of transition-state theory. These also appear in Table 2.5. The two sets of best-fit parameters are identical within experimental error.

The mechanism for HRP-I reduction is very similar to that for HRP-II reduction. There is one major difference. The HRP-I reduction is influenced by only one ground state ionization. The pK_a of any group associated with the heme will be shifted to lower pK_a values with increasing positive charge at the active site. Therefore the ionization of HRP-I at $pK_3 = 5.3$ may be due to the same ionizable group which has an ionization with $pK_a = 8.5$ in HRP-II since HRP-I has one more oxidizing equivalent than HRP-II. It is rather difficult to explain the shift of $pK_1 < 2$ to $pK_3 = 5.3$ with increasing positive charge. Hence, of the two ionizations influencing the HRP-II reaction, it is probable that only the ionizable group associated with a $pK_2 = 8.5$ in the HRP-II reaction affects the HRP-I reaction with an observed $pK_3 = 5.3$.

Results published earlier for the HRP-I-ferrocyanide reaction (Hasinoff and Dunford, 1970) for $pH < 5$ were interpreted in terms of an additional pK_a^{\ddagger} at about 4. This would suggest an additional $pK_a < 2$. However, such an interpretation is based upon two experiments performed

at pH ~ 4 where the reaction rate was very fast and the ferrocyanide system was known to be unstable. It is difficult to weight these two experimental values very heavily. The data obtained for the HRP-I-p-aminobenzoic acid would appear not to justify the inclusion of any further parameters beyond those of Fig. 2.9. Although the possibility that the ionization associated with the $pK_1 < 2$ in HRP-II reduction affecting the HRP-I reaction cannot be ruled out, it would appear that the pH profile for the HRP-I-ferrocyanide reaction has only one major ground-state ionization.

2.4 Discussion

The evidence presented above indicates that the proton-transfer mechanisms involved in the reduction of HRP-I and HRP-II by ferrocyanide are identical, over a wide range of pH, regardless of the organic hydroperoxide used as oxidizing substrate. The two ionizable groups previously identified in the acid region of pH for HRP-II reduction, when hydrogen peroxide was used as oxidizing substrate, do not appear to be significant when the experimental errors are considered carefully. This implies that the same mechanism is operable no matter what the oxidizing agent. In each case the active site must be structurally the same.

Recently, O^{18} labelling studies (Hager *et al.*, 1972) in compound I formation from chloroperoxidase and product studies from HRP-I formation (Schonbaum and Lo,

1972) provide rather strong evidence for the incorporation of a single oxygen atom of the oxidizing substrate upon formation of the intermediate compounds. These results, together with the experimental data presented here, would suggest an O-O bond cleavage on HRP-I formation with the oxygen-containing organic fragment functioning as the leaving group. It is probable that the OH group is retained at the sixth co-ordination position in HRP-I. Reduction of this intermediate compound involves the abstraction of an electron from the reducing substrate with the OH group being retained at the active site in HRP-II. Protonation of a group which is integrally involved with the heme's electronic environment would be expected to accelerate the electron-transfer process. The slower reduction of HRP-II must involve not only an electron-transfer, but also the displacement of the OH group. Protonation of this group obviously will enhance the required transfer of electronic charge to the oxygen in the bond-breaking step leaving a weakly co-ordinated water molecule in the sixth position of the native enzyme. Such a model is compatible with recent studies (Moss *et al.*, 1969; Dolphin *et al.*, 1971; Felton *et al.*, 1971) which indicate that quadrivalent iron is present in both HRP-I and HRP-II but the former shows characteristics typical of π -cation radicals. This suggests that HRP-I reduction results from charge transfer to the porphyrin ring but HRP-II reduction involves charge transfer

to the iron upon Fe-O bond cleavage.

CHAPTER 3

AROMATIC AMINE PEROXIDATION CATALYZED BY
HORSERADISH PEROXIDASE

3.1 Introduction

The proton-transfer mechanisms for the peroxidase-catalyzed reactions of compounds I and II with several inorganic reducing agents (Hasinoff and Dunford, 1970; Roman; 1972) as well as for the reaction of HRP-II with p-cresol (Critchlow and Dunford, 1972a) have been investigated. The characteristics of the pH dependence of the reaction rates were different for each substrate. This would suggest that either more than one mechanism is operative, or each substrate may interact in a unique manner with a sterically restrictive active site. A further study by Critchlow and Dunford (1972b) has attempted to explain the observed kinetics for HRP-II reduction with iodide, ferrocyanide and p-cresol in terms of a single mechanism involving an intramolecular proton transfer. However, no information was available concerning HRP-II reduction with the aromatic amines, a major class of organic substrates.

In order to determine whether proton-transfer mechanisms were similar for the oxidation of aromatic amines and phenols, p-aminobenzoic acid (PABA) was chosen as a representative of amine reducing substrates. PABA has long been implicated as a bacterial growth factor. It is one of the raw materials used for the biosynthesis of

folic acid. Lipmann (1941) was one of the first to report the oxidation of PABA by HRP. Under steady-state conditions, he observed the development of a red colour which he attributed to a rather complex mixture of oxidation products. Saunders *et al.*, (1964), Saunders and Stark (1967), Holland and Saunders (1969, 1971) and Holland *et al.*, (1969) have studied the oxidation products of a variety of substituted anilines, and Chance (1951) has reported rate constants for aniline and PABA at pH of 7. Little evidence has been published regarding the mechanism of the initial reaction in amine oxidation.

PABA was readily available in the neutral form and as the potassium salt, a white crystalline solid containing < 1% impurity. The potassium salt, being readily soluble in water, made the preparation of solutions much easier. The reported rates at pH = 7 (Chance, 1951) indicated that the reaction was slow enough to permit the study of both HRP-I and HRP-II reduction. Since the oxidation of p-cresol exhibited kinetics which were nonlinear with increasing substrate concentration, and a substrate interaction with native HRP had been reported for aniline (Critchlow and Dunford, 1972a), a slow rate of reaction was desirable to allow the characterization of the kinetics over a wide range of substrate concentration. The protonation of the carboxyl group at the position para to the amino group enhances its electron-withdrawing effect. A study of the

dependence of the rate on pH in the vicinity of the pK_a of the substrate carboxyl group should provide information about substituent effects.

3.2 Experimental

Materials:

HRP was obtained from Boehringer-Mannheim as a highly purified ammonium sulphate suspension. It was dialyzed, filtered and assayed as described in Chapter 2.

PABA, both as the free acid and as its potassium salt, were obtained from Sigma Chemical Company as Crystalline 99+% Grade 1-P. The molar absorptivity at pH = 7.6 was determined from the absorbance at 265 nm and found to be within 1% of the literature value of $1.45 \times 10^4 \text{ M}^{-1} \text{ cm}^{-1}$ (Rekker and Nauta, 1956). The substrate was observed spectrophotometrically at 265 nm in typical buffered solutions of ionic strength 0.11 over the entire pH and concentration range of the study and found to be stable, having molar absorptivities similar to those published. NMR analysis showed no spectral anomalies.

Water was distilled from alkaline potassium permanganate, then redistilled. The H_2O_2 was stored as described previously. Reagent grade aniline from Allied Chemical and USP sodium benzoate from Fisher Scientific were used without further purification. The concentrations of these reagents and PABA were monitored spectrophotometrically in phosphate buffer (pH = 7.6) with the following

molar absorptivities: PABA, $\epsilon_{265}^{25} = 1.45 \times 10^4 \text{ M}^{-1} \text{ cm}^{-1}$, aniline, $\epsilon_{281}^{25} = 1.37 \times 10^3 \text{ M}^{-1} \text{ cm}^{-1}$ (Lang, 1971), sodium benzoate $\epsilon_{270}^{25} = 6.0 \times 10^3 \text{ M}^{-1} \text{ cm}^{-1}$ (Perkampus *et al.*, 1971).

Stopped-Flow Experiments:

The techniques used in stopped-flow experiments have been described in Chapter 2. The PABA investigations were performed using comparable methods. The reduction of HRP-II was followed at 425 nm and HRP-I reduction at 411 nm. At low pH values the rates for reduction of the two intermediate compounds of HRP were similar. With substantial amounts of both HRP-I and HRP-II in solution, kinetics typical of two pseudo-first-order reactions occurring in series were obtained at 425 nm (Frost and Pearson, 1961). This would be expected if HRP-I was reduced through two one-electron transfers rather than a single two electron transfer as occurs in the oxidation of iodide (Roman and Dunford, 1972). As a result, it was imperative to insure that no HRP-I was present when observing the HRP-II reduction. This was accomplished by monitoring the reaction at 411 nm on the stopped-flow apparatus prior to each set of experiments. Since HRP and HRP-II are isobestic at this wavelength no change in absorbance should be observed. A narrow band pass was insured by using a slit width of <0.2 mm. Unlike the HRP-II reduction where interference from HRP-I decay may be eliminated by converting HRP-I entirely to HRP-II, in the HRP-I reduction

HRP-II is formed as a product. The presence of HRP-II cannot be eliminated, but the contribution to the observed absorbance change due to the decay of HRP-II may be minimized to a point where it is insignificant. This is not a major consideration if the rates at which these two intermediates are reduced are well separated in time. However if these rates are approximately the same, it becomes important to experimentally define the wavelength at which HRP and HRP-II are isosbestic (~411 nm). To establish this wavelength precisely, the monochromatic light source was set to obtain no change in absorbance for an HRP-HRP-II mixture. One was assured, then, that the absorbance change resulting from product decay was not significant. The HRP-HRP-II mixture was removed from the feed syringe, an enzyme preparation containing largely HRP-I was added, the instrument flushed and the resulting stopped-flow traces monitored for any given PABA concentration.

The potassium salt rather than the free acid of PABA was used because the latter dissolved much more easily. Both were found to give the same kinetic results. The PABA aqueous stock solutions were stored in the dark to prevent spontaneous oxidation. Although it was found that solutions stored for several days produced kinetic results similar to those from freshly prepared solutions, PABA solutions were prepared prior to each day's experiments as a precaution. Use of the PABA potassium salt in acid solutions often

required an adjustment of pH prior to each set of experiments. This was particularly true for studies involving the dependence of the observed rate constant on PABA concentration. Over the large concentration range used it was difficult to buffer the solution adequately and, at the same time, avoid buffer effects. As a result the buffer's ionic strength contribution was always maintained at 0.01 and the pH of the solution containing the PABA, buffer and nitrate was adjusted to a constant pH value by the addition of microliter quantities of 1M nitric acid. The total ionic strength was always maintained at 0.11. Whenever ionic strength contributions from the nitric acid or the PABA were significant (>2%) appropriate adjustments were made in the KNO_3 concentration. Immediately following each set of experiments the pH of the solution was measured with an Orion pH meter in conjunction with a Fisher combination electrode.

Reactions, conducted at 25°C, had half-times from 5 milliseconds to several seconds. The PABA was always at least in ten-fold excess over the HRP intermediate compound insuring pseudo-first-order conditions. The resulting absorbance changes were normally <0.04 absorbance units; hence, observed voltage changes could be regarded as proportional to the change in absorbance (see Appendix 1). An average rate constant with standard deviation was obtained from 8 to 12 traces for each set of conditions.

The Order of Reaction with Respect to HRP-II:

The order of the reaction with respect to HRP-II when the reaction proceeds slowly (half-times > 1 min.) was observed to deviate significantly from unity. This investigation was carried out on the Cary-14 spectrophotometer with a 0 - 0.1 absorbance slide wire. The method used to observe the slow decay of HRP-II was identical to that described from the HRP-II-ferrocyanide reaction at high pH.

The pK_a Values for PABA:

Under conditions comparable to those of the kinetic experiments ($\mu = 0.11$, temperature 25°C) the two ionization constants of PABA were determined spectrophotometrically on the Cary-14. The pH, maintained by buffers in which the reaction had been investigated, was measured for each sample directly in the cuvette using a Fisher combination microprobe electrode. The sample contained PABA at a total concentration of 10^{-4} M. Both sample and reference solutions contained 0.1 M potassium nitrate and buffer ($\mu = 0.01$). Absorbance measurements were made at 265 nm, the wavelength at which the spectrum appeared most sensitive to the changing concentrations of the three states of ionization of PABA. The system was investigated at 31 different pH values from 9.37 to 1.40. The curve obtained when the absorbance was plotted against pH was analyzed using a nonlinear least-squares program in terms of two

pK_a values.

Binding to Native HRP:

Absorbance changes upon the addition of PABA to a buffered solution of the native enzyme were studied spectrophotometrically over the range 380 - 440 nm on the Cary-14 spectrophotometer. These equilibrium experiments were normally conducted at pH = 5.0 using acetate buffer. All solutions were maintained at a total ionic strength of 0.11 by suitable adjustments in the KNO₃ concentration. Because the spectral changes were generally < 5%, a 0 - 0.1 absorbance slide wire was used and the absorbance change observed by difference spectroscopy. Typically, 10⁻⁵ M HRP solutions were pipetted as 2 ml aliquots into both sample and reference cuvettes. To each cuvette was added 10⁻⁶ M p-cresol. This was too low a concentration to affect the HRP spectrum but insured that any intermediate HRP compounds, possibly formed from the inadvertent introduction of oxidizing agent, were promptly reduced. A predetermined amount of PABA was added to the sample cuvette with a micro-syringe followed by a similar addition of distilled water to both the reference and sample to bring the total volume to 2.2 mls. The solutions were stirred with a Teflon plumper. The pH was measured directly in the cuvette after obtaining the difference spectrum with the use of a micro-probe electrode. Similar studies were performed using benzoic acid and aniline.

Steady-State Experiments:

The steady-state investigation used techniques identical with those already described for the ferrocyanide study. The rates were monitored at 265 nm for PABA concentrations $< 10^{-4}$ M and at 320 nm at higher PABA concentrations. Experiments were performed in carbonate buffer ($\mu = 0.01$) with 0.1 M KNO_3 making the total ionic strength 0.11. The initial horseradish peroxidase concentration $[\text{HRP}]_0$, was 7.4×10^{-7} M, with $[\text{H}_2\text{O}_2]_0 = 6.3 \times 10^{-6}$ M and $[\text{PABA}]_0 = 5 \times 10^{-5}$ M to 1.3×10^{-4} M at 265 nm, and up to 5×10^{-4} M at 320 nm.

3.3 Results

The pK_a Values for PABA:

The dependence of absorbance on pH for three different states of ionization of the same chemical species may be shown to be (see Appendix 3):

$$A = \frac{\left(\frac{\epsilon_{\text{H}_2\text{B}} [\text{H}^+]}{K_{1s} K_{2s}} + \frac{\epsilon_{\text{HB}} [\text{H}^+]}{K_{1s}} + \epsilon_{\text{B}} \right) [\text{B}]_0}{\frac{[\text{H}^+]}{K_{1s} K_{2s}} + \frac{[\text{H}^+]}{K_{1s}} + 1} \quad (3.1)$$

where A is the absorbance at a given hydrogen ion concentration, $\epsilon_{\text{H}_2\text{B}}$, ϵ_{HB} and ϵ_{B} the molar absorptivities for the three ionizable species, $[\text{B}]_0$ the total substrate concentration and K_{1s} , K_{2s} the two dissociation constants. The

data obtained are shown in Fig. 3.1 with the best-fit curve obtained from the nonlinear least-squares analysis using the molar absorptivity of the species in alkaline solution (ϵ_B) of $1.45 \times 10^4 \text{ M}^{-1} \text{ cm}^{-1}$. The molar absorptivity for the neutral species (ϵ_{HB}) was estimated at $(9.78 \pm 0.08) \times 10^3 \text{ M}^{-1} \text{ cm}^{-1}$. For the fully protonated form ϵ_{H_2B} was calculated to be $(3.2 \pm 0.3) \times 10^2 \text{ M}^{-1} \text{ cm}^{-1}$. The values of K_{1s} and K_{2s} were estimated at $(1.68 \pm 0.08) \times 10^{-5} \text{ M}$ and $(3.54 \pm 0.30) \times 10^{-3} \text{ M}$. The value for the protonation of the amino group is less well defined than that for protonation of the carboxyl because of the inability to work in the low pH region where this group is completely protonated. The pK_a values $pK_{1s} = 4.77 \pm 0.02$ (carboxyl) and $pK_2 = 2.45 \pm 0.04$ (amino) are in good agreement with those determined potentiometrically (Albert and Goldacre, 1942; Lumme, 1957). The spectrophotometric results of Robinson and Biggs (1957) (see Ref. 208) are also in agreement and verify the proposed group assignments.

The Order of the Reaction in HRP-II:

The simple exponential traces usually obtained from stopped-flow kinetics below pH = 7 demonstrated that the reaction was first-order in HRP-II. The rate constant was determined from the voltage changes observed for each trace using a nonlinear least-squares program. A typical semilogarithmic plot obtained at pH = 5.17 in acetate buffer is shown in Fig. 3.2. With a small excess of PABA (PABA concentrations in 10~100 fold excess of HRP) the slow

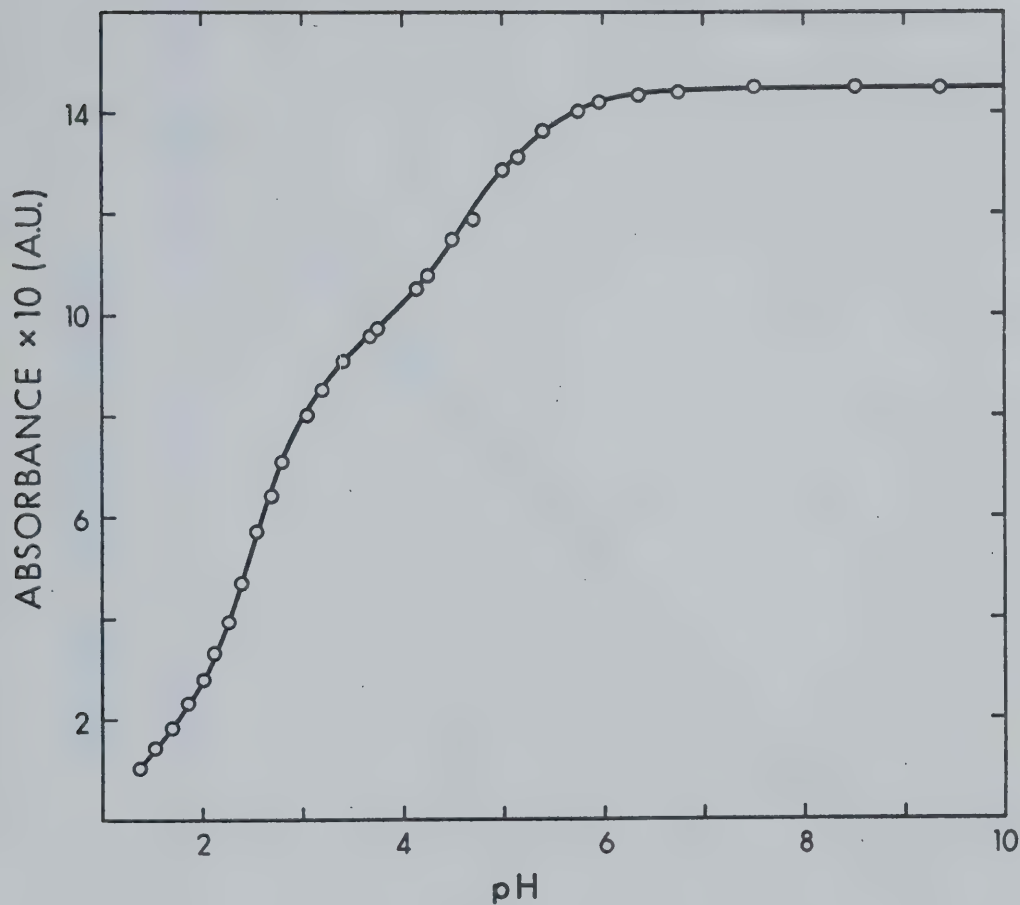


Fig. 3.1: Plot of absorbance *vs.* pH for PABA at 10^{-4} M in buffer solutions of total ionic strength 0.11 (25°C). The curve represents the nonlinear best-fit to Eq. 3.1. Parameters from the statistical analysis are to be found in the text. The pK_a values of 4.77 ± 0.02 for the carboxyl and 2.45 ± 0.04 for the amino group were obtained. The errors representing the standard deviations from the analysis.

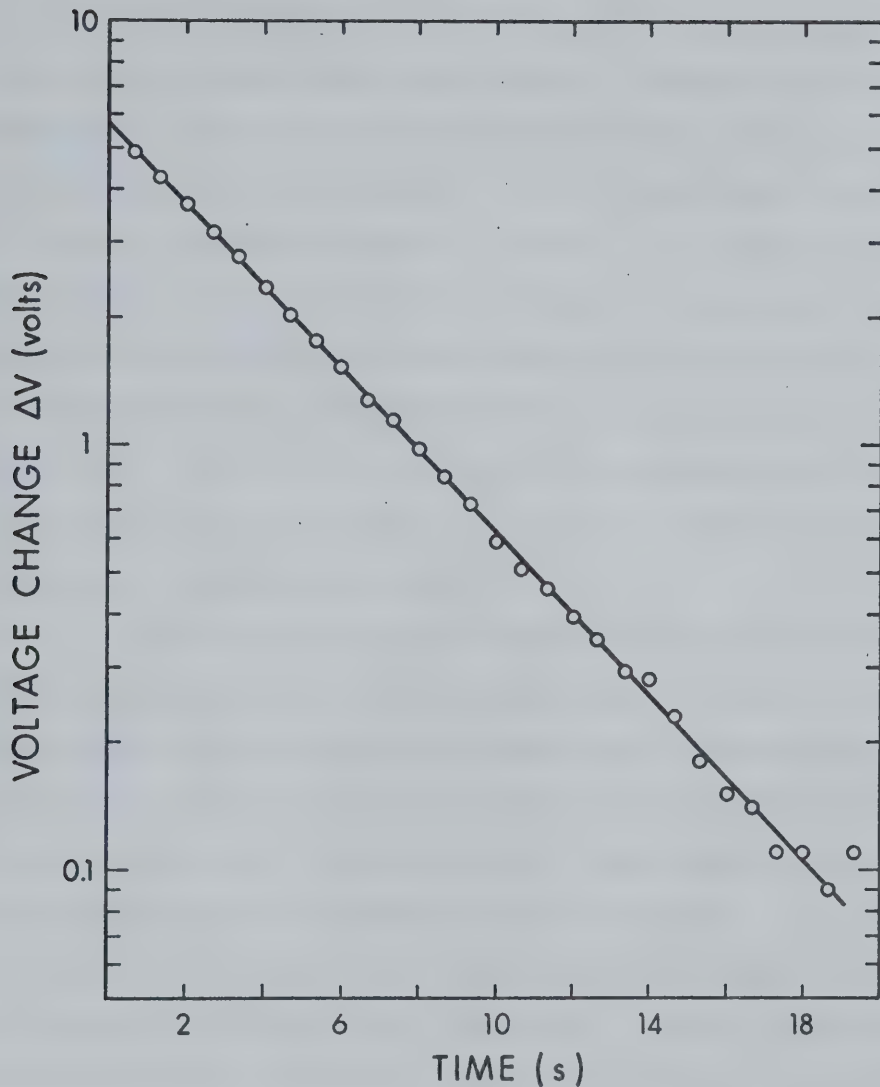


Fig. 3.2: Semilogarithmic plot of the voltage change, Δv , against time for the HRP-II reduction with PABA at pH = 5.17 in acetate buffer. This experiment was performed on the stopped-flow apparatus for $[PABA] = 10^{-4} M$ and $[HRP-II]_0 \sim 8 \times 10^{-7} M$ at a wavelength of 425 nm.

rate of HRP-II reduction at alkaline pH values can be studied on the Cary spectrophotometer. However, under such conditions, the reaction showed significant deviations from a pseudo-first-order response. A semilogarithmic plot of the data obtained at pH = 7.08 (Fig. 3.3) illustrates the nature of the observed log absorbance change (ΔA) *vs.* time trace at 425 nm and PABA concentration of 2×10^{-5} M. An identical response was observed over the Soret spectral region 390 - 440 nm. Therefore, it is unlikely that such a reaction trace is a result of another, spectrally distinguishable, intermediate of HRP.

The data of Fig. 3.3 suggest two parallel first-order reactions as a possible explanation. Similar deviations from the expected first-order rate law have been observed in the hydrolysis of diethyl-t-butyl-carbinyl chloride (Brown and Fletcher, 1949). The observed departure from first-order kinetics may be treated in an analogous fashion for HRP-II reduction by PABA (see Appendix 4 for a detailed mathematical treatment). Such a treatment implies that the HRP intermediate may be reduced to HRP by way of two parallel pseudo-first-order reactions which probably provides the simplest explanation of the results:



This would suggest that either two spectrally indistinguish-

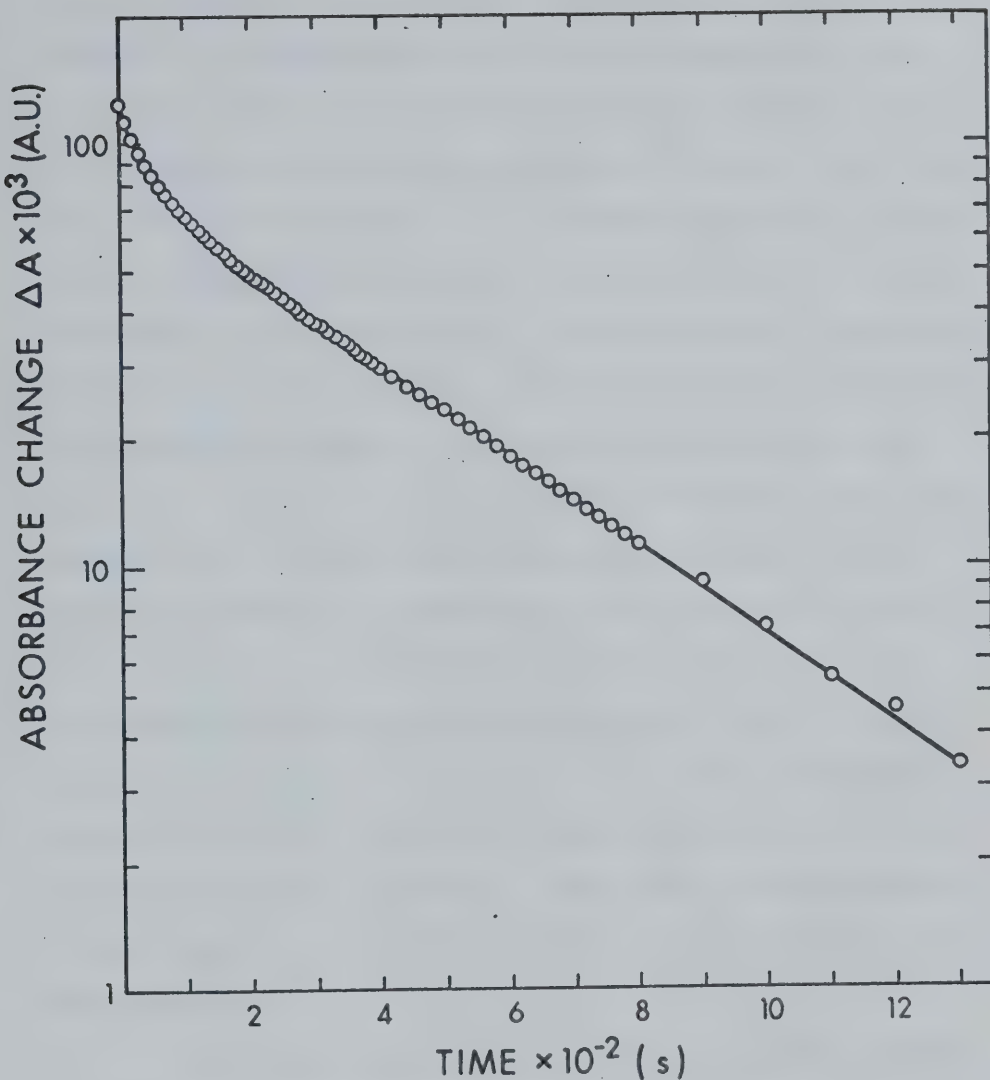


Fig. 3.3: Semilogarithmic plot of absorbance change at 425 nm against time for HRP-II reduction with $[PABA] = 2 \times 10^{-5} M$, pH = 7.08, phosphate buffer. This experiment was performed on the Cary 14 spectrophotometer.

able but kinetically different forms of HRP-II exist or that HRP-II is reduced by two different species. The kinetic parameters of each reaction may be determined by first analyzing the linear portion that occurs after the first half-time of Fig. 3.3. In this region only one of the reactions predominates and the system may be treated as a simple first-order case. Extrapolation of the linear best-fit line to zero time, then, allows one to calculate the absorbance change in the initial phase due to this reaction. As a result, the absorbance change due to the simultaneous reaction which contributes significantly initially (causing the deviation from linearity) may be determined. This calculated absorbance change for the simultaneous reaction is plotted against time in a semi-logarithmic fashion in Fig. 3.4. The linear response is a positive test for the pseudo-first-order nature of the interfering initial reaction. From these considerations, the data appear to fit the proposal of two parallel first-order reactions.

Although the separation of the initial curvature and the final linear portion of the curve becomes less well defined above PABA concentrations of 10^{-4} M, an attempt to study both reactions over the substrate concentration range 2×10^{-5} M - 2×10^{-4} M resulted in reproducible traces similar to that of Fig. 3.3. The dependence of the rate on substrate concentration is shown in Fig. 3.5 for

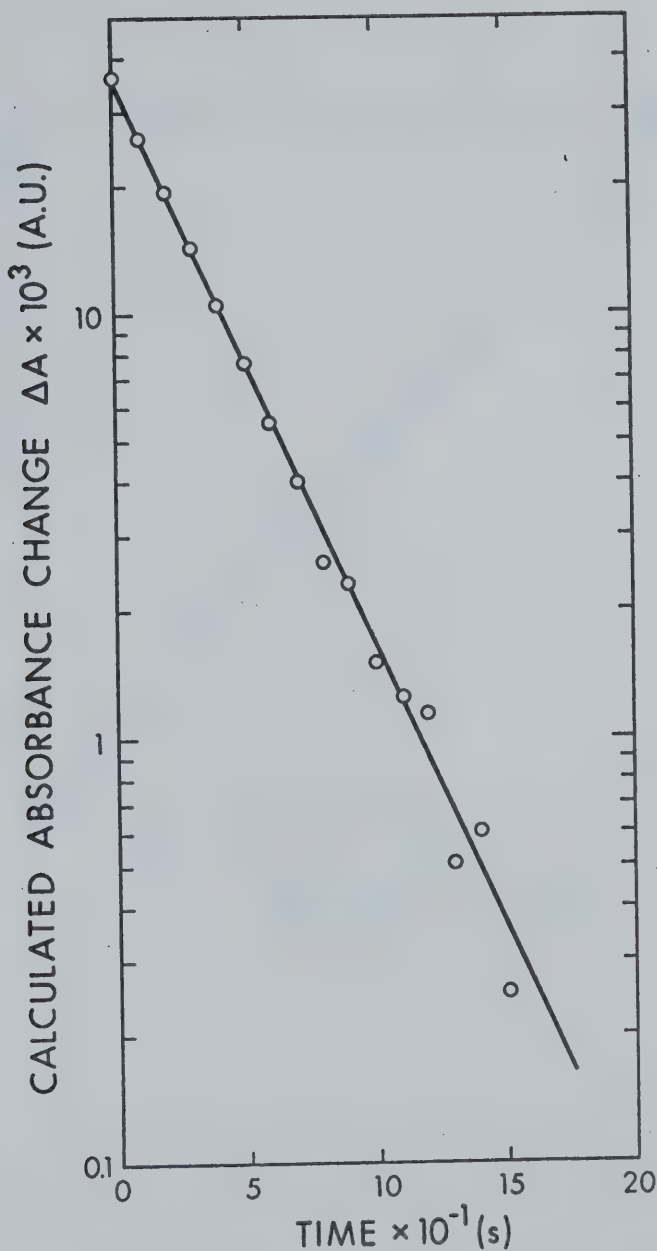


Fig. 3.4: Semilogarithmic plot of the calculated absorbance change *vs.* time for the observed deviation from linearity in the initial portion of the plot in Fig. 3.3. The results conform to the first-order rate law.

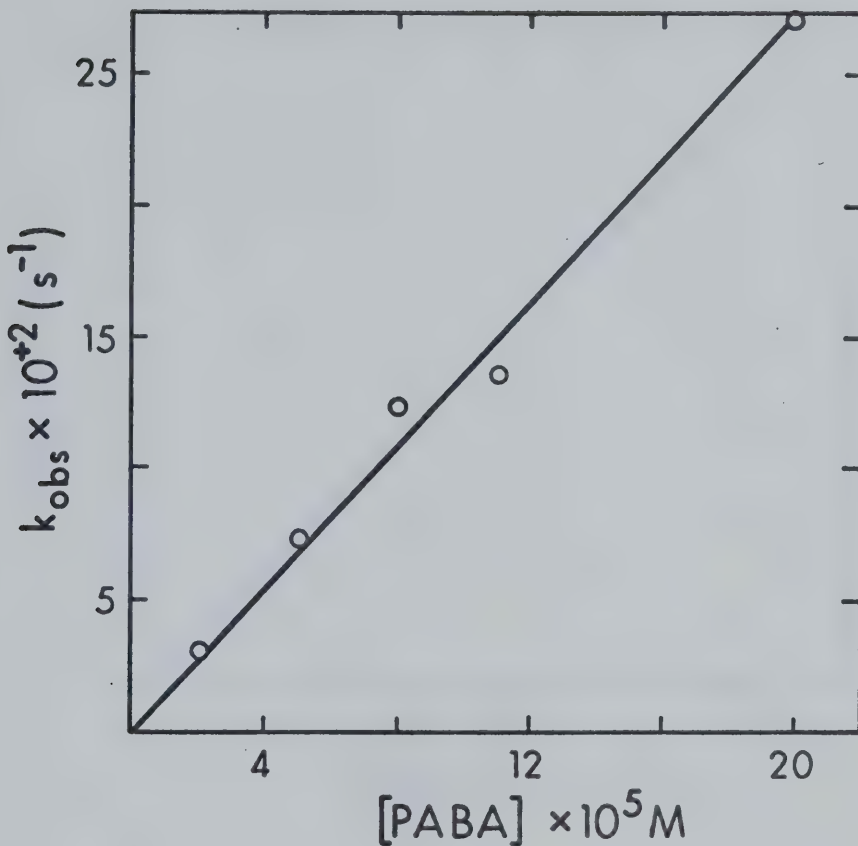


Fig. 3.5: Plot of the k_{obs} vs. $[PABA]$ for the first-order initial reaction proposed for typical kinetic responses such as Fig. 3.3 (pH = 7.08, phosphate buffer). The apparent second-order rate constant calculated from the slope is $1.35 \times 10^3 M^{-1} sec^{-1}$

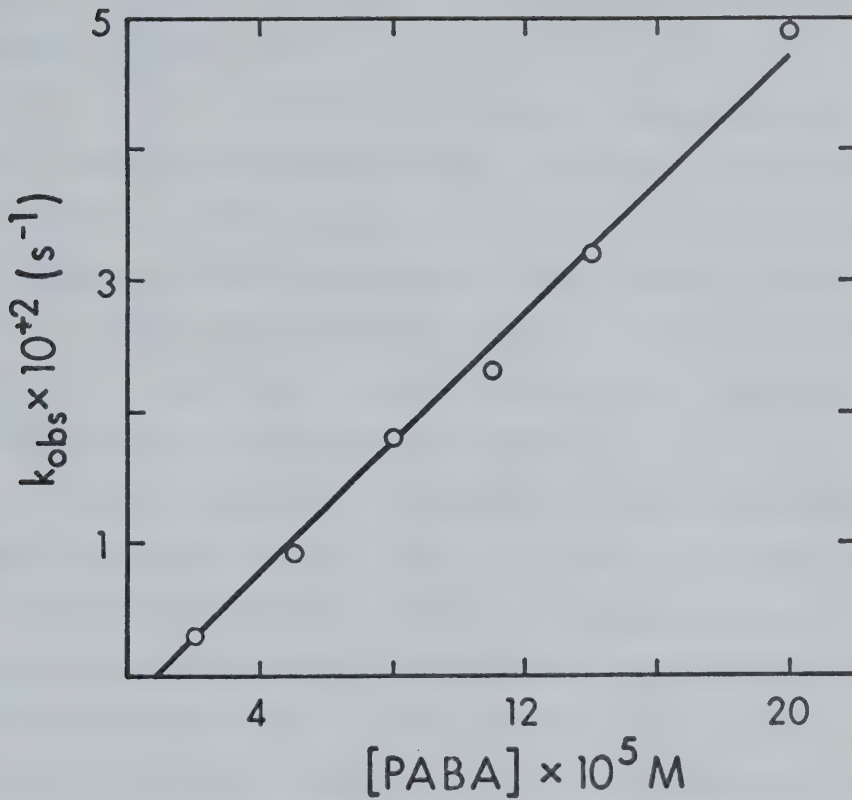


Fig. 3.6: Plot of the k_{obs} vs. $[PABA]$ for the final linear portion of the reaction trace typified by Fig. 3.3 (pH = 7.08, phosphate buffer). The apparent second-order rate constant determined from the slope is $2.35 \times 10^2 M^{-1} sec^{-1}$

the initially dominant reaction and in Fig. 3.6 for the finally dominant reaction. The correlations shown in both figures indicate that the rate constants of Eqs. 3.2 and 3.3 are linearly dependent on substrate concentration. The small negative intercept of Fig. 3.5 may be a manifestation of deviations from linearity caused by the slow accumulation of reaction products absorbing in this spectral region.

The proposed reaction scheme for the reduction of HRP-II by PABA, which involves two parallel first-order reactions, may be interpreted in several ways. If the native enzyme preparation consisted of two kinetically different isoenzymes of HRP such as the acid form, HRP(I) and the neutral form, HRP(III) (using the nomenclature of Stigbrand and Paul (1970) which is not to be confused with the designations HRP-I or HRP-III for the intermediate compounds) present in about equal concentrations, one would expect a kinetic response similar to that just described. One would predict that the observed deviation from overall first-order kinetics in the initial time interval should be independent of substrate concentration and the deviation should be clearly defined at high concentrations. Fig. 3.7 is a semilogarithmic plot of the voltage change *vs.* time observed on the stopped-flow apparatus for HRP-II reduction in phosphate buffer ($\text{pH} = 7.10$) at an initial concentration of 3×10^{-3} M PABA. No significant deviation from the first-order rate law was observed. Traces similar to those

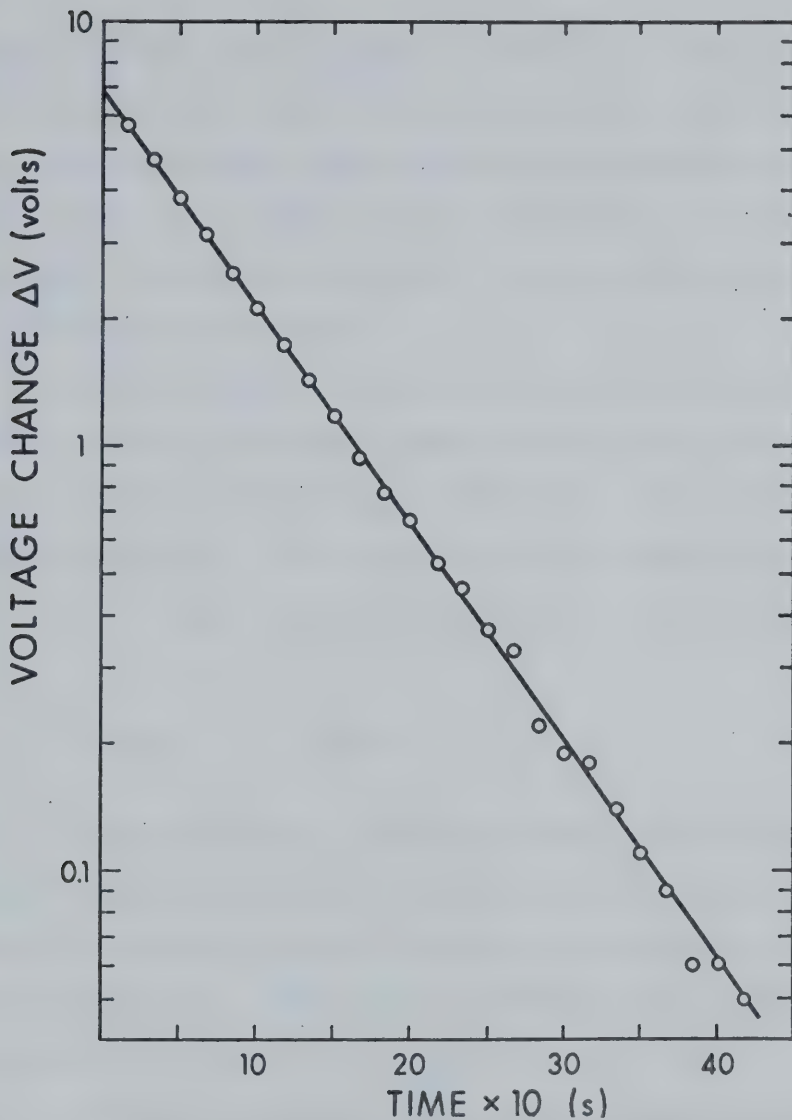


Fig. 3.7: Semilogarithmic plot of the voltage change *vs.* time for HRP-II reduction on the stopped-flow apparatus by $[PABA] = 3 \times 10^{-3}$ M ($pH = 7.10$, phosphate buffer). The linearity of this trace is in sharp contrast to Fig. 3.3 obtained at lower $[PABA]$. The apparent second-order rate constant from this experiment was calculated to be $k_{3app} = (4.00 \pm 0.05) \times 10^2 \text{ M}^{-1} \text{ sec}^{-1}$.

obtained on the Cary-14 spectrophotometer at PABA concentrations of about 2×10^{-4} M were obtained using the stopped-flow technique, which indicated that the psuedo-first-order response was not a result of the different experimental technique. Therefore, a mixture of HRP isoenzymes is not an adequate explanation.

If the PABA contained small amounts of a reactive impurity which reacted much faster with HRP-II, then, a kinetic anomaly dependent upon substrate concentration might be expected. This would lead to a second-order rate law for the initial reaction and Eq. 3.2 would be replaced by:



where i is the impurity. With increasing substrate concentration, the concentration of the reacting impurity would gradually increase until it became large compared to the HRP concentration. Under such conditions the kinetic response of Fig. 3.7 would be expected.

That this may not be the case is indicated by the observation that the initial reaction always appears to satisfy a first-order rate law. However, the response of the system to successive additions of hydrogen peroxide provides the most convincing evidence that an impurity cannot account for the observed kinetics for these experiments. On the Cary 14 spectrometer 0.8 molar equivalent hydrogen

peroxide and 0.4 molar equivalents of p-cresol were added simultaneously to a buffered solution of native HRP containing a 10 molar excess of PABA. Prior to the initial response of the instrument, the peroxide formed HRP-I which rapidly decayed to HRP-II upon reduction with p-cresol. The HRP-II then reacted with PABA to give the typical kinetic response of Fig. 3.3. If the initial non-linear portion were attributable to an impurity, then, following the complete decay of HRP-II to HRP, a second addition of peroxide and p-cresol should give a good first-order linear response since all the impurity would have reacted. However, upon five successive additions of peroxide and p-cresol, the observed kinetics were unchanged from those of the first turnover of the enzyme. Thus, a highly reactive impurity cannot be responsible for the observed deviations from the first-order rate law.

The apparent second-order rate constant calculated from Fig. 3.5 and Fig. 3.6 are not in agreement with that of Fig. 3.7. Instead, the rate of high substrate concentration (Fig. 3.7) is approximately the same as that obtained from the initial slope of Fig. 3.3. This suggests an alternative mechanism. Instead of the parallel reactions of Eqs. 3.2 and 3.3, a more likely possibility is the sequential mechanism



These consecutive reactions imply that HRP-II reacts initially with PABA, and that the products formed alter the activity of the enzyme intermediate. The results obtained upon successive addition of peroxide and p-cresol, described earlier, would indicate that, if HRP-II interacts with product, this product species must be transient in nature. This is suggestive of a free radical interaction occurring during the first half-life. Examination of Fig. 3.3 shows that, on reduction of half the HRP-II, sufficient free radicals have been produced to alter the remaining enzyme intermediate's activity. Therefore, as a tentative proposal let us consider a mechanism involving a type of product inhibition:



where P. represents the initial free radical formed on PABA oxidation and PROD. the products resulting from P. reacting with PABA. The radicals, PROD. and P., may undergo further reactions with substrate or other product species in the usual free radical chain propagation and termination reactions.

When $k' [\text{HRP II}] > k_p [\text{PABA}]$ the log ΔA vs. time traces

exhibit a distinct initial curvature which is concave to the time axis. With increasing [PABA] this curvature is extended into the linear portion until reaction 3.6 dominates. A pseudo-first-order kinetic response will be observed when $k' [HRP-II] \ll k_{3app} [PABA]$. This mechanism is the only one of those discussed which has the merit of offering a reasonable explanation consistent with all the observations.

At sufficiently low pH with excess PABA, the reduction of HRP-II conformed to the pseudo-first-order rate law (Fig. 3.2) and disappearance of HRP-II may be expressed as:

$$\frac{-d[HRP-II]}{dt} = k_{3obs} [HRP-II] \quad (3.10)$$

The same rate law applies in the alkaline region of pH at sufficiently large excess of PABA. A similar kinetic response was also observed for the HRP-I suggesting that the same arguments would apply. However, this reaction was not well documented. At the faster rates, it was not possible to study the reaction on the Cary spectrophotometer.

The Order of the Reaction with Respect to Substrate:

In the alkaline region of pH the oxidation of PABA by HRP-II was studied over a wide range of substrate concentration (up to 10^{-2} M). At PABA concentrations in

sufficient excess for eq. 3.10 to apply, the system showed good linear responses when k_{obs} was plotted against the PABA concentration. These kinetics may be described by:

$$k_{3obs} = k_{3app} [PABA] \quad (3.11)$$

Such a correlation is shown in Fig. 3.8 at pH = 6.15 in cacodylic acid buffer. The rate measured at $[PABA] = 10^{-2}$ M (not plotted in Fig. 3.8) of $k_{obs} = 4.92 \text{ sec}^{-1}$ demonstrated a pseudo-first-order response over a concentration range of two orders of magnitude. Although small positive intercepts were encountered below pH = 6, they were never greater than 0.3 sec^{-1} . Similar results were obtained in the case of ferrocyanide and p-cresol oxidation by HRP-II. These small intercepts are believed to be attributable to small amounts of reducing agent inadvertently introduced as impurity.

At pH values < 5, a nonlinear response was observed in the k_{3obs} vs. [PABA] plots. This is readily apparent from the data at pH = 4.17 in acetate buffer shown in Fig. 3.9. This kinetic response was studied over the range of pH from 2.4 to 5.0. The investigation was necessarily terminated at pH = 2.4 because the rapid rates did not permit one to determine the rate constants over a large enough range of substrate concentrations. Above pH = 5.01 excessively concentrated solutions of substrate ($< 5 \times 10^{-2}$ M) were required to define accurately the dependence of k_{obs}

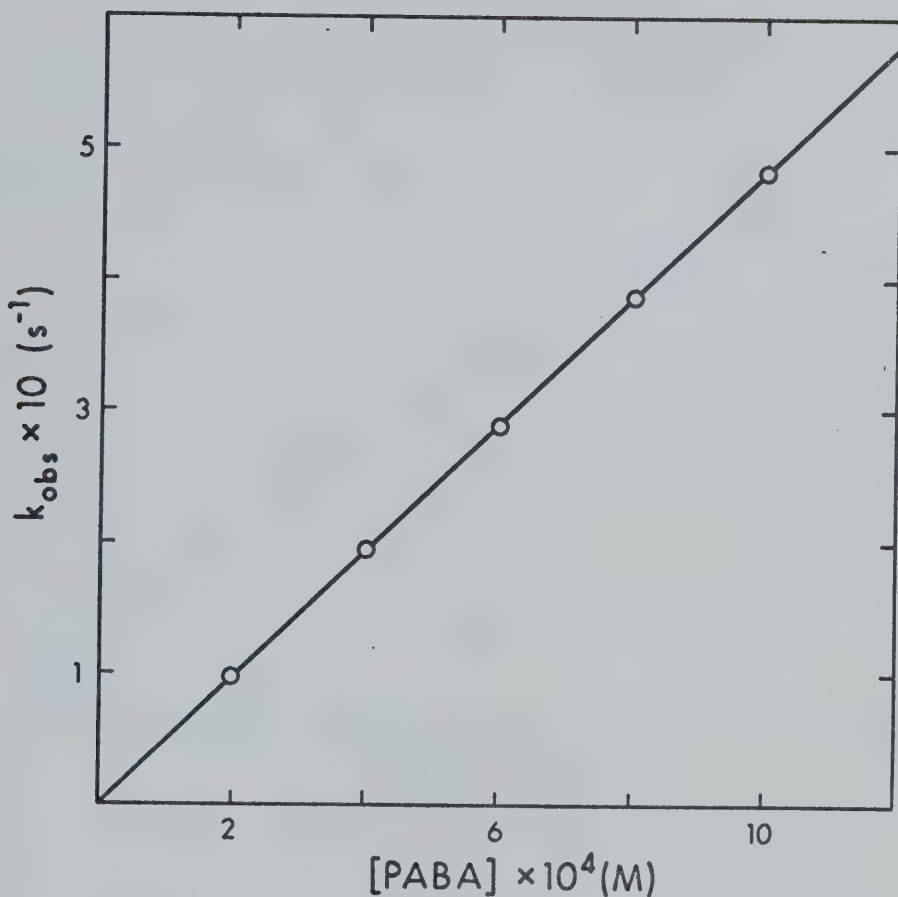


Fig. 3.8: Plot of the pseudo-first-order rate constant against [PABA] for the stopped-flow experimental results obtained at pH = 6.15 in cacodylic acid buffer. The good linear response demonstrates that the reaction, under these conditions, is first order in PABA.

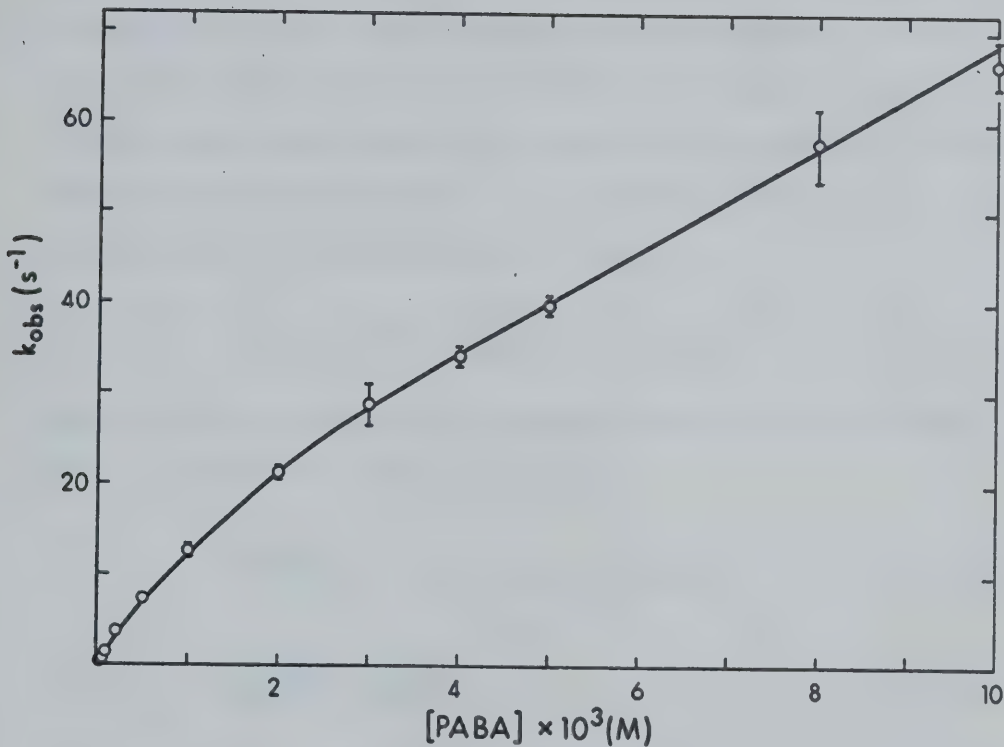


Fig. 3.9: A plot of the observed pseudo-first-order rate constant, k_{obs} , against $[\text{PABA}]$ for HRP-II reduction at pH = 4.17, acetate buffer. The nonlinear response illustrates the deviation from first-order behaviour in PABA. The error bars are the standard deviations calculated from experimental traces at each set of conditions.

on substrate concentration.

This nonlinear response of the k_{obs} with increasing PABA concentration behaviour may be described by a binding interaction between the two reactants. The simplest mechanism one might consider is the Michaelis-Menten case where substrate binds to the enzyme in a rapid equilibrium step to form an enzyme-substrate complex which then reacts in a unimolecular slow step:



where K_M is the Michaelis constant and k_3 a first-order rate constant. For this mechanism

$$\frac{-d[\text{HRP-II}]}{dt} = k_3 [\text{HRP-II-PABA}] \quad (3.13)$$

$$\text{Since } K_M = \frac{[\text{HRP-II}][\text{PABA}]}{[\text{HRP-II-PABA}]} \quad (3.14)$$

$$\text{and } [\text{HRP-II}]_0 = [\text{HRP-II}] + [\text{HRP-II-PABA}] \quad (3.15)$$

where $[\text{HRP-II}]_0$ is the concentration of the enzyme intermediate prior to mixing with PABA, then substitution of eqs. 3.14 and 3.15 into eq. 3.13 demonstrates that:

$$k_{3\text{obs}} = \frac{k_3 [\text{PABA}]}{K_M + [\text{PABA}]} \quad (3.16)$$

One would predict a hyperbolic curve when k_{obs} is plotted against [PABA]. A saturation effect occurring at high sub-

strate concentration causes the observed rate to become independent of substrate concentration. The data of Fig. 3.9 show no such saturation effect. The Lineweaver-Burk plot of the data in Fig. 3.9 is shown in Fig. 3.10. The straight line represents the linear correlation estimated from the data at low substrate concentration. All of the data are not plotted in Fig. 3.10 to allow suitable expansion of the co-ordinates in order to demonstrate the systematic deviation from linearity at high PABA concentrations. The marked nonlinearity of Fig. 3.10 illustrates the inadequacy of the Michaelis-Menten mechanism as a model for the observed kinetics.

The linear dependence of rate on PABA concentration at high substrate concentrations suggests a reaction of an enzyme-substrate complex with an additional molecule of PABA (see Fig. 3.9). Reaction of such an enzyme-substrate intermediate would be first-order in substrate.

That is:



where the $k_{4\text{app}}$ is a pH dependent second-order rate constant. Because of the two linear portions of the k_{obs} vs. [PABA] plot, two reactions that are first-order in substrate are indicated. The simplest mechanism involving an enzyme-substrate interaction which adequately describes these results is:

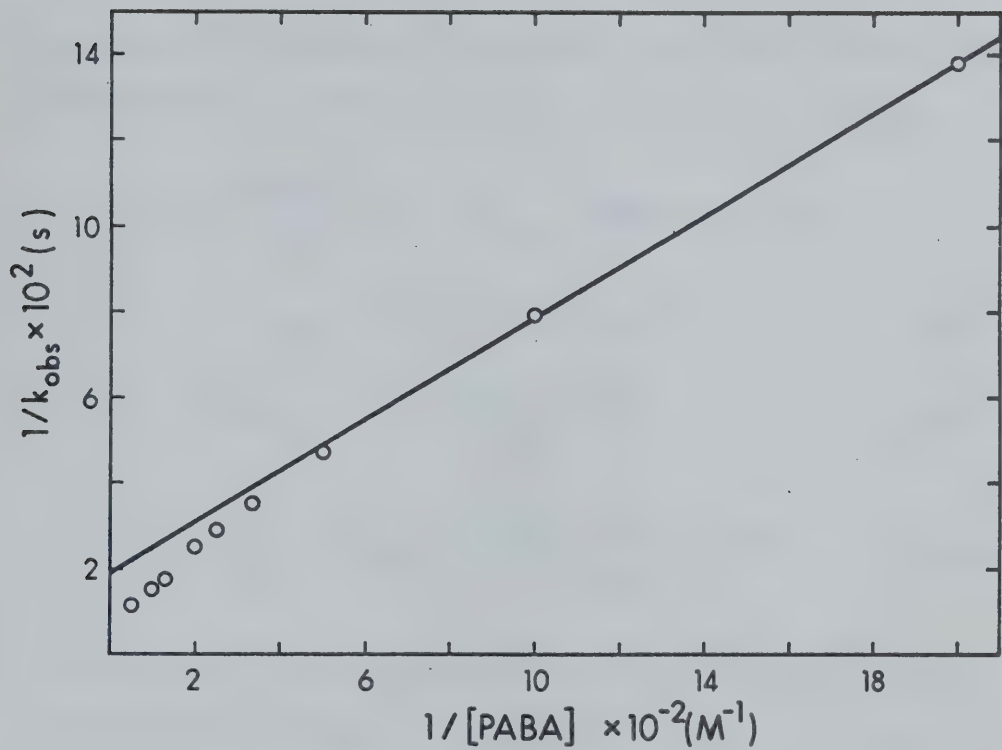
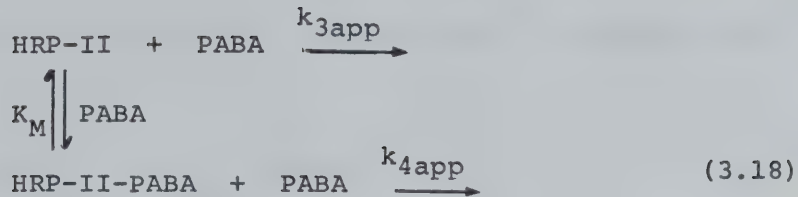


Fig. 3.10: Lineweaver-Burk plot of the data of Fig. 3.9. The linear correlation shown has been estimated from the data at lower substrate concentration. The expanded scale of the co-ordinates does not allow all data to be plotted but does indicate the deviation from simple Michaelis-Menten kinetics.



In a manner completely analogous to the simple Michaelis-Menten case, an expression may be derived for the k_{obs} :

$$\frac{-d[\text{HRP-II}]}{dt} = k_{3\text{app}} [\text{PABA}] [\text{HRP-II}] + k_{4\text{app}} [\text{PABA}] [\text{HRP-II-PABA}] \quad (3.19)$$

$$[\text{HRP-II}] = \frac{\text{K}_M [\text{HRP-II-PABA}]}{[\text{PABA}]} \quad (3.20)$$

$$[\text{HRP-II-PABA}] = \frac{[\text{PABA}] [\text{HRP-II}]}{1 + [\text{PABA}]/\text{K}_M} \quad (3.21)$$

The $[\text{HRP-II}]_o$ represents the total concentration of HRP-II as defined previously. Substitution of Eqs. 3.20 and 3.21 into Eq. 3.19 shows that:

$$k_{3\text{obs}} = \frac{k_{3\text{app}} [\text{PABA}] + k_{4\text{app}} [\text{PABA}]^2/\text{K}_M}{1 + [\text{PABA}]/\text{K}_M} \quad (3.22)$$

When $[\text{PABA}] \ll \text{K}_M$ then $[\text{PABA}]/\text{K}_M \ll 1$ and $[\text{PABA}]^2 \ll [\text{PABA}]$, therefore,

$$k_{3\text{obs}} = k_{3\text{app}} [\text{PABA}] \quad (3.23)$$

and the second-order rate constant may be determined from

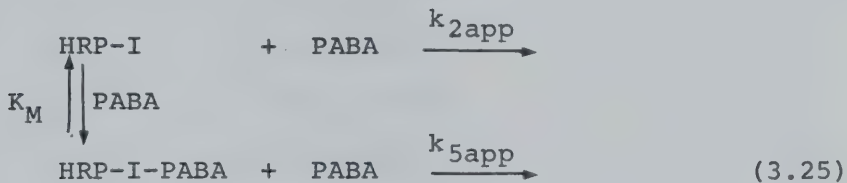
the slope of the $k_{3\text{obs}}$ vs. [PABA] plot. Similarly when $[PABA] \gg K_M$

$$k_{3\text{obs}} = k_{4\text{app}} [\text{PABA}] + k_{3\text{app}} K_M \quad (3.24)$$

and $k_{4\text{app}}$ then may be determined from the slope of a plot of $k_{3\text{obs}}$ vs. [PABA].

A nonlinear least-squares analysis was used to determine the best-fit curves (see Fig. 3.9) and the three kinetic parameters. At $[PABA] \ll K_M$, a condition which applies to all results obtained at $\text{pH} > 5$, the reaction of the complex with substrate is insignificant and the single parameter, $k_{3\text{app}}$, may be obtained from a linear least-squares analysis of the $k_{3\text{obs}}$ vs. [PABA] data. Results for the HRP-II reaction are shown in Tables 3.1 and 3.2.

A similar kinetic response for the HRP-I reaction suggests an identical mechanism to that for HRP-II:



where $k_{2\text{app}}$ and $k_{5\text{app}}$ are the appropriate second-order rate constants. Analogous to Eq. 3.22 the first-order rate constant $k_{2\text{obs}}$ may be related to the three kinetic parameters:

$$k_{2\text{obs}} = \frac{k_{2\text{app}} [\text{PABA}] + k_{5\text{app}} [\text{PABA}]^2 / K_M}{1 + [\text{PABA}] / K_M} \quad (3.26)$$

Table 3.1: The second-order rate constants determined for the HRP-II-PABA reaction at 25°C and $\mu = 0.11$ under conditions such that Eq. 3.10 and Eq. 3.23 apply.

pH ^a	k_{3app} ($M^{-1}s^{-1}$) ^b	Buffer ^c
2.48 ^d	(6.8±0.1)×10 ⁵	GNH
3.10 ^d	(1.2±0.2)×10 ⁵	GNH
3.39 ^d	(6.3±0.6)×10 ⁴	GNH
3.78 ^d	(2.5±0.1)×10 ⁴	A
4.35	(8.8±0.1)×10 ³	A
4.54	(5.4±0.1)×10 ³	A
4.88	(2.8±0.1)×10 ³	A
5.17	(1.6±0.1)×10 ³	A
5.43	(8.9±0.1)×10 ²	A
5.75	(6.4±0.1)×10 ²	A
6.15	(4.8±0.1)×10 ²	CA
6.35	(4.8±0.1)×10 ²	P
6.58	(4.3±0.1)×10 ²	CA
6.77	(4.0±0.1)×10 ²	P
7.30 ^d	(4.0±0.1)×10 ²	P
7.66	(3.8±0.1)×10 ²	T
8.08 ^d	(3.4±0.1)×10 ²	T
8.31	(3.2±0.1)×10 ²	T
8.70	(2.3±0.1)×10 ²	T

(Table continued on next page)

Table 3.1 continued

pH ^a	$k_{3\text{app}}$ ($\text{M}^{-1}\text{s}^{-1}$) ^b	Buffer ^c
9.12 ^d	$(1.0 \pm 0.1) \times 10^2$	C
9.34 ^d	$(6.3 \pm 0.3) \times 10$	C
9.53	$(5.1 \pm 0.1) \times 10$	C
9.61 ^d	$(4.1 \pm 0.1) \times 10$	C

^aErrors in pH values estimated at ± 0.02

^bErrors of rate constants represent the standard deviation calculated from data at a given pH.

^cBuffer abbreviations are the same as for Table 2.1 with GNH being glycine-nitric acid.

^dOnly these data represent a set of experiments performed at the given pH and single [PABA]. In all other cases the first-order dependence on [PABA] was established.

Table 3.2: Parameters from the nonlinear least-squares analysis of the dependence of the pseudo-first-order rate constant $k_{3\text{obs}}$ on PABA concentration for the HRP-II-PABA reaction under conditions where Eq. 3.22 applies.

pH^{a}	$k_{3\text{app}} \text{ (M}^{-1}\text{s}^{-1}\text{)}^{\text{b}}$	$k_{4\text{app}} \text{ (M}^{-1}\text{s}^{-1}\text{)}^{\text{b}}$	$1/k_M \text{ (M}^{-1}\text{)}^{\text{b}}$	[PABA] Range (M) $\times 10^5$	Buffer ^c
2.39	(9.9 \pm 0.4) $\times 10^5$	(6.2 \pm 2.4) $\times 10^5$	(6.0 \pm 8) $\times 10^3$	(1-20)	GNH
2.59	(4.7 \pm 0.1) $\times 10^5$	(2.5 \pm 0.4) $\times 10^5$	(7 \pm 3) $\times 10^3$	(1-30)	GNH
2.85	(2.1 \pm 0.2) $\times 10^5$	(1.2 \pm 0.6) $\times 10^5$	(7.4 \pm 2.1) $\times 10^3$	(5-200)	CT
3.64	(4.9 \pm 0.2) $\times 10^4$	(2.5 \pm 0.1) $\times 10^4$	(1.5 \pm 0.5) $\times 10^3$	(5-500)	A
3.97	(1.8 \pm 0.1) $\times 10^4$	(9.5 \pm 0.5) $\times 10^3$	(8.6 \pm 2.3) $\times 10^2$	(2-800)	A
4.17	(1.5 \pm 0.1) $\times 10^4$	(5.3 \pm 0.3) $\times 10^3$	(5.3 \pm 0.7) $\times 10^2$	(2-1000)	A
4.28	(1.2 \pm 0.1) $\times 10^4$	(5.5 \pm 0.3) $\times 10^3$	(2.8 \pm 0.5) $\times 10^2$	(2-1500)	A
4.51	(8.6 \pm 0.2) $\times 10^3$	(3.8 \pm 0.3) $\times 10^3$	(3.1 \pm 0.6) $\times 10^2$	(5-1000)	A
4.72	(4.8 \pm 0.1) $\times 10^3$	(1.9 \pm 0.1) $\times 10^3$	(1.5 \pm 0.2) $\times 10^2$	(50-3750)	A
5.01	(2.7 \pm 0.1) $\times 10^3$	(7.0 \pm 1.5) $\times 10^2$	(4.2 \pm 0.8) $\times 10$	(20-5000)	A

(Table continued on next page)

Table 3.2 continued

^aErrors in pH values estimated at ± 0.02

^bErrors of rate constants represent the standard deviation calculated from data at a given pH.

^cBuffer abbreviations are the same as for Table 2.1 with GNH being glycine-nitric acid.

Thus, the HRP-I reaction with PABA was conveniently interpreted in terms of a binding mechanism important over the same range of pH as in the HRP-II-PABA reaction. At pH > 5 the reaction may then be represented as:



from which $k_{2\text{app}}$ may be obtained from $k_{2\text{obs}}$:

$$k_{2\text{obs}} = k_{2\text{app}} [\text{PABA}] \quad (3.28)$$

The data are tabulated in Tables 3.3 and 3.4. The Michaelis constant determined for the HRP-I and HRP-II at any given pH were the same within the experimental error. Apparently the differences in the active site for these enzyme intermediates have had little effect on this parameter. As a result, no attempt has been made to distinguish between the K_M 's for the two reactions. Data for $k_{2\text{app}}$, $k_{3\text{app}}$ and $1/K_M$ are plotted as a function of pH in Fig. 3.11.

Although the interpretation of the data in terms of an enzyme-substrate complex offers an adequate and reasonable explanation, an alternative explanation might be briefly considered. As already pointed out, the PABA appeared stable under all experimental conditions. However, the change in the observed rates with increasing concentration might suggest a change in the activity of PABA in the aqueous solution. Let us consider the various possible interactions which may occur between molecules of a benzoic

Table 3.3: The second-order rate constants determined for the HRP-I-PABA reaction (25°C , $\mu = 0.11$) under conditions such that the rate was first-order in both reactants.

pH ^a	$k_{2\text{app}} (\text{M}^{-1}\text{s}^{-1})^b$	Buffer ^c
2.51	$(1.1 \pm 0.5) \times 10^4$	GNH
2.59	$(1.1 \pm 0.5) \times 10^4$	GNH
2.73	$(1.3 \pm 0.1) \times 10^4$	GNH
2.95	$(1.9 \pm 0.1) \times 10^4$	GNH
3.05	$(1.9 \pm 0.1) \times 10^4$	GNH
3.07	$(1.9 \pm 0.1) \times 10^4$	GNH
3.64	$(2.4 \pm 0.1) \times 10^4$	A
3.78	$(2.3 \pm 0.1) \times 10^4$	A
4.09	$(2.4 \pm 0.1) \times 10^4$	A
4.51	$(2.5 \pm 0.1) \times 10^4$	A
4.89 ^d	$(1.7 \pm 0.1) \times 10^4$	A
5.02	$(1.7 \pm 0.1) \times 10^4$	A
5.06	$(1.6 \pm 0.1) \times 10^4$	A
5.19	$(1.6 \pm 0.1) \times 10^4$	A
5.32	$(1.4 \pm 0.1) \times 10^4$	A
5.41	$(1.3 \pm 0.1) \times 10^4$	A
5.49	$(9.7 \pm 0.2) \times 10^3$	A
5.67	$(9.7 \pm 0.1) \times 10^3$	A
5.81	$(8.0 \pm 0.1) \times 10^3$	A

(Table continued on next page)

Table 3.3 continued

pH ^a	$k_{2\text{app}}$ ($\text{M}^{-1}\text{s}^{-1}$) ^b	Buffer ^c
6.15	$(6.8 \pm 0.1) \times 10^3$	CA
6.36	$(6.2 \pm 0.2) \times 10^3$	P
6.58	$(5.5 \pm 0.1) \times 10^3$	CA
6.76 ^d	$(5.8 \pm 0.1) \times 10^3$	P
6.95	$(4.7 \pm 0.1) \times 10^3$	T
7.10	$(4.6 \pm 0.1) \times 10^3$	P
7.56	$(4.3 \pm 0.2) \times 10^3$	T
8.03	$(4.3 \pm 0.1) \times 10^3$	T
8.23	$(4.4 \pm 0.2) \times 10^3$	T
8.61	$(4.2 \pm 0.1) \times 10^3$	T
9.39 ^d	$(4.8 \pm 0.1) \times 10^3$	C

^a Errors in pH values estimated at ± 0.02

^b Errors of rate constants represent the standard deviation calculated from data at a given pH.

^c Buffer abbreviations are the same as for Table 2.1 with GNH being glycine-nitric acid.

^d Study of the dependence of $k_{2\text{obs}}$ on [PABA] from which $k_{2\text{app}}$ was calculated from the slope.

Table 3.4: Parameters from the nonlinear least-squares analysis of the dependence of the pseudo-first-order rate constant, $\kappa_{2\text{obs}}$ on PABA concentration for the HRP-I-PABA reaction under conditions where Eq. 3.26 applies.

pH ^a	$\kappa_{2\text{app}}$ ($M^{-1}s^{-1}$) ^b	$\kappa_{5\text{app}}$ ($M^{-1}s^{-1}$) ^b	$1/K_M (M^{-1})$ ^b	[PABA] Range (M) $\times 10^4$	Buffer ^c
2.85	$(1.5 \pm 0.1) \times 10^4$	$(1.2 \pm 0.1) \times 10^4$	$(4.0 \pm 3) \times 10^3$	(0.1-30)	GNH
3.23	$(2.3 \pm 0.1) \times 10^4$	$(1.4 \pm 0.1) \times 10^4$	$(3.1 \pm 1.1) \times 10^3$	(0.2-30)	GNH
3.44	$(2.6 \pm 0.1) \times 10^4$	$(1.4 \pm 0.3) \times 10^4$	$(2.9 \pm 1.8) \times 10^3$	(0.2-20)	C
3.97	$(2.9 \pm 0.1) \times 10^4$	$(1.4 \pm 0.1) \times 10^4$	$(1.2 \pm 0.2) \times 10^3$	(0.2-80)	A
4.28	$(2.3 \pm 0.1) \times 10^4$	$(9.4 \pm 0.6) \times 10^3$	$(3.8 \pm 0.7) \times 10^2$	(1-100)	A
4.72	$(2.0 \pm 0.1) \times 10^4$	$(8.8 \pm 0.3) \times 10^3$	$(1.8 \pm 0.4) \times 10^2$	(1-120)	A

^aErrors in pH values estimated at ± 0.02

^bErrors of rate constants represent the standard deviation calculated from data at a given pH.

^cBuffer abbreviations are the same for Table 2.1 with GNH being glycine-nitric acid.

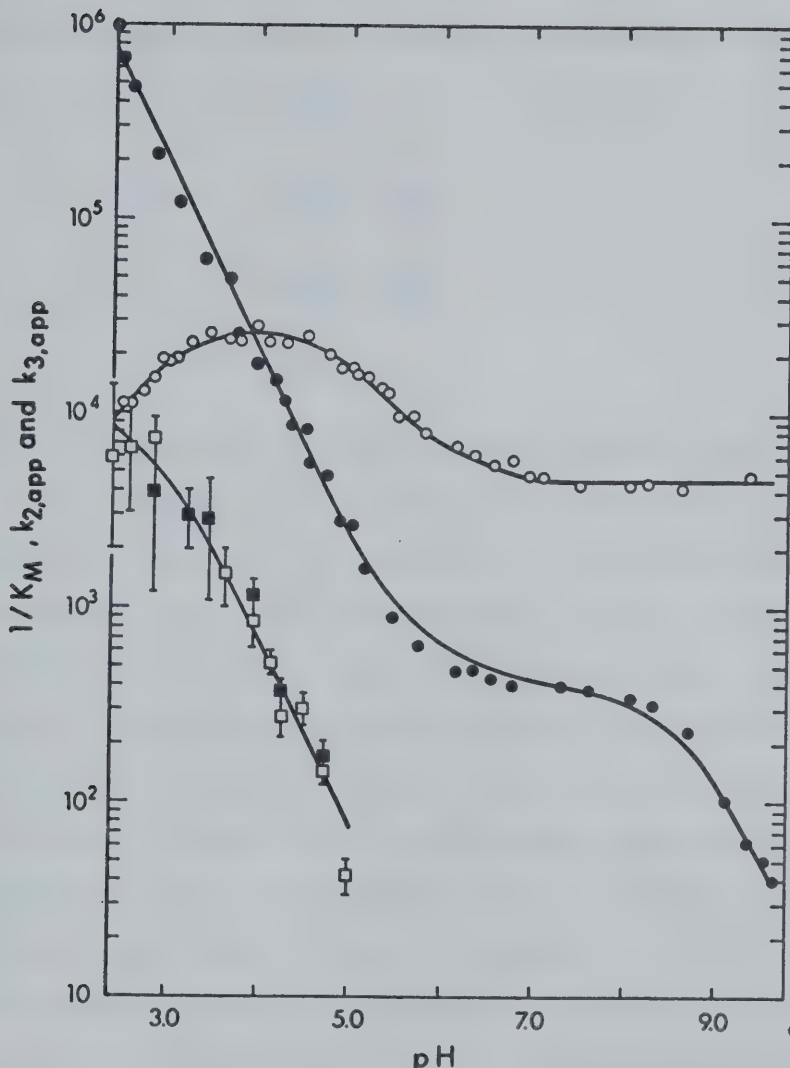
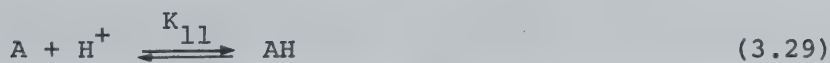


Fig. 3.11: Semilogarithmic plot of $1/K_M$ for the HRP-II (\square) and HRP-I reaction with PABA (\blacksquare) as well as the rate constant for the HRP-I-PABA reaction $k_{2,app}$ (\circ), and the rate constant for the HRP-II-PABA reaction, $k_{3,app}$ (\bullet), against pH. The curves were calculated from a nonlinear least-squares fit of the data to Eq. 3.60 for $1/K_M$ and Eq. 3.56 and Eq. 3.50 for $k_{2,app}$ and $k_{3,app}$.

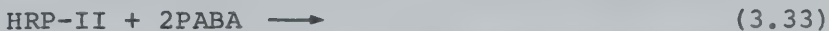
acid in aqueous solution (Martin and Rossotti, 1959):



where A represents the unprotonated benzoate anion and the K's are association constants. It would appear that a reasonable case for the dominance of the monomolecular ionization (Eq. 3.29) has been made for $[A] < 5 \times 10^{-2}$ M, a concentration above which the PABA oxidation was not studied. The polynuclear equilibria become significant only at higher concentrations. The hydrogen dibenzoate (benzoate - benzoic acid) ion has been shown to exist in aqueous solution at concentrations of benzoate above 0.1 M (Kolthoff and Bosch, 1932a). Although it is difficult to determine the effect of hydrophobic association, some hydrophobic interaction has been proposed for butyric acid in aqueous solution (Nash and Monk, 1957). However, the trends for the various dissociation equilibria are in the order of that expected for ion-ion, ion-dipole and dipole-dipole interactions; that is, $K_{11} > K_{22} > K_{12} > K_A$ which suggests that the dimer prefers the extended form of Eq. 3.30. The system is further complicated by the presence of

the acetic acid-acetate buffer. At [Acetate] = 0.7 M the amount of the acid-acetate dimer is reported to be about 10%.

Kolthoff and Bosch (1932b) have determined an activity coefficient of 1.00 (within a 2% error) for 2.66×10^{-2} M benzoic acid in a 0.09 M KNO_3 aqueous solution. The dissociation constant as defined by Eq. 3.30 at 2×10^{-2} M acid was $K_{12} = 1.6$ M. If at least 90% of the aromatic acid were associated at 2×10^{-2} M and pH = 5.0, as it must be if we are to interpret the results by this mechanism, then, $[\text{HA}_2] = 9 \times 10^{-3}$ M, $[\text{A}] \approx [\text{HA}] = 10^{-3}$ M and $K_{12} \approx 10^{-4}$ M. The experimentally determined value for K_{12} is much too large for any significant amount of the dimer to be present at 2×10^{-2} M. Furthermore, the ultraviolet spectrum of PABA has been studied over the pH range 1.1 - 11.5 in 2×10^{-4} M aqueous solution (Rekker and Nauta, 1956). The interpretation involves only monomolecular dissociations of the type in Eq. 3.29. Therefore, it would appear unlikely that association of the acid in these dilute aqueous solutions is significant. One may conclude that the mechanism:



although kinetically indistinguishable from a reaction of the proposed HRP-II complex with substrate (Eq. 3.18), is not a viable alternative explanation.

Spectrophotometric Evidence for an Enzyme-Substrate Interaction:

Conceivably, the formation of an enzyme-substrate complex, implied in Eq. 3.18, could result in an observable spectral change if there were a large enough difference in the molar absorptivities of HRP-II and HRP-II-PABA. Because of the transient nature of HRP-II in the presence of PABA, the amplitude of the stopped-flow trace resulting from HRP-II reduction is the most convenient parameter to monitor such a spectral change. To determine whether the change in molar absorptivity upon HRP-II reduction was sensitive to the enzyme-substrate interaction, a preliminary set of experiments was performed. The amplitude at low PABA concentration at pH = 5.01, acetate buffer ($[PABA] = 10^{-3}$ M) was observed ($\Delta V = 5.2$ volts) at 425 nm. The syringe containing the PABA solution was quickly replaced with PABA at 5×10^{-2} M, the stopped-flow flushed, and the amplitude again noted ($\Delta V = 4.9$ volts). Under these conditions at time zero for each experiment there will be about 50% of the total HRP-II present as a complex. In the instrument dead-time (~7 ms) < 20% of the reactive intermediates will have decayed. Similar results at 420 nm and 430 nm also indicated no significant change in the amplitude. Apparently, any complex formed does not affect the change in molar absorptivity enough to be experimentally observable. This is in contrast to the results obtained for p-cresol where the

amplitude for HRP-II reduction at 10^{-3} M p-cresol and 426 nm (pH = 9.84) was reported to be about 20% of its value at 10^{-5} M (Critchlow and Dunford, 1972a).

Since any spectral change upon HRP-II-PABA complex formation was, apparently, too small to be detected by monitoring the amplitude of the stopped-flow signal, it seemed reasonable to investigate the native enzyme for small spectral changes indicative of enzyme-substrate interaction. Difference spectroscopy has been used previously to define quantitatively spectral changes of < 3% in terms of the binding of p-cresol (Critchlow and Dunford, 1972b). A similar approach has been used to study the effect of pH on spectra of HRP (Theorell and Paul, 1944) and turnip peroxidase (Ricard *et al.*, 1972). A preliminary investigation showed that small spectral changes in the Soret region were dependent upon PABA concentration. A typical difference spectrum is shown in Fig. 3.12 at pH = 5.0 in acetate buffer. A recently published dissociation constant for the binding of aniline to HRP determined by difference spectroscopy (Critchlow and Dunford, 1972b) as well as the small spectral changes resulting from the interaction of HRP with organic acids (Ricard *et al.*, 1968; Gasper *et al.*, 1972) indicated that both functional groups of PABA may be involved. To further complicate the system, acetate buffers have been shown to cause small spectral changes in the Soret region (Horne, 1967). As a result, it was decided to investigate

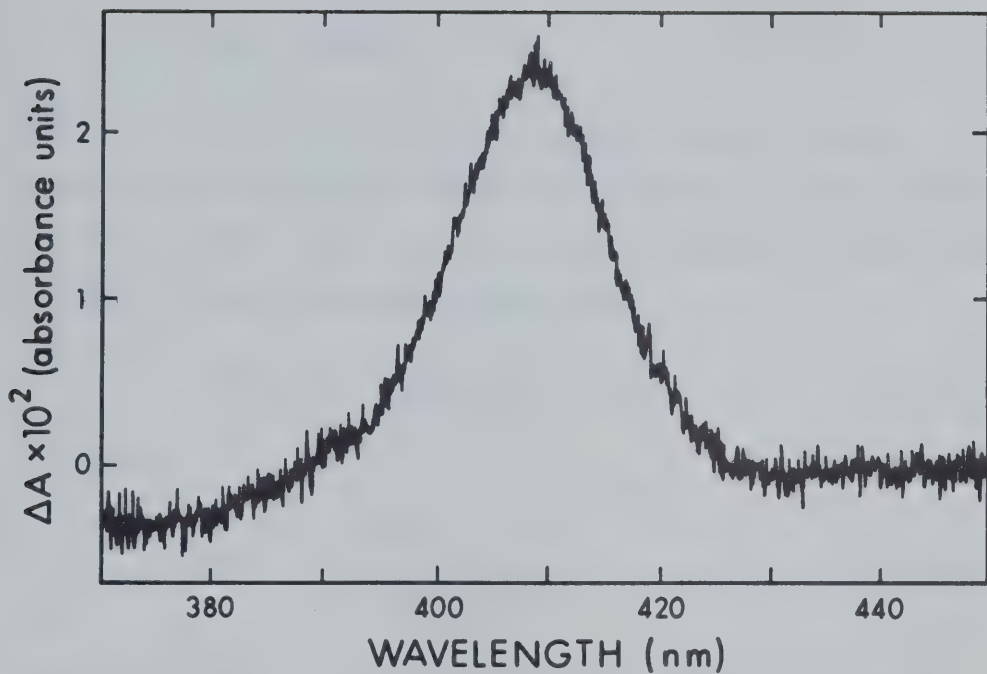


Fig. 3.12: The difference spectrum of the native enzyme in the presence of 7.5×10^{-3} M PABA relative to HRP. Enzyme concentration in both sample and reference was 1.6×10^{-5} M in acetate buffer (contribution to the total ionic strength 5.5×10^{-2}) pH = 5.0.

acetate buffer, aniline, benzoic acid and PABA at pH = 5.0.

First, consider the binding of any substrate S to the native enzyme assuming a 1:1 stoichiometry:



where K_S is the dissociation constant for the complex. The total concentration of native HRP originally added to the cuvette, $[\text{HRP}]_0$, will be distributed between the free native enzyme form HRP and its complex HRP-S:

$$[\text{HRP}]_0 = [\text{HRP}] + [\text{HRP-S}] \quad (3.35)$$

Therefore:

$$[\text{HRP}] = \frac{[\text{HRP}]_0}{1 + [S]/K_S} \quad (3.36)$$

Since no substrate is added to the reference cuvette the absorbance A_R will be:

$$A_R = \epsilon_{\text{HRP}} [\text{HRP}]_0 \quad (3.37)$$

where ϵ_{HRP} is the molar absorptivity of the enzyme. For the sample cuvette the absorbance A_S will be the sum of the absorbances of the two species present

$$A_S = \epsilon_{\text{HRP}} [\text{HRP}] + \epsilon_{\text{HRP-S}} [\text{HRP-S}] \quad (3.38)$$

where $\epsilon_{\text{HRP-S}}$ is the molar absorptivity of the complex.

Expressing $[\text{HRP-S}]$ in terms of $[\text{HRP}]$ and substituting the

the value of [HRP] from Eq. 3.36 one obtains:

$$A_S = (\epsilon_{HRP} + \epsilon_{HRP-S} [S]/K_S) \frac{[HRP]_O}{1 + [S]/K_S} \quad (3.39)$$

Therefore, the difference in absorbance upon addition of the substrate to the sample cuvette may be expressed as:

$$\Delta A = A_R - A_S = \frac{(\epsilon_{HRP} - \epsilon_{HRP-S}) [HRP]_O [S]/K_S}{1 + [S]/K_S} \quad (3.40)$$

If ΔA_S is defined as the absorbance difference observed at infinitely high [S] where all the enzyme is present as the complex ($[HRP]_O = [HRP-S]$) then:

$$\Delta A_S = A_R - A_{S,\infty} = (\epsilon_{HRP} - \epsilon_{HRP-S}) [HRP]_O \quad (3.41)$$

and $\Delta A = \frac{\Delta A_S [S]/K_S}{1 + [S]/K_S} \quad (3.42)$

The effect of the acetate buffer upon the Soret spectrum of the native enzyme was investigated initially at pH = 5.0. For these studies the total ionic strength was maintained at 0.11 by adjusting the concentration of KNO_3 in solution. In the reference cuvette the buffer contributed 4.5×10^{-3} to the total ionic strength. The difference spectrum was obtained as a function of buffer concentration by varying the acetate buffer's contribution to the total ionic strength in the sample cuvette from 4.5×10^{-3} to 0.10. A typical spectrum is shown in Fig.

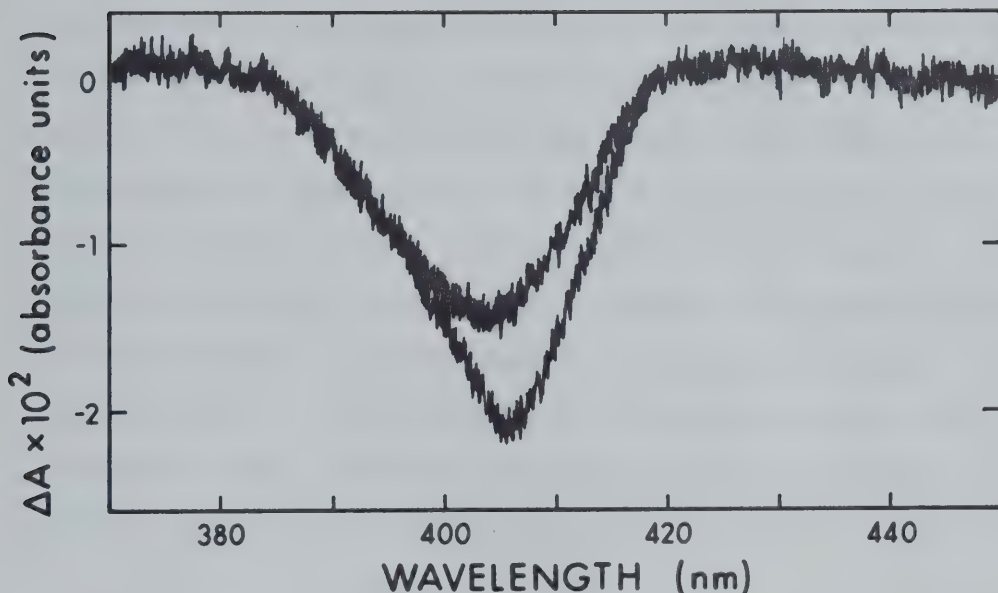


Fig. 3.13: The difference spectra of the native enzyme in the presence of aniline and acetic acid-acetate buffer relative to HRP.

Upper Curve: $[Aniline] = 3 \times 10^{-2} M$; $[HRP] = 8 \times 10^{-6} M$; acetate buffer ($\mu' = 5.5 \times 10^{-2}$); pH = 5.0.

Lower Curve: Sample consisted of acetate buffer at $\mu' = 0.1$ and reference consisted of acetate buffer at $\mu' = 4.5 \times 10^{-3}$, total ionic strength of solutions 0.11; $[HRP] = 8 \times 10^{-6} M$; pH = 5.0.

3.13. Since the position of the base line may be subject to small errors arising from the presence of extraneous matter either in solution or on the cuvette, the difference in absorbance differences between sample and reference at 410 nm and 395 nm, $\Delta A'$, was used as a monitor. The simple model of Eq. 3.34 may be used to describe the observed dependence of this spectral change with increasing ionic strength of the buffer. The quantity $\Delta A'$ will obey a relation analogous to Eq. 3.42. Because the acetate concentration will be proportional to its ionic strength contribution μ' at any given pH and constant total ionic strength of the solution without regard to the concentrations of its state of ionization:

$$\Delta A' = \frac{\Delta A'_S c\mu'}{1 + c\mu'} \quad (3.43)$$

where $c\mu' = [S]/K_S$. $[S]$ now refers to the total acetate-acetic acid concentration and c is a proportionality constant. The results obtained for $\Delta A'$ at different ionic strengths for the acetate buffer are plotted in Fig. 3.14. The solid curve represents the nonlinear least-squares best-fit to the data. From the analysis the values of the two parameters $\Delta A'_S$ and $1/c$ were calculated. The results together with standard deviations are tabulated in Table 3.5. For any given value of μ' the value of $[S]/K_S$ may be determined.

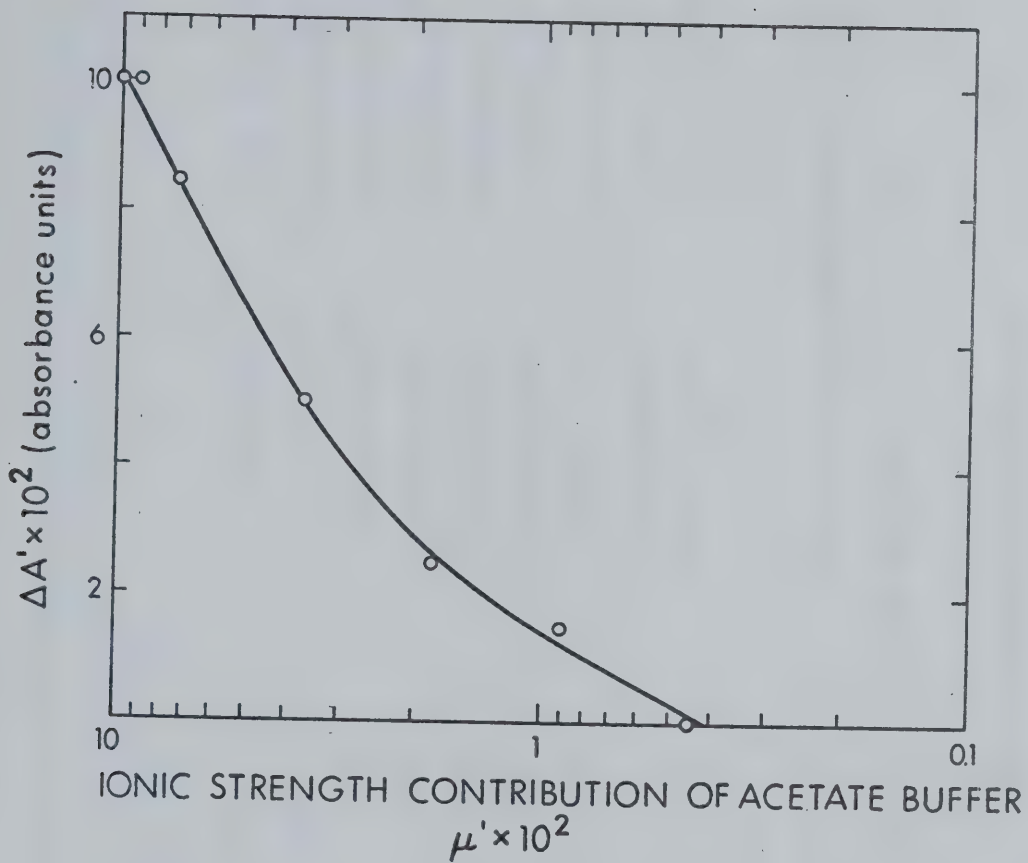


Fig. 3.14: Plot of $\Delta A_{410} - \Delta A_{395}$ for the changing absorbance difference against the contribution which the acetate buffer makes to the constant total ionic strength (0.11). The abscissa is logarithmic. The best-fit to Eq. 3.43 is shown. $[HRP] = 8 \times 10^{-6}$ M. $pH = 5.0$

Table 3.5. Parameters obtained for the binding of PABA and related substrates to HRP

Substrate	pH	Contribution of Acetate to μ (10^{-1})	K_S^a	ΔA^a
Acetate Buffer	5.0	0.045 ~ 1.0	(1.7±0.6) x 10 ⁻¹ ^b	(2.8±0.6) x 10 ⁻²
Acetate Buffer	4.4	0.045 ~ 1.0	(1.3±0.4) x 10 ⁻¹ ^b	(1.4±0.7) x 10 ⁻¹ ^d
Benzoic Acid	5.0	0.55	(3.0±0.2) x 10 ⁻²	(2.2±0.7) x 10 ⁻¹ ^c
Benzoic Acid	5.0	1.0	(2.6±0.3) x 10 ⁻²	(2.7±0.8) x 10 ⁻¹ ^c
Aniline ^f	5.0	0.55	(6.5±1.4) x 10 ⁻²	(4.5±0.6) x 10 ⁻² ^c
Aniline ^f	5.0	1.0	(4.2±0.9) x 10 ⁻²	(3.7±0.5) x 10 ⁻² ^c
PABA	5.0	0.55	(2.3±0.4) x 10 ⁻²	(9.2±0.5) x 10 ⁻² ^e
PABA	5.0	1.0	(1.8±0.3) x 10 ⁻²	(1.6±0.3) x 10 ⁻¹ ^d
PABA	4.4	0.55	(8.2±2.0) x 10 ⁻³	(1.7±0.2) x 10 ⁻¹ ^d

^a Errors estimated as the standard deviation of the nonlinear least-squares analysis^bThe parameter reported is not K_S but 1/c from Eq. 3.43^c [HRP] = 8 x 10⁻⁶ M

(Table continued on next page)

$$d_{[HRP]} = 3.2 \times 10^{-5} \text{ M}$$

$$e_{[HRP]} = 1.6 \times 10^{-5} \text{ M}$$

$$f_{\Delta A'} = \Delta A_{395} - \Delta A_{435}$$

Benzoic acid was examined in acetate buffer ($\text{pH} = 5.0$) for spectroscopic evidence of an enzyme-substrate interaction. Again, the spectral change (Fig. 3.15) was monitored using the difference in the absorbance difference at 410 nm and 395 nm. The data were analyzed by a nonlinear least-squares method using as a model competitive binding of benzoic acid and acetic acid at a single enzyme site. Such an assumption seemed reasonable. That the data conformed to this model was shown, within the limits of experimental error, by studying the binding of benzoic acid at a buffer ionic strength $\mu' = 0.10$ as well as $\mu' = 5 \times 10^{-3}$ and obtaining similar results (see Table 3.5). In both cases the acid concentrations used to calculate the K_S were the total of its protonated and unprotonated forms. At a constant buffer concentration it may be shown that:

$$\Delta A' = \frac{\Delta A'_B [B] / K_B}{1 + [A]/K_A + [B]/K_B} \quad (3.44)$$

in an analogous fashion to Eq. 3.42. In this equation $[A]$ and $[B]$ represent the concentrations of acetate-acetic acid and benzoate-benzoic acid, K_A and K_B the dissociation constants of their respective complexes with the enzyme and $\Delta A'_B$ the absorbance difference at infinite $[B]$ as indicated by the difference $\Delta A_{410} - \Delta A_{395}$. The results, together with the best-fit curve, are shown in Fig. 3.16.

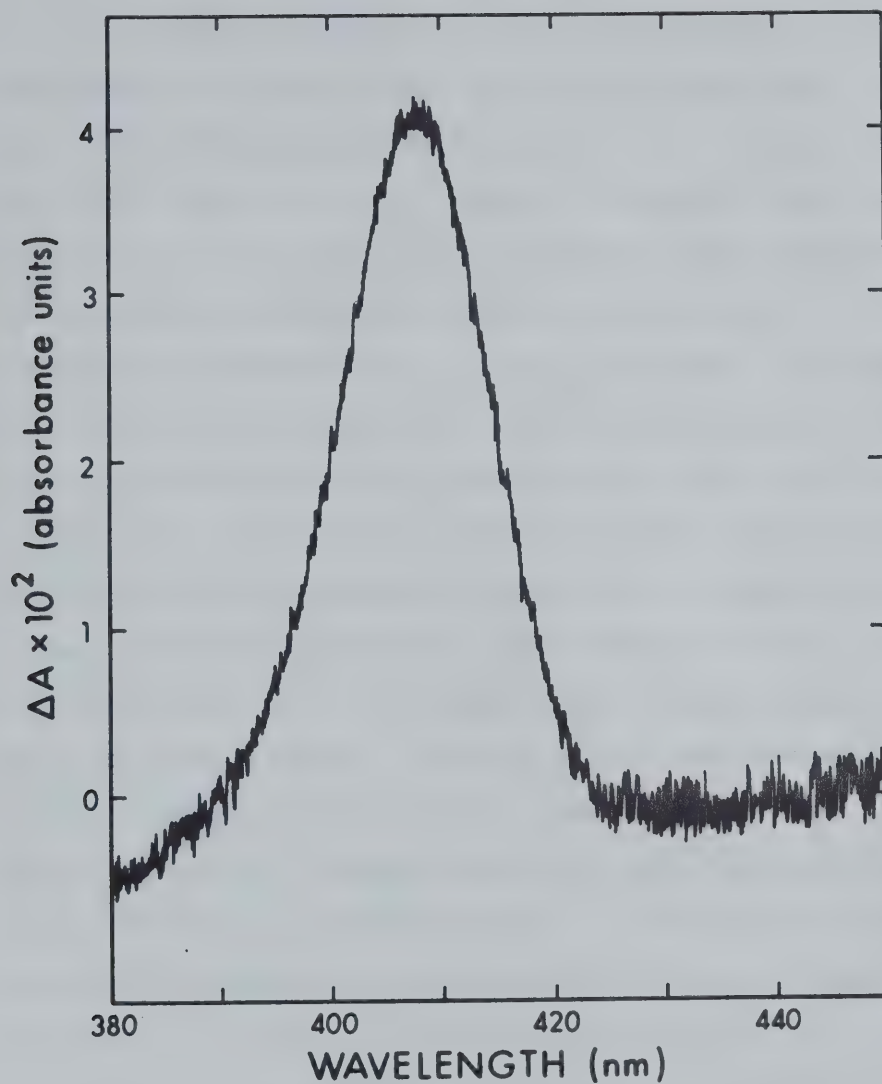


Fig. 3.15: The difference spectrum of HRP in the presence of 7.5×10^{-3} M benzoic acid relative to HRP. Enzyme concentration in both sample and reference was 8×10^{-6} M in acetate buffer (contribution to ionic strength 5.5×10^{-2}); pH = 5.0.

Using a similar approach, the binding of aniline and PABA were investigated in acetate buffer ($\text{pH} = 5.0$). From the difference spectra of Fig. 3.13 it is apparent that the difference $\Delta A_{410} - \Delta A_{395}$, although a good monitor for the spectral change with increasing PABA concentration, is insensitive to changing aniline concentration. As a result the difference $\Delta A_{395} - \Delta A_{435}$ was used. The data were analyzed by a nonlinear least-squares method assuming that each substrate binds competitively with acetate at a single site. The results from the analysis are plotted in Fig. 3.16 and tabulated in Table 3.5. Results at different buffer concentrations were similar for both aniline and PABA indicating that competitive binding with acetate is a reasonable model. Using Eq. 3.43, the parameters for acetate buffer at $\text{pH} = 4.4$ were determined and the experimental procedure repeated for PABA at this pH (see Table 3.5). Attempts to work below $\text{pH} = 4$ resulted in nonreproducibility which may be attributed to enzyme denaturation. At 2×10^{-2} M PABA in phosphate buffer at $\text{pH} = 7.0$ no spectral changes were observed suggesting that the dissociation constant was too large to be determined experimentally.

With aniline, benzoic acid and acetate buffer present, the data is consistent with competitive binding. At a constant buffer concentration, an expression for the absorbance change $\Delta A' = \Delta A_{410} - \Delta A_{395}$ may be derived in a

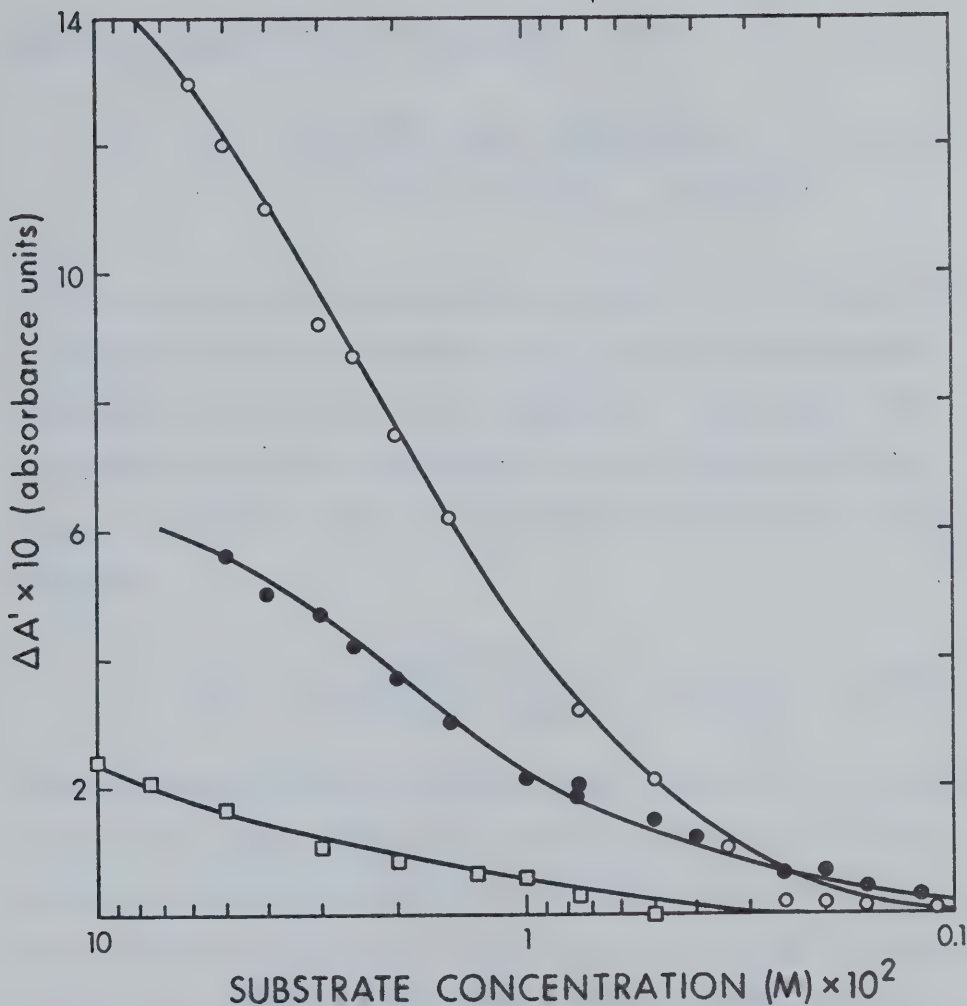


Fig. 3.16: Plot of the changing absorbance difference against the substrate concentration. The abscissa is logarithmic. For benzoic acid (O) $\Delta A' = \Delta A_{410} - \Delta A_{395}$, $[HRP] = 8 \times 10^{-6}$ M; PABA (●) $\Delta A' = \Delta A_{410} - \Delta A_{395}$, $[HRP] = 1.6 \times 10^{-5}$ M, aniline (□) $\Delta A' = \Delta A_{435} - \Delta A_{395}$, $[HRP] = 8 \times 10^{-6}$ M. In each case $pH = 5.0$ acetate buffer ($\mu' = 5.5 \times 10^{-2}$).

similar manner to Eq. 3.42 and Eq. 3.44:

$$\Delta A' = \frac{\Delta A'_{An} [An]/K_{An} + \Delta A'_{B} [B]/K_B}{1 + [A]/K_A + [An]/K_{An} + [B]/K_B} \quad (3.45)$$

where $[An]$ is the aniline concentration without regard to its state of protonation and K_{An} is the dissociation constant for the HRP-aniline complex. Since $\Delta A'_{An}$, the absorbance change as monitored by the difference $\Delta A_{410} - \Delta A_{395}$ at infinite $[An]$, is approximately zero, Eq. 3.45 becomes:

$$\Delta A' = \frac{\Delta A'_{B} [B]/K_B}{1 + [A]/K_A + [An]/K_{An} + [B]/K_B} \quad (3.46)$$

Using the previously determined parameters for aniline and benzoic acid the value of $\Delta A'$ may be calculated for any given set of concentrations. At $[An] = 2 \times 10^{-2} M$ (pH = 5.0, acetate buffer) the concentration of benzoic acid was varied and the $\Delta A'$ determined from the difference spectra. These values are plotted against the values calculated from Eq. 3.46 at the same concentrations in Fig. 3.17. The solid line represents the expected relation if aniline and benzoic acid bind competitively. Within the experimental error, deviations from Eq. 3.46 are not significant. Using a previously published dissociation constant (Critchlow and Dunford, 1972b) and a value of $\Delta A'_s$ deter-

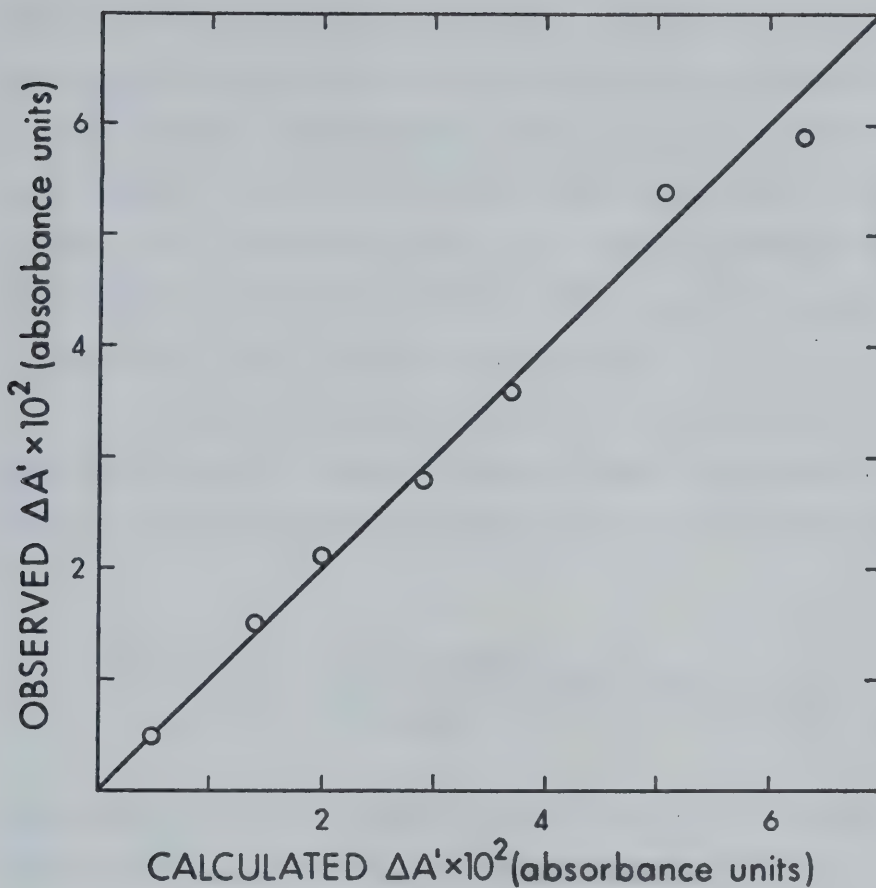


Fig. 3.17: Changing absorbance difference ($\Delta A' = \Delta A_{410} - \Delta A_{395}$) observed plotted against the $\Delta A'$ calculated from Eq. 3.46 with $[Aniline] = 2 \times 10^{-2} M$, $[HRP] = 8 \times 10^{-6} M$, $[Benzoic\ acid] = 10^{-3} M - 2 \times 10^{-2} M$, $pH = 5.0$, Acetate buffer ($\mu' = 5.5 \times 10^{-2}$). The linear relation shown having a 45° slope represents the predicted relation if the experimental data conform to the Eq. 3.46, a criterion for competitive binding.

mined experimentally for p-cresol, the spectral change with increasing p-cresol concentration in the presence of 2×10^{-2} M PABA was observed at pH = 5.0. A plot of these data against the $\Delta A'$ calculated from an expression analogous to Eq. 3.45 is shown in Fig. 3.18. Again, deviations from the competitive binding of PABA and p-cresol, represented by the solid line, are not significant.

Using an approach completely analogous to that used to derive Eq. 3.42, it may be shown for benzoic acid and aniline binding at two different sites on the enzyme that:

$$\Delta A' = \frac{\Delta A'_B [B]/K_B + \Delta A'_{An,B} [An][B]/K_{An,B} K_{An}}{1 + [A]/K_A + [An]/K_{An} + [B]/K_B + [An][B]/K_{An,B} K_{An}} \quad (3.47)$$

Where $\Delta A'_{An,B}$ is the limiting value of $\Delta A'$ at infinite concentrations of both aniline and benzoic acid and $K_{An,B} = [HRP-An][B]/[B-HRP-An]$. If one assumes that the binding of aniline or benzoic acid is not affected by the complex formed by the other substrate then $K_{An,B} = K_B$ and $\Delta A'_{An,B} = \Delta A'_B + \Delta A'_{An}$. With this latter assumption, the values obtained for $\Delta A'$ at various benzoic acid concentrations ($[An] = 2 \times 10^{-2}$ M, pH = 5.0, acetate buffer) are plotted in Fig. 3.19 against values calculated from Eq. 3.47 at these same concentrations. Unlike Fig. 3.17 in which the data were tested for competitive binding, the model requiring two binding sites does not represent as

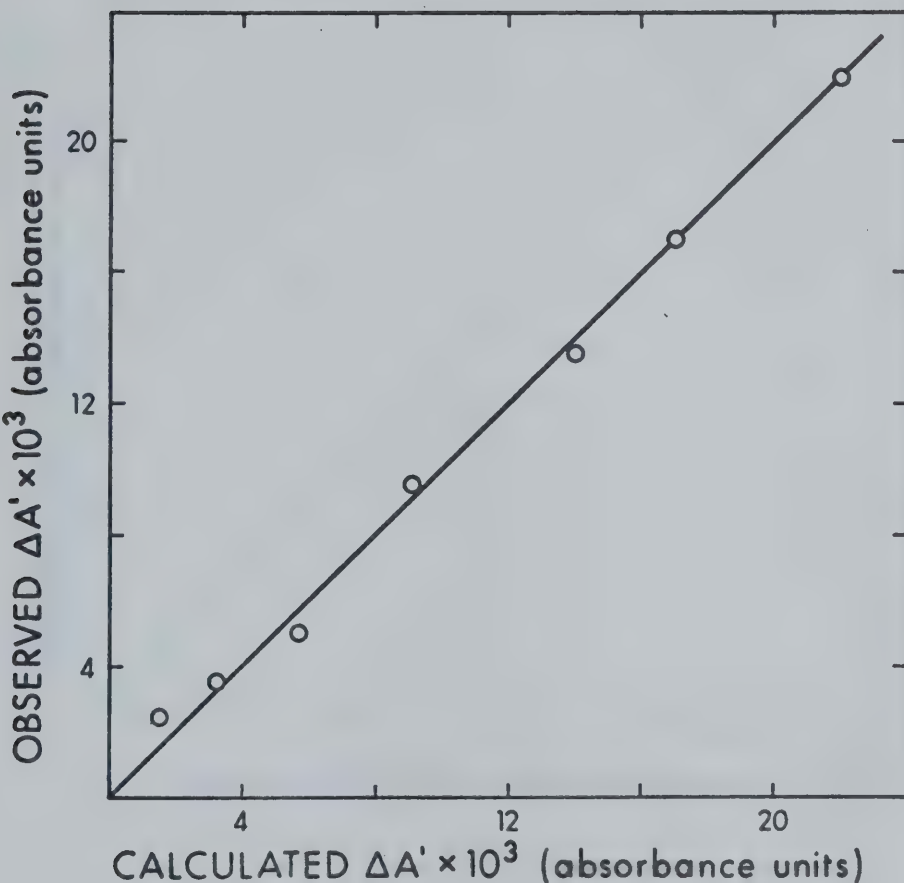


Fig. 3.18: The changing absorbance difference ($\Delta A' = \Delta A_{410} - \Delta A_{395}$) plotted against the $\Delta A'$ calculated from a relation of the same form as Eq. 3.45 for $[PABA] = 2 \times 10^{-3}$ M, $[HRP] = 9.5 \times 10^{-6}$ M, $[p\text{-cresol}] = 1.2 \times 10^{-3}$ M - 10^{-2} M, pH = 5.0 Acetate ($\mu' = 5.5 \times 10^{-2}$). The linear relation represents the predicted relation for competitive binding of PABA and p-cresol.

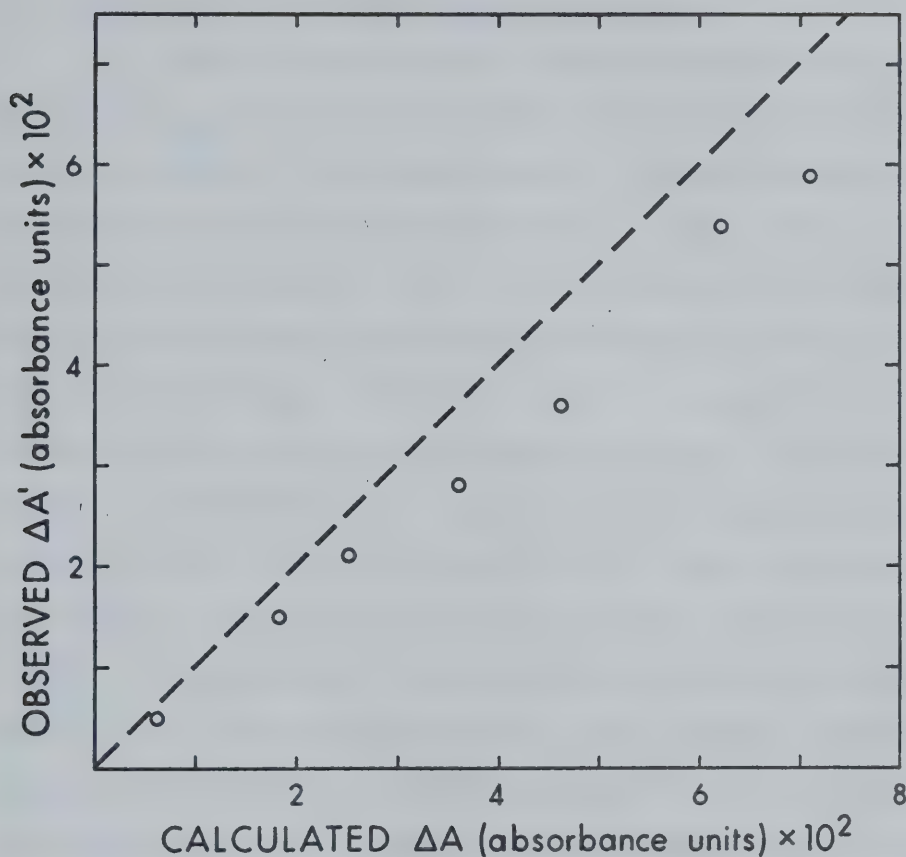


Fig. 3.19: The changing absorbance difference ($\Delta A' = \Delta A_{410} - \Delta A_{395}$) observed plotted against the $\Delta A'$ calculated from Eq. 3.47 under the same conditions as indicated in Fig. 3.17. The broken line with a 45° slope represents the predicted relation if the experimental data conform to Eq. 3.47.

good a description of the experimental results.

Dependence of the Kinetic Parameters on pH:

The data plotted as a function of pH in Fig.

3.11 for k_{3app} , the second-order rate constant for the reduction of HRP-II by PABA, shows a remarkable similarity to that for the HRP-II-ferrocyanide reaction. There are two major differences. The rates are slower by a factor of fifty and a small shift of the positive inflection (with increasing pH) in the log rate *vs.* pH profile to a lower value on the abscissa occurs upon going from ferrocyanide to PABA oxidation. Apparently the same proton-transfer mechanisms must apply for both substrates as indicated by the overall similarity of the two pH-rate curves. The reduction of HRP-II with both PABA and ferrocyanide are influenced by the same two ionizable groups neither of which can be readily assigned to the substrate. The dependence on pH of both reactions appears to be substrate independent. A consideration of transition-state theory and the two possible pairing schemes, already discussed in considerable detail in Chapter 2, should result in similar arguments for PABA as for ferrocyanide oxidation. These will not be reconsidered at this point. The log k_{3app} *vs.* pH profile was analyzed by a nonlinear least-squares program fitting the data to the phenomenological equation of Eq. 2.7 reproduced here for convenience:

$$k_{3\text{app}} = \frac{A_1 [H^+] (1 + [H^+]/A_2)}{(1 + [H^+]/A_3)} \quad (3.48)$$

In a completely analogous fashion to that for the HRP-II-ferrocyanide reaction, one may assume a single mechanism to describe the log rate-pH profile over the entire range of pH. Assigning the two pK_a values to ionizable groups on the enzyme, the transition-state approach leads to an expression for $k_{3\text{app}}$ similar to Eq. 2.9:

$$k_{3\text{app}} = \frac{k'_3 (1 + [H^+]/K_2^\ddagger + [H^+]^2/K_1^\ddagger K_2^\ddagger)}{(1 + [H^+]/K_2 + [H^+]^2/K_1 K_2)} \quad (3.49)$$

where k'_3 is a pH independent rate constant at high pH, K_1^\ddagger and K_2^\ddagger are transition-state acid dissociation constants having values of $pK_1^\ddagger = 5.7$ and $pK_2^\ddagger > 10$ and K_1 and K_2 , the ground state acid dissociation constants having values $pK_1 < 2$ and $pK_2 = 8.6$. When the terms making a negligible contribution to the observed pH dependence are neglected, eq. 3.49 becomes:

$$k_{3\text{app}} = \frac{k'_3 [H^+]/K_2^\ddagger (1 + [H^+]/K_1^\ddagger)}{(1 + [H^+]/K_2)} \quad (3.50)$$

Eq. 3.48 and Eq. 3.50 are of the same form which allows the identification of the parameters estimated from the non-linear analysis with acid dissociation constants. The non-

linear correlation is shown in Fig. 3.11 and the results are tabulated in Table 3.6.

For the HRP-II reduction by PABA, the rates are insensitive to the protonation of the carboxyl or amino group on the substrate. Because protonation of the carboxyl anion will result in a stronger withdrawal of electrons reducing the electron density at the amino nitrogen, electron transfer would be expected to be more difficult and the influence of the substrate pK_a should appear in the pH profile. Such a result has been observed for protonation of the p-cresolate anion (Critchlow and Dunford, 1972a). Protonation of the amino group should also influence electron transfer but, again, no inflection in the appropriate region of the pH-rate profile is observable. One explanation of these results may be that all three forms of the substrate react with HRP-II at the same rate because of the fortuitous cancellation of all factors affecting the rate. This must be regarded as unlikely. A second possible explanation may be that the protonated form of the enzyme as it exists at $\text{pH} < 2$ reacts with PABA by way of a diffusion-controlled process. In such a case a reaction will occur whenever this protonated form of the enzyme encounters a molecule of PABA having the correct orientation for reaction no matter what its state of ionization. Although the various protonated forms of PABA may have the potential to react at different rates with the enzyme, the diffusion-controlled limit

Table 3.6. Parameters obtained from a nonlinear least-squares analysis for the HRP-II reduction by PABA

	Parameters related to:	Numerical value ^a
Eq. 3.47	Eq. 3.49	Eq. 3.53
A_1	$k_3^{\ddagger}/K_2^{\ddagger}$	$\frac{k_3''}{K_1^{\ddagger}} + \frac{k_3'}{K_2^{\ddagger}}$ $(1.9 \pm 0.2) \times 10^{11} \text{ M}^{-2} \text{ s}^{-1}$
A_2	K_1^{\ddagger}	$(k_3'/k_3'') (K_1^{\ddagger} K_2/K_2^{\ddagger}) + K_2$ $(2.1 \pm 0.2) \times 10^{-6} \text{ M}$
A_3	K_2	$(2.6 \pm 0.3) \times 10^{-9} \text{ M}$
A_1^b		$(9.5 \pm 0.9) \times 10^{10} \text{ M}^{-2} \text{ s}^{-1}$

^aErrors estimated from the standard deviations of the fit.

^bCalculated from values of $k_{4\text{app}}$ using A_2 and A_3 as fixed parameters.

essentially levels all rates to a single value. Probably, this approach offers the simplest explanation.

Therefore, the reaction is influenced only by two ionizable groups on the enzyme. One of these groups may be a hydroxyl group located at the iron's sixth coordination position. Protonation of this species will greatly enhance its ability to function as a leaving group. The protonated hydroxyl group need not physically leave the active site when the reduction of HRP-II occurs but simply may revert electronically to a neutral water molecule weakly associated at the iron's sixth position. With this group protonated, the active site is potentially capable of reacting with the reducing substrate at every encounter. Hence, it is not unreasonable to assign K_1 to this hydroxyl group. The second ionizable group may influence the electronic configuration of the heme in the alkaline region of pH because of a change in its state of protonation. On the other hand, because of its possible strategic location (in close proximity to the hydroxyl group), it may be capable of protonating the hydroxyl species by intramolecular transfer of a proton (Fig. 2.7). If this latter situation were the case, then, the reduction of HRP-II should be influenced by protonation of this hydroxyl group over the entire range of pH. Since reaction with HRP-II containing the protonated hydroxyl group is diffusion-controlled, reduction should be insensitive to substrate ionizable groups at both acid and

alkaline pH values. However, the substrate pK_a for p-cresol oxidation has a value > 10 . If one accepts the fact that a similar proton transfer mechanism likely governs phenol and aromatic amine oxidation, this piece of evidence, together with the insensitivity to the substrate pK_a values at $pH < 6$, favours the mechanism involving two ionizable groups each independently affecting the heme's electronic environment. The protonated form of the species having $pK_1 < 2$ reacts at the diffusion-controlled rate with the substrate whereas the protonated form of the group having a $pK_2 = 8.6$ does not. The two ionizations may be thought of as influencing the reaction independently rather than one group assisting protonation of the other in the alkaline region of pH. This mechanism has been discussed in Chapter 2 and the resulting log rate -pH profile shown schematically in Fig. 2.8.

In the oxidation of PABA, it is conceivable that electron transfer may occur at the carboxyl rather than the amino group. Protonation of the carboxyl group increases the electron density at the oxygen. The peroxidatic reactivity of phenols is greatly enhanced by protonating the phenolic anion, as has been shown for p-cresol (Critchlow and Dunford, 1972a). These considerations might suggest that the reaction of PABA with HRP-II may occur by way of an electron transfer from the protonated carboxyl oxygen rather than from the aromatic amine. Since the reaction is

diffusion-controlled, the kinetic data cannot yield any information about the center at which electron transfer occurs nor about its state of protonation. More will be said of this later in connection with the HRP-I reaction.

If the log rate-pH relation is considered to result from two ionizations independently influencing the reaction, the pH dependent second-order rate constant may be expressed as the sum of two independent rate constants each influenced by a single ionizable group:

$$k_{3\text{app}} = \frac{k_3''(1 + [H^+]/K_1^\ddagger)}{(1 + [H^+]/K_1)} + \frac{k_3'(1 + [H^+]/K_2^\ddagger)}{(1 + [H^+]/K_2)} \quad (3.51)$$

where k_3' and k_3'' are pH independent rate constants at high pH for reactions influenced by the ground state acid dissociation constants K_2 and K_1 respectively. This transition-state approach adheres to the convention established earlier in this thesis. That is, the pH independent rate constants are arbitrarily taken as the limiting values at high pH. One could have defined the pH independent constants as limiting values at low pH ($k_{3,1}$ and $k_{3,2}$). The resulting equation would then be:

$$k_{3\text{app}} = \frac{k_{3,2}(1 + K_1^\ddagger/[H^+])}{(1 + K_1/[H^+])} + \frac{k_{3,1}(1 + K_2^\ddagger/[H^+])}{(1 + K_2/[H^+])} \quad (3.52)$$

Since $K_1^\ddagger/[H^+] \ll 1$ and $K_2^\ddagger/[H^+] \ll 1$, eq. 3.52 may be simp-

lified to:

$$k_{3\text{app}} = \frac{k_{3,2}}{(1 + K_1/[H^+])} + \frac{k_{3,1}}{(1 + K_2/[H^+])} \quad (3.53)$$

This is tantamount to saying that the transition state acid dissociations are not observed; therefore, they need not be considered in order to define the pH-log rate profile.

However, in order to show that the phenomenological equation used to describe the data will differ only in the interpretation of the parameters A_1 and A_2 (Eq. 3.48), let us return to the original expression of Eq. 3.51. Over the observable pH range $[H^+]/K_1 \ll 1$, $[H^+]/K_1^\ddagger \gg 1$ and $[H^+]/K_2^\ddagger \gg 1$; therefore, upon rearrangement Eq. 3.51 becomes:

$$k_{3\text{app}} = \frac{(k''_3/K_1^\ddagger + k'_3/K_2^\ddagger) [H^+] (1 + [H^+]/(k'_3/k''_3 (K_1^\ddagger K_2/K_2^\ddagger) + K_2))}{(1 + [H^+]/K_2)} \quad (3.54)$$

Thus, the original transition-state dissociation constant K_1^\ddagger identified with A_2 now no longer has any simple significance in terms of transition-state theory but the non-linear least-squares analysis of the data remains unchanged regardless of mechanistic considerations.

The pH dependence of $k_{4\text{app}}$, the second-order rate constant for the HRP-II-PABA complex reacting with PABA, is shown in Fig. 3.20 with tabulated results in Table 3.6. The solid line is the best-fit to the data using Eq. 3.48

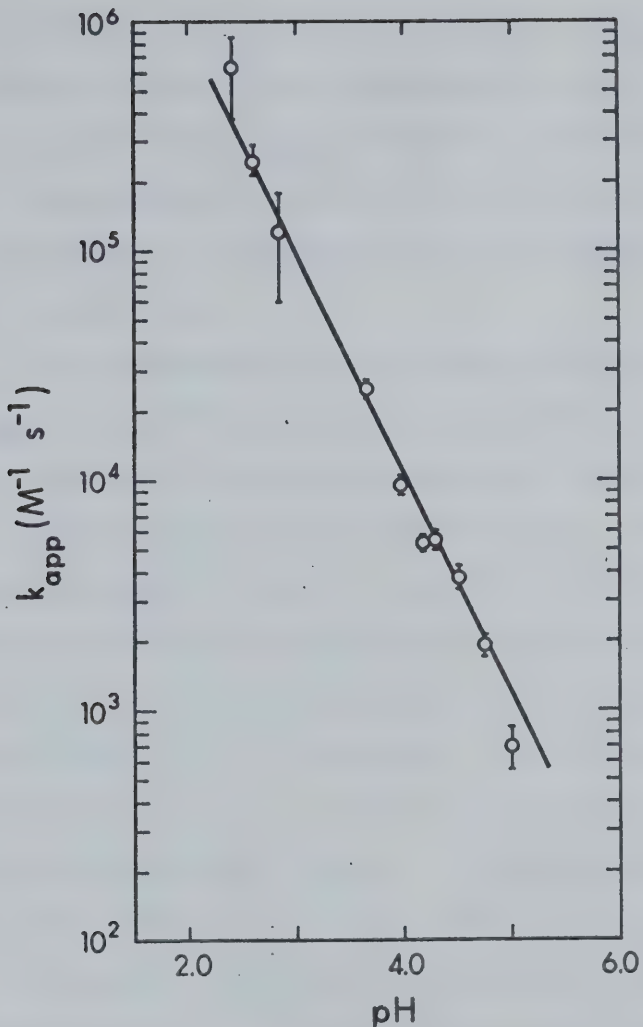


Fig. 3.20: Semilogarithmic plot of $k_{4\text{app}}$ for the HRP-II complex reacting with a second molecule of PABA against pH. The linear relation was determined from a nonlinear least-squares fit to Eq. 3.48 using parameters of Table 3.6. The error bars represent the standard deviation for $k_{4\text{app}}$ estimated from the statistical analysis.

and the parameters of Table 3.6 determined for $k_{3\text{app}}$. The results suggest a similar pH dependence for $k_{3\text{app}}$ and $k_{4\text{app}}$ over the pH range where $k_{4\text{app}}$ could be conveniently investigated. This implies that the proton-transfer mechanisms for the complexed and uncomplexed forms of HRP-II reacting with PABA are the same.

The pH dependence of the second-order rate constant, $k_{2\text{app}}$, for HRP-I reduction with PABA is shown in Fig. 3.11. The solid curve represents the best-fit from a nonlinear least-squares analysis of the data. Again, the similarity of the HRP-I reaction with PABA and ferrocyanide is evident. This similarity between the two pH curves would suggest that one of the ground state pK_a 's for the HRP-I reduction by PABA should be assigned to an ionizable group on the enzyme ($pK_a = 5.1$). This is completely analogous to the HRP-I-ferrocyanide reaction. The other pK_a may be assigned to the amino group on the substrate ($pK_a = 2.7$).

It would be difficult to rationalize the assignment of the pK_a of 5.1 to the substrate's carboxyl group if one assumes that the amino group is the only site for electron transfer. The ground state dissociation constant, $pK_3 = 5.1$, has a value very close to that determined spectrophotometrically for the carboxyl group of PABA. However, protonation of this group should reduce the electron density at the aromatic amine's nitrogen, which should retard the reaction. If the pK_a of 5.1 were assigned to the substrate,

then, the protonated form must react at a faster rate than the anion. This result may be expected only if protonation of the carboxyl group enhances its ability to function as a site for electron transfer. There appears to be very little evidence to support this hypothesis. The literature contains no reports of aromatic acids acting as reducing substrates in the peroxidatic reaction with HRP, whereas the oxidation of aromatic amines is well established (Saunders *et al.*, 1964). The HRP catalyzed oxidations of p-nitroaniline, p-aminoacetophenone, and benzoic acid at pH = 7 are very slow ($k_{app} < 10$) if, indeed, there is any reaction at all (Saunders *et al.*, 1964). No significant reaction was observed for benzoic acid (acetate buffer, pH = 3.8). At benzoic acid concentrations of 5×10^{-3} M and at an enzyme concentration of 8×10^{-6} M the spontaneous decay of HRP-II was observed. The absence of an observable reaction with benzoic acid does not necessarily mean that PABA, with its electron donating amino group, does not react by way of a protonated carboxyl group. But, a decrease of four orders of magnitude upon going from the unsubstituted to the para-amino-substituted aromatic acid (PABA at pH = 3.8 has a rate constant for oxidation by HRP-I and HRP-II of $2.5 \times 10^4 \text{ M}^{-1} \text{ s}^{-1}$) is rather difficult to explain. Studies of HRP-I reduction by iodide, sulfite, and ferrocyanide all exhibit a ground-state pK_a near this value which suggests that it is substrate independent. Therefore,

existing evidence favours the assignment of the pK_a of 5.1 to the enzyme rather than substrate. The schematic diagram of Fig. 3.21 shows a pairing mechanism in which the ground-state acid dissociation constant on the enzyme, K_3 , is paired with the transition-state dissociation constant K_3^\ddagger . The ground-state acid dissociation appearing at pH = 2.7 has been assigned to a substrate acid dissociation K_4 . This ground-state dissociation constant has been paired with the transition-state acid dissociation K_4^\ddagger at pH < 2. Using transition-state theory, the general form of Eq. 2.8 becomes:

$$k_{2\text{app}} = \frac{k'_2(1 + [H^+]/K_3^\ddagger + [H^+]^2/K_3^\ddagger K_4^\ddagger)}{(1 + [H^+]/K_3)(1 + [H^+]/K_4)} \quad (3.55)$$

where k'_2 is the pH independent rate constant observed at high pH. Since the third term in the numerator is always much less than one over the pH range of the study, Eq. 3.55, which describes the pH dependence of $k_{2\text{app}}$ can be written in the form

$$k_{2\text{app}} = \frac{k'_2 (1 + [H^+]/K_3^\ddagger)}{(1 + [H^+]/K_3)(1 + [H^+]/K_4)} \quad (3.56)$$

The parameters obtained by fitting the observed kinetic data to Eq. 3.56 by the method of least-squares are given in Table 3.7. The ionization at $pK_4 = 2.7$ has been assigned

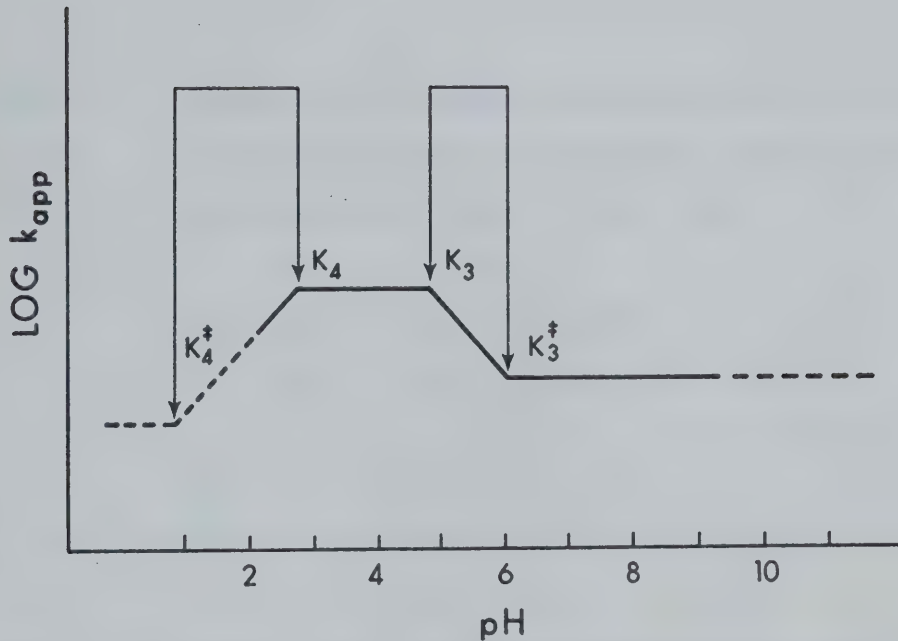


Fig. 3.21: Plot of $\log k_{\text{app}}$ vs. pH for PABA oxidation shown schematically. The solid line represents the experimental curve, whereas the broken line represents the unobservable hypothetical curve at $\text{pH} < 2$. The pairing mechanism consistent with Fig. 2.9 is shown.

Table 3.7: Parameters^a obtained from a nonlinear least-squares analysis for the HRP-I reduction by PABA using Eq. 3.55 for the fit.

$$k_2' = (4.5 \pm 0.1) \times 10^3 \text{ M}^{-1}\text{s}^{-1}$$

$$K_3 = (8.0 \pm 0.9) \times 10^{-6} \text{ M}$$

$$K_4 = (2.1 \pm 0.2) \times 10^{-3} \text{ M}$$

$$K_3^\ddagger = (1.3 \pm 0.1) \times 10^{-6} \text{ M}$$

^aErrors estimated from the standard deviations of the fit.

to the substrate's amino group. No ionization in this region has been observed for either the iodide or sulphite reactions. Protonation of the amino group would be expected to retard the reaction since it blocks the electron pair. The proposed mechanism for the HRP-I reduction with PABA is then, a simple extension of the ferrocyanide reaction with the influence of a substrate protonation appearing at low pH. This would seem to be a reasonable conclusion considering the similarity of the HRP-II reduction with the two substrates, PABA and ferrocyanide.

The values for k_{5app} , the rate constant for the HRP-I-PABA complex reacting with PABA, are tabulated in Table 3.4. There were not sufficient data to allow an accurate nonlinear least-squares estimate of the two parameters K_3 and K_4 controlling the pH dependence of the rates. However, the trend is similar to that for k_{2app} .

Fig. 3.11 summarizes the results obtained for the dissociation constant K_M as a function of pH. The analysis of data obtained for reaction rates measured at the same pH for both HRP-I and HRP-II reduction produced dissociation constants which were, within experimental error, the same. Because of the fast rates which must be measured for the HRP-II reaction in order to investigate conditions of significant binding, the K_M values become less well defined at low pH as the reaction rates increase. Below pH = 2.4, reaction rates could not be measured at

sufficiently high substrate concentration to allow reliable estimation of K_M for the HRP-II-PABA complex. In the HRP-I reaction, the traces for the much slower rates become distorted because of enzyme denaturation at pH < 3. The large error bars of Fig. 3.11, representing the standard deviation from the nonlinear analysis of the rate vs. [PABA] correlations, are a manifestation of these two problems. At pH > 5, the large values of K_M required concentrations of PABA above 5×10^{-2} M. As mentioned previously, above this concentration, substrate interaction may become significant and the kinetics difficult to interpret.

The effect of pH on Michaelis constants has been discussed in detail by Dixon and Webb (1964). The trend toward a pH independent maximum at low pH appeared to justify the analysis of the data in terms of a single ionizable group on either the enzyme or substrate. Because of the unit positive change in slope with decreasing pH, Dixon's (1953) rules eliminate the possibility of this inflection being assigned to an ionization on the complex. Since the ionizable group has a pK_a very close to that expected for the amino group of PABA, it has been tentatively assigned to the substrate. It may be shown that the pH dependent dissociation constant, K_M , defined by the total concentrations of all protonated forms of enzyme $[E]_o$, substrate $[S]_o$ and complex $[ES]_o$:

$$K_M = \frac{[E]_o [S]_o}{[ES]_o} \quad (3.57)$$

may be expressed in terms of a pH independent constant, K'_M , defined by the concentrations of the particular ionic forms of the substrate which affect the reaction:

$$K'_M = \frac{[E]_o [S]}{[ES]_o} \quad (3.58)$$

Since the state of protonation of E and ES, in this case, do not affect the rates, they may be ignored. The concentration term [S] may be defined as the concentration of the protonated amino species, in which case K'_M becomes the pH independent constant at $\text{pH} < 2$. Then K_M and K'_M are related by the Michaelis pH function for the two protonated forms of the PABA amino group:

$$K_M = K'_M (1 + K_4 / [H^+]) \quad (3.59)$$

where K_4 is the dissociation constant for the substrate.

$$\text{Therefore: } \frac{1}{K_M} = \frac{1}{K'_M} \left(\frac{[H^+]}{[H^+] + K_4} \right) \quad (3.60)$$

A nonlinear least-squares analysis resulted in the best-fit curve to this equation in Fig. 3.11. The values of the two variable parameters of this fit, $1/K'_M$ and K_4 are tabulated in Table 3.8.

The dependence of K_M on pH, therefore, indicates

Table 3.8: Parameters^a obtained from a nonlinear least-squares analysis of the $1/K_M'$ fitted to Eq. 3.59

$$K_4 = (1.5 \pm 0.5) \times 10^{-3} \text{ M}$$

$$1/K_M' = (8.6 \pm 0.6) \times 10^{-5} \text{ M}^{-1}$$

^aErrors estimated from the standard deviations of the fit.

the preferential binding of the completely protonated form of the substrate's amino group to a electronegative site on the enzyme. This site, apparently, remains unchanged upon reduction of HRP-I to HRP-II. Any conformational or electronic change occurring in the HRP-I reduction has little effect upon complex formation. No spectral change was observed which could account for a complex with HRP-II. If the magnitude of this spectral change were similar to that observed for the native enzyme it would not be detected by monitoring the amplitude of the stopped-flow trace. This lends credence to the possible explanation that PABA binds near the active site, either on the porphyrin ring or adjacent protein structure. Complex formation then hinders the reaction sterically or changes the electronic nature of the conjugated iron-porphyrin electron-transfer system. Negatively charged species such as ferrocyanide would not associate readily with a basic enzyme site and no complexing would be observed. Although p-cresol may bind to the same site as PABA, the complex formed must be intrinsically different as manifested in the large spectral change upon binding of p-cresol to HRP-II and the much greater inhibitory effect that complex formation has on the enzyme's activity (Critchlow and Dunford, 1972a).

The Steady-State Reaction:

Although observation of the steady-state reaction is potentially a source of considerable information, PABA

oxidation forms a variety of oxidation products (following formation of the initial free radical) which absorb in the UV and visible spectral region. A preliminary investigation in which the initial PABA concentration, $[PABA]_0$, was varied and the initial H_2O_2 concentration, $[H_2O_2]_0$ was held constant, demonstrated that the absorbance change was not a simple function of $[PABA]_0$. In the study of the reaction with H_2O_2 at a much lower concentration than PABA, it was observed that termination of the reaction results from depletion of the oxidizing agent. Therefore, at constant $[H_2O_2]_0$, the total absorbance change, that is, the amplitude of the trace, should always be independent of $[PABA]_0$. However a 7% decrease in the total absorbance change was observed for a three-fold change in $[PABA]_0$ which indicated that this was not the case. Doubling the $[H_2O_2]_0$ should result in an increase in the total absorbance change by a factor of two. Adding equal increments of H_2O_2 to a system containing an excess of PABA, allowing the reaction to consume all the oxidizing agent, then scanning through the UV and visible regions in order to find an area of the spectrum in which the absorbance change was proportional to the $[H_2O_2]_0$, located two potentially useful areas at 440 nm and 320 nm. The absorbance change in the region of 440 nm was too small to provide a good monitor for the reaction. The absorbance change observed at 320 nm was due to absorption by one of the products. The steady-state

kinetic results at 320 nm were the same as obtained at 265 nm but the reduced intensity of this peak allowed one to work at much higher substrate concentrations. Over a five-fold range of $[PABA]_o$ and constant $[H_2O_2]_o$, the latter being present at concentrations much less than the reducing substrate concentration, the total absorbance change was not independent of $[PABA]_o$. The results of a study of the steady-state reaction under such conditions would be difficult to interpret unambiguously. It was therefore decided that this approach was untenable.

3.4 Discussion

The kinetic scheme, summarized in Eq. 3.18 and Eq. 3.25, may be a result of productive or unproductive complex formation. That is, the PABA molecule binding to the HRP intermediate compound may remain complexed upon reduction, in which case it does not partake in the electron-transfer process but only partially inhibits the reaction. Such behaviour would be described as unproductive. On the other hand, the molecule bound to the enzyme may be integrally involved in the electron-transfer process; hence, it may be converted to oxidized product. Then the complex would be productive requiring the second PABA molecule only to trigger substrate oxidation. These two possible situations are kinetically indistinguishable.

This kinetic ambiguity has been discussed in detail for the oxidation of p-cresol by HRP-II (Critchlow

and Dunford, 1972a). Because the dissociation constant for the HRP-II-p-cresol complex and the second-order rate constant for p-cresol oxidation do not depend on a common ionizing group, these authors have argued that the complex is unproductive. Such an argument cannot be applied to PABA oxidation. The pK_4 of 2.8 for the complex formation is probably related to the pK of 2.7 for HRP-I reduction by PABA. The presence of a common ionizable group may argue in favour of productive binding only if it can be assigned to the enzyme and not to the substrate. However, other available evidence implies an unproductive complex. A small spectral change upon complex formation, similar K_M values for all three enzymatic forms, similar pH profiles for the reduction of the complexed and uncomplexed HRP intermediates and the two pieces of evidence discussed earlier, all indicate that PABA does not bind to the iron's sixth coordination position. The complex is unproductive in the sense that it does not promote the peroxidatic activity, but whether the complexed or uncomplexed molecule of PABA that participates in the HRP-I and HRP-II reactions is oxidized cannot be determined unequivocally.

An adequate explanation is desirable for the insensitivity of PABA oxidation by HRP-II to the substrate's ionizable groups. It is difficult to argue that the availability of electrons at the amine's nitrogen atom does not affect the reaction rates. The second-order rate constant

for HRP-II reduction with aniline has been reported as $7 \times 10^4 M^{-1} s^{-1}$ at pH = 7.0 (see Chapter 1). No reaction has been observed for the para-substituted anilines containing strong electron-withdrawing groups such as the acetyl or nitro group (Saunders *et al.*, 1964). If electron density does not explain the disparity in the overall reaction rates, then, oxidation must proceed through a mechanism unique to each substituted aromatic amine. Contrary to this point of view, such structurally different substrates as PABA and ferrocyanide appear to have similar proton-transfer mechanisms. At pH > 7 p-cresol oxidation with HRP-II also exhibits the same pH dependent response.

A diffusion-controlled rate for PABA at pH < 6 adequately explains the lack of sensitivity to the ionizable groups of PABA. Protonation of these groups does alter the electron availability in the transition state to which the oxidation mechanism must be sensitive. However, because the completely protonated form of the substrate reacts at every encounter with the active site of HRP-II, the potentially faster rates of the other two protonated forms of PABA are not observed. These latter two forms cannot react any faster than the diffusion-controlled rate.

The fifty-fold difference between the PABA and ferrocyanide rates of oxidation by HRP-II at pH < 6 may be explained in terms of a larger diffusion-controlled rate constant for the ferrocyanide reaction. Two primary factors

may be involved. In the first case, the effect of the electrostatic interactions between the two reactants must be considered. A theoretical interpretation using equations of Debye (Alberty and Hammes, 1958) suggests that the minimum allowable diffusion-controlled rate involving a positive center (HRP-II) and a highly negatively charged species, such as ferrocyanide, will be faster than for a less negatively charged species such as PABA. The difference in rates may be as large as an order of magnitude ($\mu \sim 10^{-3}$) depending upon the effective charge on the reactants. As the ionic strength increases, the difference in these theoretically permissible values decreases. At ionic strengths comparable to those at which the HRP-II reductions were investigated, the difference in rates predicted likely will be less than an order of magnitude if one assumes that the product of the charges on the reactants is about 8. The second factor deals with the role of orientation constraints on a bimolecular diffusion-controlled rate constant (Schmitz and Schurr, 1972). Using as a model for the reaction a mobile orientable sphere (the substrate) and a localized stationary site on a plane (active site), it was demonstrated, at least qualitatively, that modest angular constraints placed on the access of substrate to the active site can produce a large reduction in the diffusion-controlled rate. It is not unreasonable to expect that the symmetrical ferrocyanide anion with six possible

sites for electron transfer will have a rate of encounters with suitable orientation for reaction which is at least an order of magnitude faster than the rate of effective encounters of the somewhat planar PABA molecule with its single nitrogen group.

The primary difference between the two intermediate compounds, HRP-I and HRP-II, appears to be the storage of an additional oxidizing equivalent in the former case. This may be described in terms of two possible structures for HRP-I. The system may be electron deficient in the conjugated π system of the porphyrin ring which gives rise to a stable porphyrin free radical (Dolphin *et al.*, 1971; Felton *et al.*, 1971). Recently, some doubt has been expressed concerning a free radical in the porphyrin ring because a spectrum resembling HRP-I, apparently, has never been generated for any model system having d-orbitals in the iron atom correctly oriented to accept an electron from the π -ring (R.J.P. Williams, private communication to H.B. Dunford). This may suggest that the unpaired electron is stored on an adjacent amino acid residue as has been described for compound I of cytochrome c peroxidase (Yonetani, 1970). Whichever may be the case, the large shift in the Soret spectral region upon formation and reduction of HRP-I indicates that the electron-transfer processes must influence the electronic configuration of the heme. Any heme-linked ionization, potentially, must be capable of affecting

the kinetics of the electron-transfer process involved in HRP-I and HRP-II reduction. Since it is highly probable that the same ionizable groups are present at the active site of both intermediates, some correlation may exist between the proton-transfer mechanisms affecting their reduction.

As mentioned previously, it has been established that oxygen is incorporated into compound I (Hager *et al.*, 1972); Schonbaum and Lo, 1972). Apparently, this alters the nature of the iron's sixth co-ordination position. It is no longer accessible to cyanide (see Chapter 4). This condition appears not to have changed in HRP-II. Since the sixth position binds cyanide in the native enzyme, the evidence would suggest that protonation of the oxygen-containing ligand at the sixth position in HRP-II (most likely a hydroxyl group) may enhance the ability of this species to function as a leaving group but not in HRP-I. This is not very different from many nucleophilic substitution reactions which are sensitive to protonation of the hydroxyl group. In the native HRP, protonation of this hydroxyl group has a pK_a of 11.0 at an ionic strength of 0.11 (Ellis, 1968). This group (OH_2^+) becomes more acid in HRP-II ($pK_a < 2$). With increasing positive charge in HRP-I, this group may be so acidic that no significant protonation occurs in the observable range of pH. Therefore, the unprotonated hydroxyl group remains at the active site upon HRP-I re-

duction, and the influence of its protonated form on the reaction rates is not significant at pH > 2. The other group, having a pK_a of 8.6 in HRP-II which is shifted to a lower value ($pK_a = 5.1$) with the increased positive charge in HRP-I, is the only ionization observed to influence both HRP-I and HRP-II reduction by PABA and ferrocyanide.

Therefore, the mechanism for the HRP-I reaction with PABA or ferrocyanide may be identified with that for HRP-II reduction at pH > 6. Neither reaction is diffusion-controlled. The HRP-I reduction by PABA is very sensitive to protonation of the amino group. One would expect to see the kinetic influence of the substrate's $pK_a \sim 4.8$ (carboxyl group); however, this is not observed. One explanation may be that the rates are not very sensitive to this ionization. If the kinetic influence of the other group on the enzyme ($pK_a = 5.1$) were dominant, the effect of the substrate pK_a would not be detected. The apparent shift of the pK_a of the amino group to a higher value, when one compares the value obtained from the HRP-II-PABA log rate-pH profile to that obtained from equilibrium studies on the free substrate, may reflect a small influence of the carboxyl group's ionization.

A simple explanation for the HRP-I reaction studied with four reducing agents now emerges. For each of these substrates, namely, PABA, ferrocyanide, iodide and sulfite, HRP-I reduction is influenced by an ionizable

group having a pK_a value of 5.1. If the pairing schemes of Fig. 2.9 and Fig. 3.21 (showing a pK_a paired with a pK_a^{\ddagger} such that $pK_a < pK_a^{\ddagger}$) apply for each reducing substrate, then, the differences in the log rate-pH profiles may be rationalized in terms of the reaction's sensitivity to protonation of this group. The difference $pK_a^{\ddagger} - pK_a$ is a measure of this sensitivity. The oxidation of iodide by HRP-I has a $pK_a^{\ddagger} > 9$. It is more sensitive to protonation of this group ($pK_a \sim 5.1$) than is ferrocyanide with a pK_a^{\ddagger} of 6.6 which, in turn, is more sensitive to protonation than PABA with a pK_a^{\ddagger} of 5.9.

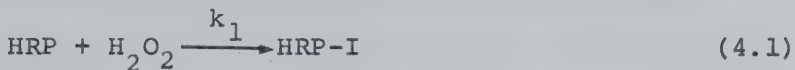
This tentative proposal is a further attempt to organize the available information concerning HRP-catalyzed oxidations and develop a basis for future experimental work. In many respects, it offers a simpler explanation than the mechanism for HRP-II reduction proposed earlier (Critchlow and Dunford, 1972b). Such a modification allows the mechanism for HRP-I reduction, as manifested in the pH dependent rates, to be incorporated readily into the overall picture without substantially changing earlier mechanistic considerations or proposing two different mechanisms for the HRP-I and HRP-II reactions. This mechanistic point of view has the unique ability of explaining the influence of a substrate ionization in the pH profile for p-cresol and the absence of influence of the two expected substrate ionizations for PABA in HRP-II reduction.

CHAPTER 4

THE KINETIC EFFECT OF CYANIDE INHIBITION ON THE
STEADY-STATE PEROXIDATION CATALYZED BY
HORSERADISH PEROXIDASE

4.1 Introduction

The following oxidation-reduction cycle of HRP is well established (George, 1952, 1953; Chance, 1952);



The reactions in Eq. 4.2 and Eq. 4.3 have been studied intensively as a function of pH as is evident from the material of Chapter 2. As well, cyanide is known to bind tightly to the heme iron of native HRP and the kinetics of both its binding and dissociation reactions have been studied (Ellis and Dunford, 1968). However, if the sixth co-ordination position of the iron is occupied by some other ligand in the enzyme's intermediate compounds, the cyanide should have restricted access to this site. Therefore, to further elucidate the nature of the active site and to provide evidence as to whether p-cresol, PABA and other substrates, which may alter the enzyme's activity, bind to this site, a study of cyanide binding to HRP-I

and HRP-II was undertaken. Two approaches were used:

(1) the effect of cyanide on the steady-state ferrocyanide oxidation was investigated, and (2) a possible spectral change in the Soret region of HRP-II upon cyanide addition was examined.

4.2 Experimental

Materials:

Horseradish peroxidase was obtained from Boehringer-Mannheim as a highly purified ammonium sulfate suspension and the solutions prepared and analyzed as described in Chapter 2. Solutions of potassium ferrocyanide, potassium nitrate and hydrogen peroxide were prepared and handled as described previously. Kinetic studies were performed in solutions with an ionic strength, μ , of 0.11 ± 0.002 with the buffer contributing 0.06μ and potassium nitrate 0.05μ at pH 7.10 and 5.00. At pH 9.00 the glycine buffer contributed 0.01 to the ionic strength and potassium nitrate 0.10. Appropriate adjustments were made in the potassium nitrate concentration when the total contribution of potassium ferrocyanide and potassium cyanide to ionic strength exceeded 2%. Solutions of potassium cyanide were analyzed by titration with a standard silver nitrate solution (Kolthoff and Sandell, 1952).

Steady-State Kinetic Studies:

The kinetic measurements were performed on a Cary 14 recording spectrophotometer equipped with a slide

wire for the absorbance range 0 to 0.1 absorbance units. The cell compartments were thermostatted at 25°C. In a typical experiment, appropriate volumes of potassium nitrate solution (1.00 M) and buffer ($\mu = 0.20$) were pipetted into a 250 ml volumetric flask to obtain a solution of $\mu = 0.22$. A 5 ml aliquot was pipetted into a 10 ml volumetric flask and solutions of HRP, ferrocyanide, and cyanide were added by microsyringe. The solution was made up to volume and 2 ml pipetted into a cuvette which was inserted into a cell compartment, and allowed to equilibrate to 25°. The reaction was initiated by stirring the solution with a plumper on which was deposited a few microliters of hydrogen peroxide. The production of ferricyanide was followed at 420 nm. An initial velocity was determined by estimating the slope at the beginning of the trace.

At any given set of conditions four traces were obtained and the estimated initial velocities were used to calculate a mean value. The pH of the solution was determined immediately upon obtaining the traces using an Orion model 801 digital pH meter in conjunction with a Fisher combination electrode. At pH 9.00 the cyanide solution was adjusted to the pH of the buffer prior to each kinetic study.

Spectral Measurements:

It was found that reasonably stable solutions containing a mixture of HRP and HRP-II could be prepared

from a 10^{-6} M HRP solution in tris-nitric acid buffer of pH 7.0 and ionic strength 0.06. Sufficient potassium nitrate was added to bring the total ionic strength to 0.11. The HRP solution was allowed to stand at room temperature for several days. Compound I was prepared by adding 0.9 molar equivalents of hydrogen peroxide, relative to the total amount of HRP, with a microliter syringe to 2.0 ml of solution in a cuvette. Compound II was obtained by reduction with 0.5 molar equivalents of p-cresol, also relative to the total amount of HRP. The resulting spectrum was isosbestic with the spectrum of native HRP at 411 nm. It showed no detectable change at 420 nm after 10 minutes, a time sufficient to permit the complete execution of the experiments.

In order to demonstrate that HRP-I had been reduced successfully to HRP-II, the prepared mixture of HRP and HRP-II was observed at 411 nm. At this wavelength any absorbance change should not be related to HRP-II conversion to HRP. Excess p-cresol was then added to the solution and the change was observed to be 10^{-3} absorbance units. Therefore, at a total enzyme concentration of 10^{-6} M, < 2.5% of the enzyme must be present as HRP-I.

A difference spectrum was obtained by removing the cuvette containing water as a reference and inserting a matching cuvette containing the original HRP solution to which 2.0×10^{-3} M potassium cyanide had been added.

Then, the sample containing the components HRP and HRP-II was scanned from 450 nm to 390 nm. Critchlow and Dunford (1972) used a similar approach in their studies of the binding of p-cresol to native HRP. Addition of 5×10^{-4} M cyanide to the sample permitted one to obtain a difference spectrum of the resulting mixture. A rapid spontaneous decay of a fraction of the HRP-II was observed, caused by small quantities of reducing agent in the cyanide which was followed by a period where the HRP-II was comparatively stable. The decay was estimated to be 10% of the total HRP-II present, and a correction was made for this concentration change in later calculations. At 5×10^{-4} M cyanide the error involved upon assuming that all of the native HRP is present as the cyanide complex is < 1%.

4.3 Results

Steady-State Kinetic Studies:

Previous work (see Chapter 2) has demonstrated that the steady-state peroxidase catalyzed oxidation of ferrocyanide obeys the double reciprocal form of Lineweaver-Burk:

$$\frac{1}{v} = \frac{K}{V} \left(\frac{1}{A} \right) + \frac{1}{V} \quad (4.4)$$

Using the nomenclature and symbolism of Cleland (1963), v is the initial velocity, A the initial concentration of the variable substrate, V the apparent maximum velocity,

and K the apparent Michaelis constant. Previous work has shown that cyanide binds to the native enzyme to form a complex over a wide range of pH (Ellis and Dunford, 1968; Chance, 1943). Thus, it functions as a dead-end inhibitor. With cyanide present the steady-state ferrocyanide oxidation should give rise to linear uncompetitive inhibition if cyanide combines reversibly with only one enzyme form, native HRP. The general form of the double reciprocal plot then becomes:

$$\frac{1}{v} = \frac{K}{V} \left(\frac{1}{A} \right) + \frac{1}{V} \left(1 + \frac{I}{K_i} \right) \quad (4.5)$$

where I is the initial inhibitor concentration, and K_i is the inhibition constant. However, if cyanide binds to more than one form of the enzyme, that is, to either or both of HRP-I and HRP-II, then the general form is one of linear noncompetitive inhibition:

$$\frac{1}{v} = \frac{K}{V} \left(1 + \frac{I}{K_{is}} \right) \left(\frac{1}{A} \right) + \left(\frac{1}{V} - \frac{1}{V} + \frac{I}{K_i} \right) \quad (4.6)$$

Thus, because of the effect of the apparent inhibition constant K_{is} , the slope of the double reciprocal plot would change with changing initial inhibitor concentration.

Based on the general reaction scheme shown in Fig. 4.1, the specific equation analogous to Eq. 4.6 is

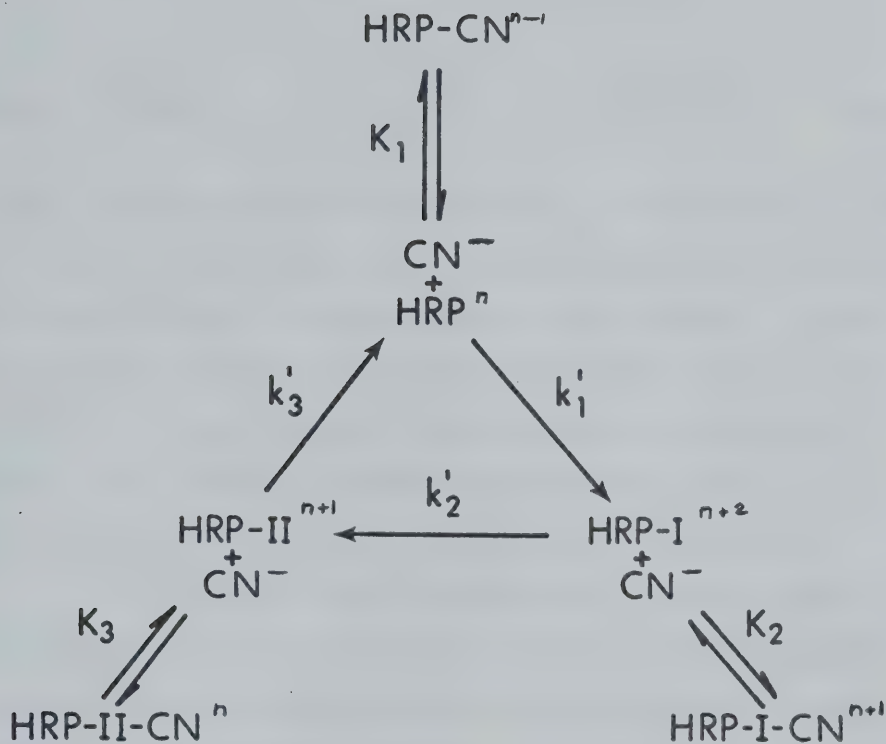


Fig. 4.1: The HRP reaction cycle, showing the possibility of cyanide binding to all forms of HRP. CN represents all forms of cyanide, $k'_1 = k_1[\text{H}_2\text{O}_2]_0$, $k'_2 = k_2[\text{Fe}(\text{CN})_6^{-4}]_0$, and $k'_3 = k_3[\text{Fe}(\text{CNO})_6^{-4}]_0$.

$$\frac{[HRP]_0}{v} = \frac{1}{2k_1[H_2O_2]_0} \left(1 + \frac{[CN]_0}{K_1} \right) + \left[\frac{k_2 + k_3}{2k_2k_3} + \left(\frac{1}{2k_2K_2} + \frac{1}{2k_3K_3} \right) [CN]_0 \right] \frac{1}{[Fe(CN)_6^{-4}]_0} \quad (4.7)$$

In this equation the initial velocity is expressed in terms of the second order rate constants, dissociation constants and concentrations of the reactants and inhibitor. The initial concentrations $[CN]_0$ and $[Fe(CN)_6^{-4}]_0$ refer to all protonated and unprotonated forms of cyanide and ferrocyanide. The relation between the constants of Eq. 4.6 and the parameters of Eq. 4.7 is shown in Table 4.1.

To minimize experimental error, optimum conditions were selected to detect cyanide binding. Initial cyanide concentrations were chosen such that an excess, as large as possible, was present without the first term of Eq. 4.7 becoming dominant. In order to use an initial cyanide concentration of 10^{-4} M or greater, a condition required for adequate experimental sensitivity to binding, a concentration of hydrogen peroxide $> 10^{-4}$ M was necessary at pH = 5.00. At an initial concentration of 7.5×10^{-4} M hydrogen peroxide the first term of Eq. 4.7 was not rate-limiting, but enzyme denaturation appeared to alter the reaction trace. However, the rate of destruction was slow and did not affect the measurement of the initial steady-

TABLE 4.1

A Table Relating Parameters from General and Specific
Steady-State Equations (Eqs. 4.6 & 4.7).

$$K = \frac{k_1(k_2 + k_3)}{k_2 k_3} [H_2O_2]_0$$

$$K_i = K_1$$

$$K_{is} = \frac{K_2 K_3 (k_2 + k_3)}{k_2 K_2 + k_3 K_3}$$

$$V = 2k_1 [HRP]_0 [H_2O_2]_0$$

state velocity. For an accurate estimate of the initial velocity, an initial absorbance change of > 0.002 absorbance units/minute was required. For this reason, the initial HRP concentration was always large enough to provide a reaction rate satisfying this minimum requirement, but small enough to permit a rapid attainment of the steady-state. Similarly, the initial ferrocyanide concentration was always large enough to provide a sufficiently linear initial portion of the absorbance *vs.* time trace but small enough to enhance the importance of the second term in the right side of Eq. 4.7.

The double reciprocal plots obtained at pH 5.00 for different cyanide concentrations are shown in Fig. 4.2. Similar results were obtained at pH 7.10 and 9.00. The slopes of the double reciprocal plots from these data are tabulated in Table 4.2. Fig. 4.3 is a plot of these slopes at pH 9.00 against the cyanide concentration. The slope of such a plot determined for all three pH values by linear least-squares analysis was zero within the estimated error limits. These results are shown in Table 4.3.

The kinetic data clearly indicate that this steady-state system satisfies the case of uncompetitive inhibition. If one considers the estimated errors in Table 4.3, then cyanide binding occurring to either HRP-I or HRP-II at pH 5.00 must be such that $(1/2 k_2 K_2 + 1/2 k_3 K_3) \leq 3.6 \times 10^{-4}$ s. If the hypothetical case is considered in which no binding

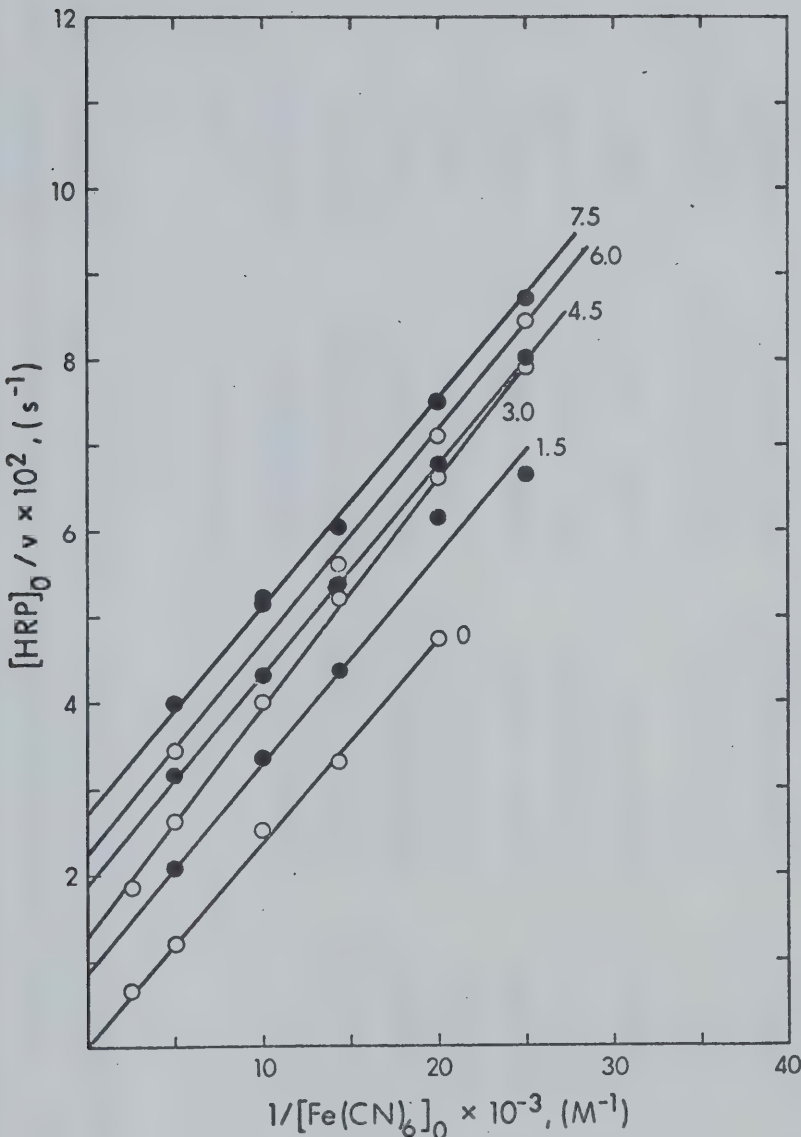


Fig. 4.2: The double reciprocal plots of $[HRP]_0/v$ vs. $1/[Fe(CN)_6]_0^{-1}$ at pH 5.00 with $[CN]_0$ varying from 0 to 7.5×10^{-4} M. The invariant slope and changing intercept is characteristic of uncompetitive inhibition.

TABLE 4.2

Slopes and Intercepts of the Double Reciprocal Plots of $[HRP]_0/v$ vs. $1/[Fe(CN)_6^{-4}]_0$ as a function of $[CN]_0$. Errors were estimated from twice the standard deviation of the linear least-squares analysis. The calculated intercepts were determined as described in the text.

PH, Buffer and Ionic Strength	$[CN]_0, M$	Slope, M-S	Observed Intercept, s	Calculated Intercept, s
5.00	0.0	$(2.3 \pm 0.1) \times 10^{-6}$	$(6.6 \pm 6.0) \times 10^{-4}$	3.3×10^{-4}
Acetic Acid	1.5×10^{-4}	$(2.5 \pm 0.2) \times 10^{-6}$	$(8.6 \pm 2.7) \times 10^{-3}$	8.1×10^{-3}
Sodium Acetate ($\mu = 0.01$)	3.0×10^{-4}	$(2.8 \pm 0.1) \times 10^{-6}$	$(1.2 \pm 0.1) \times 10^{-2}$	1.2×10^{-2}
KNO ₃ ($\mu = 0.10$)	4.5×10^{-4}	$(2.4 \pm 0.1) \times 10^{-6}$	$(1.9 \pm 0.1) \times 10^{-2}$	1.8×10^{-2}
	6.0×10^{-4}	$(2.5 \pm 0.3) \times 10^{-6}$	$(2.3 \pm 0.1) \times 10^{-2}$	2.3×10^{-2}
	7.5×10^{-4}	$(2.3 \pm 0.1) \times 10^{-6}$	$(2.8 \pm 0.1) \times 10^{-2}$	2.8×10^{-2}
7.10	0.0	$(2.1 \pm 0.3) \times 10^{-5}$	$(4.6 \pm 16.2) \times 10^{-3}$	3.3×10^{-4}
KH ₂ PO ₄ -Na ₂ HPO ₄ ($\mu = 0.06$)	1.5×10^{-4}	$(2.3 \pm 0.1) \times 10^{-5}$	$(2.4 \pm 0.8) \times 10^{-2}$	2.1×10^{-2}
	3.0×10^{-4}	$(2.2 \pm 0.1) \times 10^{-5}$	$(3.2 \pm 1.2) \times 10^{-2}$	4.2×10^{-2}
	4.5×10^{-4}	$(2.1 \pm 0.2) \times 10^{-5}$	$(6.7 \pm 2.0) \times 10^{-2}$	6.3×10^{-2}

(Table continued on next page)

Table 4.2 continued

PH, Buffer and Ionic Strength	[CN] ₀ , M	Slope, M-s	Observed Intercept, s	Calculated Intercept, s
KNO ₃ (μ = 0.05)	6.0x10 ⁻⁴	(2.2±0.1)x10 ⁻⁵	(5.1±0.8)x10 ⁻²	8.3x10 ⁻²
	7.5x10 ⁻⁴	(2.5±0.2)x10 ⁻³	(7.4±1.0)x10 ⁻²	1.0x10 ⁻¹
9.00	0.0	(1.4±0.1)x10 ⁻⁴	-(7.3±4.6)x10 ⁻³	3.3x10 ⁻⁴
Glycine-sodium Glycinate (μ = 0.01)	5.0x10 ⁻⁴	(1.4±0.1)x10 ⁻⁴	-(3.5±4.8)x10 ⁻³	2.7x10 ⁻²
	1.0x10 ⁻³	(1.3±0.1)x10 ⁻⁴	(8.0±2.2)x10 ⁻³	5.3x10 ⁻²
	1.5x10 ⁻³	(1.4±0.1)x10 ⁻⁴	(1.1±0.6)x10 ⁻¹	7.9x10 ⁻²
	2.0x10 ⁻³	(1.4±0.1)x10 ⁻⁴	(1.0±0.3)x10 ⁻¹	1.0x10 ⁻²
KNO ₃ (μ = 0.10)				

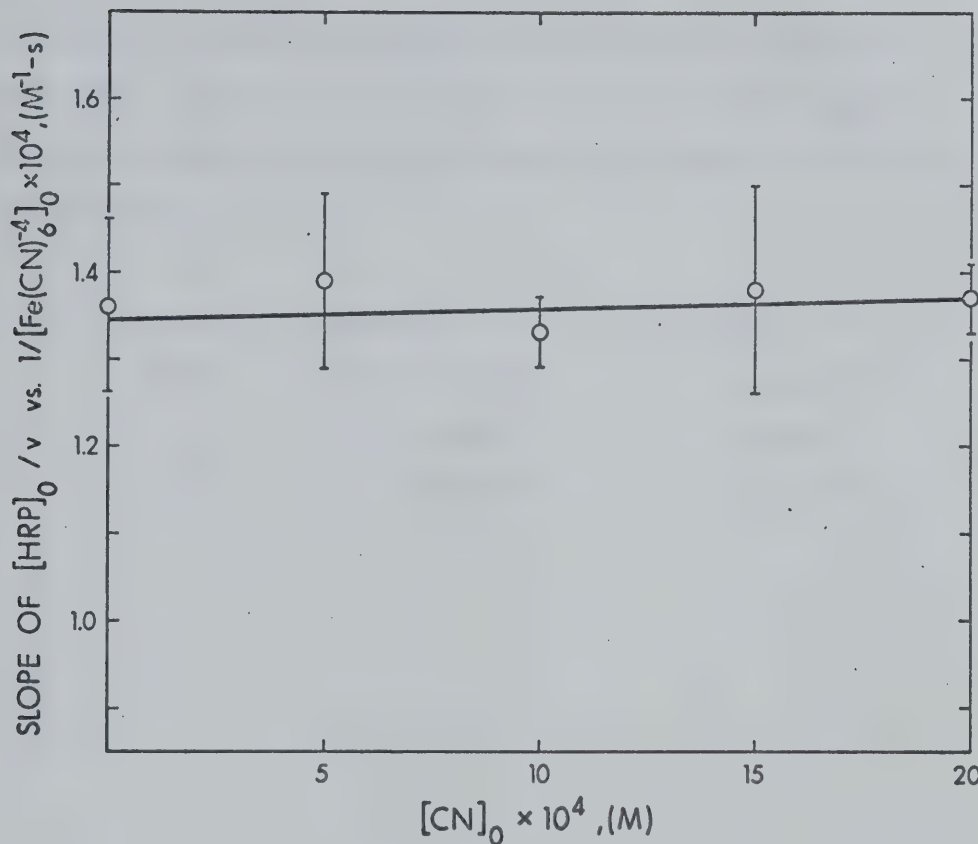


Fig. 4.3: The slopes of $[HRP]_0/v$ vs. $1/[Fe(CN)_6]_0^{-4}$ plots as a function of cyanide concentrations of pH 9.00. The error bars indicate twice the standard deviation obtained from a weighted linear least-squares determination of the slopes.

TABLE 4.3

The slope of $[HRP]_0 [Fe(CN)_6^{4-}]_0 / v$, the slopes of Table 4.2, vs. $[CN]_0$. The estimated errors represent the standard deviation determined by the linear least-squares analysis of the data.

pH	Slope, s	Intercept, M-s
5.00	$-(1.6 \pm 3.6) \times 10^{-4}$	$(2.5 \pm 0.2) \times 10^{-6}$
7.10	$(3.0 \pm 2.6) \times 10^{-3}$	$(2.1 \pm 0.1) \times 10^{-5}$
9.00	$(1.4 \pm 2.6) \times 10^{-3}$	$(1.3 \pm 0.1) \times 10^{-4}$

occurs to HRP-II then $K_2 \geq 1.9 \times 10^{-4}$ M. Similarly, if no binding occurs to HRP-I, then $K_3 \geq 6.9 \times 10^{-3}$ M. The spectrophotometrically determined K_1 for HRP-CN was 2.0×10^{-6} M. Therefore, any binding which occurs to HRP-I and HRP-II must be smaller by factors of 10^2 and 3.5×10^3 than that which occurs to HRP at pH 5.00. Similarly at pH 7.10 $K_2 \geq 2.4 \times 10^{-4}$ M, $K_3 \geq 9.3 \times 10^{-3}$ M, and at pH 9.00 $K_2 \geq 4.6 \times 10^{-4}$ M, $K_3 \geq 6.6 \times 10^{-2}$ M.

Using the general scheme for first order series and parallel reactions described in detail by Matsen and Franklin (1950), a computer program was written in order to calculate the pre-steady-state changes in intermediate concentrations. The relevant equations and a brief description of the program are to be found in Appendix 2. The program considered the steady-state cycle as outlined in Eqs. 4.1 - 4.3 and the case of cyanide binding to the native enzyme, as was indicated experimentally. It made no provision for changing hydrogen peroxide or ferrocyanide concentrations, which are components of the system present in sufficient excess to ensure pseudo-first-order conditions. Published rate constants for the oxidation of ferrocyanide (Chapter 2) and the reversible binding of cyanide (Ellis and Dunford, 1968) were used in the calculations. The computed results showed that, for all conditions used, the steady-state concentrations of enzyme species were attained to within 99% after 10 seconds, the approximate dead-time

of the instrument. The linear correlation obtained by plotting the initial velocity *vs.* HRP concentration at pH 5.00, shown in Fig. 4.4, provides experimental evidence of the validity of the steady-state approximation. A significant spontaneous reaction in the absence of HRP was observed only at pH 5.00 in the presence of cyanide. This spontaneous rate was never more than 20% of the observed initial velocity and could be completely accounted for as a small increase in the intercept of the Lineweaver-Burk double reciprocal plot shown in Fig. 4.4.

From published parameters (Ellis and Dunford, 1968; Chance, 1949) the intercepts from the double reciprocal plots were calculated. These are tabulated in Table 4.2 along with experimentally determined intercepts. The measured spontaneous rate was added to the calculated intercepts at pH 5.00, and it is the sum of these two quantities which is reported in Table 4.2. Satisfactory agreement with the observed intercepts was obtained. The value of K_3 , $2.0 \times 10^5 \text{ M}^{-1} \text{ s}^{-1}$, calculated from the results at pH 5.00, is in good agreement with a previous value obtained for the steady-state ferrocyanide oxidation of $1.9 \times 10^5 \text{ M}^{-1} \text{ s}^{-1}$. Similarly, the k_3 value calculated from results at pH 9.00 of $3.8 \times 10^3 \text{ M}^{-1} \text{ s}^{-1}$ is in good agreement with previous results (Hasinoff and Dunford, 1970).

At pH 7.10 with phosphate present at ionic strength 0.06, total ionic strength 0.11, the calculated

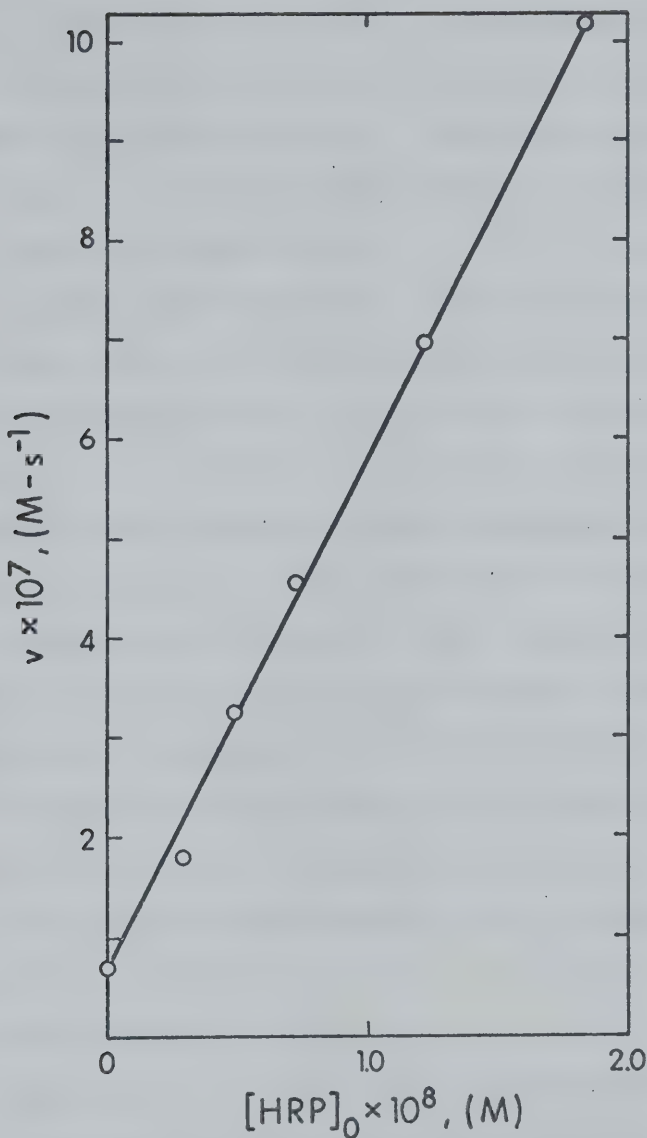


Fig. 4.4: The initial velocity plotted against $[\text{HRP}]_0$ at pH 5.00. The linear correlation demonstrates that the initial rate is first order with respect to $[\text{HRP}]_0$ under steady-state conditions with $[\text{CN}]_0 = 3 \times 10^{-4} \text{ M}$.

value of k_3 was $2.4 \times 10^4 \text{ M}^{-1} \text{ s}^{-1}$. This result was about 50% larger than would have been predicted for the steady-state system from previous work. Experiments performed in tris-nitric acid buffer, under otherwise identical conditions, gave a k_3 value of $1.4 \times 10^4 \text{ M}^{-1} \text{ s}^{-1}$ in agreement with the earlier investigations. The rate constant calculated from a duplicate set of double reciprocal plots at pH 7.20 and phosphate buffer at $\mu = 0.01$ (potassium nitrate $\mu = 0.10$) was $1.4 \times 10^4 \text{ M}^{-1} \text{ s}^{-1}$. This provided good evidence for a buffer effect observed in the phosphate buffer with the larger contribution to the total ionic strength. At pH 7.0 in tris buffer the second order rate constant was $7.0 \times 10^4 \text{ M}^{-1} \text{ s}^{-1}$ at a total ionic strength of 0.02. Therefore, there were two effects observed at neutral pH. The rate was accelerated by increasing the concentration of phosphate while the ionic strength was invariant. In addition, the rate decreased sharply with increasing ionic strength of the solution.

Spectral Measurements:

The spectral results were obtained from solutions of HRP-II and HRP to which cyanide had been added. If it is assumed that no cyanide binds to HRP-II, then the only enzyme species present in solution in appreciable amounts are HRP-II and HRP-CN. The change in the spectrum at any given wavelength upon cyanide addition is then related to the absorbance change occurring upon conversion of HRP to

HRP-CN:

$$\Delta A_D = \epsilon_{\text{HRP}}[\text{HRP}] - \epsilon_{\text{CN}}[\text{HRP-CN}] \quad (4.8)$$

The difference in the absorbance between the two spectra, without and with excess cyanide, is ΔA_D , and ϵ_{CN} is the molar absorptivity of the HRP-CN. From a spectrum of the HRP-CN complex the molar absorptivity was determined at any wavelength relative to the calibration value of $9.4 \times 10^4 \text{ M}^{-1} \text{ cm}^{-1}$ at 423 nm (Keilin and Hartree, 1951). The calculated and observed values for ΔA_D are presented in Table 4.4 for a number of wavelengths. Within the estimated error there is good agreement. Thus, the spectral changes occurring upon cyanide addition may be accounted for in terms of only two species present in the cyanide solution, namely, HRP-CN and HRP-II. Other species which may be formed upon cyanide addition either must have spectra very similar to HRP-CN and HRP-II or the total contribution which they make to the observed absorption at any given wavelength must be less than about 10%.

4.4 Discussion

The results obtained provide no evidence for extensive binding of cyanide to either of the two intermediate enzyme forms. Any major interaction of cyanide with HRP-I or HRP-II, if it occurs (Fridovich, 1963), must take place at some site removed from the prosthetic group. This must necessarily cause only small, undetectable conformational

TABLE 4.4

Calculated and observed changes in absorbances at several wavelengths in the Soret region for mixtures of HRP and HRP-II with and without cyanide present. Concentrations: [HRP] = 2.0×10^{-7} M, [HRP-II] = 8.0×10^{-7} M, [HRP-CN] = 2.2×10^{-7} M.

(A.U. : absorbance units)

Wavelength nm	$\epsilon_{\text{HRP}}' \text{ M}^{-1} \text{cm}^{-1}$	$\epsilon_{\text{CN}} \text{M}^{-1} \text{cm}^{-1}$	$\Delta A_D, \text{CAL}, \text{A.U.}$ cal.	$\Delta A_D, \text{OBS}', \text{A.U.}$ obs.
390	7.6×10^4	2.8×10^4	$(9.1 \pm 0.5) \times 10^{-2}$	$(8.5 \pm 0.5) \times 10^{-2}$
400	8.9×10^4	4.3×10^4	$(8.4 \pm 0.5) \times 10^{-2}$	$(8.5 \pm 0.5) \times 10^{-2}$
410	8.4×10^4	6.2×10^4	$(3.0 \pm 0.5) \times 10^{-2}$	$(2.5 \pm 0.5) \times 10^{-2}$
420	5.2×10^4	9.3×10^4	$-(1.0 \pm 0.5) \times 10^{-1}$	$-(9.5 \pm 0.5) \times 10^{-2}$
430	3.1×10^4	1.1×10^5	$-(9.5 \pm 0.5) \times 10^{-2}$	$-(9.5 \pm 0.5) \times 10^{-2}$
440	1.9×10^4	3.2×10^4	$-(3.3 \pm 0.5) \times 10^{-2}$	$-(4.0 \pm 0.5) \times 10^{-2}$
450	1.4×10^4	2.0×10^2	$-(1.5 \pm 0.5) \times 10^{-2}$	$-(2.3 \pm 0.5) \times 10^{-2}$

or electronic changes at the active site. In such a case, the binding would be not only unobservable with the techniques used, but also, under these conditions, of little kinetic significance.

It is generally accepted that the observed complex formation with native HRP involves the interaction of cyanide with the heme at the sixth co-ordination position (Smith and Williams, 1970). Apparently, in HRP-I and HRP-II this binding site is occupied by a tightly co-ordinated species which cyanide is unable to displace. This is in agreement with recent O^{18} labelling experiments on chloroperoxidase (Hager *et al.*, 1973). It is also in agreement with the point of view discussed in Chapter 3 that the displacement of the bound species in HRP-II is accelerated by protonation of this bound group. The influence of ionic strength on the reaction rate indicates that reduction of HRP-II with ferrocyanide involves the approach of oppositely charged species. The large effect of ionic strength suggests that the species involved have large electrostatic charges associated with them as one would expect in the case of the ferrocyanide anion interacting with a positive center. Thus, the data offer reasonable support to the argument of Chapter 3 in which the electrostatic interaction of the reactants for the HRP-II reduction was used to explain, at least in part, the possible difference in the diffusion-controlled rates for ferrocyanide and PABA oxidation.

References

1. AGNER, K. (1941), *Acta Physiol. Scand.* 2, Suppl. 8.
2. AGNER, K. (1958), *Acta Chem. Scand.* 12, 89.
3. ALBERT, A. and GOLDACRE, R. (1942), *Nature* 149, 245.
4. ALBERTY, R.A. and BLOOMFIELD, V. (1963), *J. Biol. Chem.* 238, 2804.
5. ALBERTY, R.A. and HAMMES, G.G. (1958), *J. Phys. Chem.* 62, 154.
6. ALTSCHUL, A.M., ABRAMS, R. and HOGNESS, T.R. (1940), *J. Biol. Chem.* 136, 777.
7. ANDREJEN, A., GERNEZ-RIEUX, C. and TACQUET, A. (1959), *Bull. Soc. Chim. Biol.* 41, 1047.
8. BACH, A.N. and CHORDAT, R. (1903), *Ber. Dtsch. Chem. Ges.* 36B, 606.
9. BAGGER, S. and WILLIAMS, R.J.P. (1971), *Acta Chem. Scand.* 25, 976.
10. BALLS, A.K. and HALE, W.S. (1934), *J. Biol. Chem.* 107, 767.
11. BARB, W.G., BAXENDALE, J.H., GEORGE, P. and HARGRAVE, K.R. (1949), *Nature* 163, 692.
12. BARB, W.G., BAXENDALE, J.H., GEORGE, P. and HARGRAVE, K.R. (1951a), *Trans. Faraday Soc.* 47, 462.
13. BARB, W.G., BAXENDALE, J.H., GEORGE, P. and HARGRAVE, K.G. (1951b), *Trans. Faraday Soc.* 47, 591.
14. BATEMAN, L. (1954), *Quarterly Reviews* 8, 147.

15. BAUMGARTNER, J. and NEUKON, H. (1972), *Chimia* 26, 366.
16. BAXENDALE, J.H. (1952), *Advances in Catalysis* 4, 31.
17. BIRK, J.P. (1969), *J. Am. Chem. Soc.* 91, 3189.
18. BLUMBERG, W.E., PEISACH, J., WITTENBERG, B.A. and WITTENBERG, J.B. (1968), *J. Biol. Chem.* 243, 1854.
19. BOESEKEN, J. (1930), *Proc. Acad. Sci. Amst.* 33, 134.
20. BRILL, A.S. (1966), *Comp. Biochem.* 14, 447.
21. BRILL, A.S. and SANDBERG, H.E. (1968), *Biochemistry* 7, 4254.
22. BRILL, A.S. and WILLIAMS, R.J.P. (1961), *Biochm. J.* 78, 253.
23. BROWN, H.C. and FLETCHER, R.S. (1949), *J. Am. Chem. Soc.* 71, 1845.
24. BROWN, S.B. and JONES, P. (1968), *Trans. Faraday Soc.* 64, 994,999.
25. BROWN, S.B., JONES, P. and SUGGETT, A. (1968), *Trans. Faraday Soc.* 64, 986.
26. BRUSCHWEILER, H. and MINKOFF, G.J. (1955), *Anal. Chim. Acta* 12, 186.
27. CHANCE, B. (1943), *J. Cell. Comp. Physiol.* 22, 33.
28. CHANCE, B. (1949a), *Arch. Biochem. Biophys.* 22, 224.
29. CHANCE, B. (1949b), *J. Biol. Chem.* 179, 1341.
30. CHANCE, B. (1949c), *Science* 109, 224.
31. CHANCE, B. (1951), *The Enzymes* 2, Part I, 428.
32. CHANCE, B. (1952a), *Arch. Biochem. Biophys.* 37, 235.

33. CHANCE, B. (1952b), *Arch. Biochem. Biophys.* 40, 153.
34. CHANCE, B. (1952c), *Arch. Biochem. Biophys.* 41, 416.
35. CHANCE, B. and PAUL, K.G. (1960), *Acta. Chem. Scand.* 14, 1711.
36. CHAPMAN, N.B. and SAUNDERS, B.C. (1941), *J. Chem. Soc.*, 496.
37. CHEN, J.H. (1968), Ph.D. Thesis (University of California, Riverside, Calif.), Order No. 69-10092, Univ. Microfilms, Ann Arbor, Mich.
38. CLELAND, W.W. (1963), *Biochim. Biophys. Acta* 67, 173.
39. COHEN, G. and HOCHSTEIN, P. (1963), *Biochemistry* 2, 1420.
40. COTTON, M.L. and DUNFORD, H.B. (1973), *Can. J. Chem.* (in press).
41. COTTON, M.L., DUNFORD, H.B. and RAYCHEBA, J.M.T. (1973), *Can. J. Biochem.* (in press).
42. CRITCHLOW, J.E. and DUNFORD, H.B. (1972a), *J. Biol. Chem.* 247, 3703.
43. CRITCHLOW, J.E. and DUNFORD, H.B. (1972b), *J. Biol. Chem.* 247, 3714.
44. CRITCHLOW, J.E. and DUNFORD, H.B. (1972c), *J. Theor. Biol.*, 37, 307.
45. DELINCÉE, H. and RADOLA, B.J. (1970), *Biochim. Biophys. Acta* 200, 204.
46. DIXON, M. (1953), *Biochem. J.* 55, 161.

47. DIXON, M. and WEBB, E.C. (1964), *Enzymes*, 2nd Ed., London, LONGMANS, GREEN, 116-145.
48. DOLIN, M.J. (1957), *J. Biol. Chem.* 225, 557.
49. DOLIN, M.J. (1961), in *The Bacteria 2*, Acad. Press, New York, N.Y., 425.
50. DOLPHIN, D., FORMAN, A., BORG, D.C., FAJER, J. and FELTON, R.H. (1971), *Proc. Nat. Acad. Sci. U.S.* 62, 614.
52. DOUZOU, P., SIREX , R. and TRAVERS, F. (1970), *Proc. Nat. Acad. Sci. U.S.* 66, 787
53. DOUZOU, P. (1971a), *Biochimie* 53, 17
54. DOUZOU, P. (1971b), *Biochimie* 53, 307.
55. DUNFORD, H.B. and ALBERTY, R.A. (1967), *Biochemistry* 6, 447.
56. ELLIOT, K.A.C. (1932), *Biochem. J.* 26, 10.
57. ELLIS, W.D. and DUNFORD, H.B. (1968a), *Can. J. Biochem.* 46, 1231.
58. ELLIS, W.D. and DUNFORD, H.B. (1968b), *Biochemistry* 7, 2054.
59. ELLIS, W.D. (1968), Ph.D. Thesis, University of Alberta, Edmonton.
60. ELLIS, W.D. and DUNFORD, H.B. (1969), *Arch. Biochem. Biophys.* 133, 313.
61. FELTON, R.H., OWEN, G.S., DOLPHIN, D. and FAJER, J. (1971), *J. Am. Chem. Soc.* 93, 6332.

62. FERGUSSON, R.R. (1956), *J. Am. Chem. Soc.* 78, 1266.
63. FLOCHE, L. (1969), *Biochem. Biophys. Acta.* 191, 541.
64. FRIDOVICH, I. (1963), *J. Biol. Chem.* 288, 3921.
65. FROST, A.A. and PEARSON, R.G. (1961), *Kinetics and Mechanism*, 2nd Ed., Wiley, New York, p. 166.
66. GALSTON, A.W. (1956), in *The Chemistry and Mode of Action of Plant Growth Substances*, Butterworth, London, 219.
67. GASPER, T., BOUCHET, M. and DARIMOT, E. (1972), *Arch. Int. Physiol. Biochem.* 80, 45.
68. GATT, R. and KREMER, M.L. (1968), *Trans. Far. Soc.* 64, 721.
69. GEORGE, P. (1952), *Nature* 169, 612.
70. GEORGE, P. (1953a), *J. Biol. Chem.* 201, 413.
71. GEORGE, P. (1953b), *Science* 117, 220.
72. GEORGE, P. (1953c), *Biochem. J.* 54, 267.
73. GEORGE, P. and IRVINE, D.H. (1956), *J. Colloid. Sci.* 11, 327.
74. GEORGE, P., BETTLESTONE and GRIFFITH, J.S. (1961), in *Hematin Enzymes*, Pergamon Press, New York, N.Y., 105.
75. GETCHELL, R.W. and WALTON, J.H. (1931), *J. Biol. Chem.* 91, 419.
76. HAGER, L.P., DOUBEK, D.L., SILVERSTEIN, R.M., HARGIS, J.H. and MARTIN, J.C. (1972), *J. Am. Chem. Soc.* 94, 4364.

77. HAGGETT, M.L., JONES, P. and WYNNE-JONES, W.F.K. (1960), *Dis. Far. Soc.* 29, 153.
78. HASINOFF, B.B. and DUNFORD, H.B. (1970), *Biochemistry* 9, 4930.
79. HASINOFF, B.B. (1970), Ph.D. Thesis, University of Alberta, Edmonton.
80. HIDAKA, H. and UDENFRIEND, S. (1970), *Arch. Biochem. Biophys.* 140, 174.
81. HIDAKA, H., NAGASAKA, A. and DEGROOT, L.J. (1971), *Endocrinology* 88, 1264.
82. HOLLAND, V.R. and SAUNDERS, B.C. (1969), *Tetrahedron* 25, 4153.
83. HOLLAND, V.R. and SAUNDERS, B.C. (1971), *Tetrahedron* 27, 2851.
84. HOLLAND, V.R., ROBERTS, B.M. and SAUNDERS, B.C. (1969), *Tetrahedron* 25, 2291.
85. HOLLENBERG, P.F. and HAGER, L.P. (1972), *Fed. Proc.* 31, 483 Abs.
86. HORNE, D.G. (1967), *The Interaction Between HRP and Buffers at Low pH*, unpublished results.
87. HOSOYA, T. (1968), *Gumma Symp. Endocrinol.* 5, 219.
88. HULTQUIST, D.E. and MORRISON, M. (1963), *J. Biol. Chem.* 238, 2843.
89. IIZUKA, T. and KOTANI, M. (1968), *Biochim. Biophys. Acta* 154, 417.

90. IIZUKA, T., KOTANI, M. and YONETANI, T. (1968), *Biochim. Biophys. Acta* 167, 257.
91. IIZUKA, T. and KOTANI, M. (1969a), *Biochim. Biophys. Acta* 181, 275.
92. IIZUKA, T. and KOTANI, M. (1969b), *Biochim. Biophys. Acta* 194, 351.
93. JOHNSON, R.M. and SIDDIQI, I.W. (1970) *Determination of Organic Peroxides*, Pergamon Press, London, Chapter 3.
94. JONES, P., TOBE, M.L. and WYNNE-JONES, W.F.K. (1959), *Trans. Faraday Soc.* 55, 79.
95. JORDAN, J. and EWING, G.J. (1962), *Inorg. Chem.* 1, 587.
96. KASINSKY, H.E. and HACKETT, D.P. (1968), *Phytochemistry* 7, 1147.
97. KAY, E., SHANNON, L.M. and LEW, J.Y. (1967), *J. Biol. Chem.* 242, 2170.
98. KEILIN, D. and HARTREE, E.H. (1951), *Biochem. J.* 49, 88.
99. KEILIN, D. and HARTREE, E.H. (1955), *Biochem. J.* 60, 310.
100. KEILIN, D. and MANN, T. (1937), *Proc. Roy. Soc.* 122B, 119.
101. KENDREW, J.C. (1962), *Brookhaven Symposia in Biology* 15, 216.
102. KITTO, G.B., WASSARMAN, P.M. and KAPLAN, N.O. (1966). *Proc. Nat. Acad. Sci. U.S.* 56, 579.

103. KOLTHOFF, I.M. and BOSCH, W. (1932a), *J. Phys. Chem.* 36, 1685.
104. KOLTHOFF, I.M. and BOSCH, W. (1932b), *J. Phys. Chem.* 36, 1695.
105. KOLTHOFF, I.M. and SANDELL, E.B. (1952), *Textbook of Quantitative Inorganic Analysis*, MacMillan Company, New York, N.Y.
106. KREMER, M.L. (1962), *Trans. Far. Soc.* 58, 702.
107. KREMER, M.L. (1963), *Trans. Far. Soc.* 59, 2535.
108. KREMER, M.L. (1965), *Trans. Far. Soc.* 61, 1453.
109. KREMER, M.L. (1967), *Trans. Far. Soc.* 63, 1208.
110. KREMER, M.L. and STEIN, G. (1959), *Trans. Far. Soc.* 55, 959.
111. KRINSKY, M.M. and FRUTON, J.S. (1971), *Biochem. Biophys. Res. Commun.* 43, 935.
112. KUHN, R., HAND, D.B. and FLORKIN, M. (1931), *Z. Physiol. Chem.* 201, 255.
113. KUROZUMI, T., INADA, Y. and SHIBATA, K. (1961), *Arch. Biochem. Biophys.* 94, 464.
114. LIPPMANN, F. (1941), *J. Biol. Chem.* 139, 977.
115. LANG, L. (1971), Editor: *Absorption Spectra in the Ultraviolet and Visible Region* 15, Acad. Press. Inc., New York, N.Y., p. 26.
116. LUMME, P.O. (1957), *Suomen Kem.* 30B, 176.
117. MAEHLY, A.C. (1961), *Nature* 192, 630.
118. MAGUIRE, R.J., DUNFORD, H.B. and MORRISON, M. (1971), *Can. J. Biochem.* 49, 1165.

119. MAGUIRE, R.J. and DUNFORD, H.B. (1972a), *Biochemistry* 11, 937.
120. MAGUIRE, R.J. and DUNFORD, H.B. (1972b), *Can. J. Chem.*, (in press).
121. MARKLUND, S. (1971), *Eur. J. Biochem.* 27, 348.
122. MARTIN, D.L. and ROSSOTTI, F.J.C. (1959), *Proc. Chem. Soc.*, 60.
123. MASON, H.S. (1957), *Advances in Enzymology* 13, 79.
124. MASON, H.S., ONOPRYENKO, I. and BUHLER, D. (1957), *Biophys. Biochim. Acta* 24, 225.
125. MATSEN, F.A. and FRANKLIN, J.L. (1950), *J. Am. Chem. Soc.* 72, 3337.
126. MAZZA, G., CHARLES, C., BOUCHET, M. and RICARD, J. (1968), *Biophys. Biochim. Acta* 167, 89.
127. MILLS, G.C., (1957), *J. Biol. Chem.* 229, 189.
128. MILLS, G.C. (1959), *J. Biol. Chem.* 234, 502.
129. MILLS, G.C. (1960), *Arch. Biochem. Biophys.* 88, 1.
130. MORITA, Y. and MASON, H.S. (1965), *J. Biol. Chem.* 240, 2654.
131. MORITA, Y., YOSHIDA, C., KITAMURA, I. and IDA, S. (1970), *Agr. Biol. Chem.* 34, 1191.
132. MORITA, Y., YOSHIDA, C. and MAEDA, Y. (1971), *Agr. Biol. Chem.* 35, 1074.
133. MORRIS, D.R. and HAGER, L.P. (1966), *J. Biol. Chem.* 241, 1763.

134. MOSS, T.H., EHRENBERG, A. and BEARDEN, A.J. (1969), *Biochemistry* 8, 4159.
135. NAKAMURA, Y., TOHJO, M. and SHIBATA, K. (1963), *Arch. Biochem. Biophys.* 102, 144.
136. NASH, G.R. and MONK, C.B. (1957), *J. Chem. Soc.*, 4274.
137. NOBLE, R.W. and GIBSON, Q.H. (1970), *J. Biol. Chem.* 245, 2409.
138. OVENSTON, T.C.J. and REES, W.T. (1950), *Analyst (London)* 75, 204.
139. PAUL, K.G. (1958), *Acta Chem. Scand.* 12, 1312.
140. PAUL, K.G. (1958), *Acta Chem. Scand.* 2, 1611.
141. PAUL, K.G. (1959), *Acta Chem. Scand.* 13, 1239.
142. PAUL, K.G. (1963), in *The Enzymes* 8B, 2nd Ed., Acad. Press, New York, N.Y., 227.
143. PAUL, K.G. and STIGBRAND, T. (1970), *Acta Chem. Scand.* 24, 3607.
144. PEISACH, J., BLUMBERG, W.E., WITTENBERG, B.A. and WITTENBERG, J.B. (1968), *J. Biol. Chem.* 243, 1871.
145. PERKAMPUS, H.H., SANDEMAN, I. and TIMMINS, C.J. (1971), Editors: *UV Atlas of Organic Compounds* 5, Butterworths, London.
146. PHELPS, C. and ANTONINI, E. (1969), *Biochem. J.* 114, 719.
147. PHELPS, C., FORLANI, L. and ANTONINI, E. (1971), *Biochem. J.* 124, 605.

148. PLANCHE (1810), *Bull. Pharm.* 2, 578.
149. PORTSMOUTH, D. and BEALE, E.A. (1971), *Eur. J. Biochem.* 29, 479.
150. RAMETTE, R.W. and SANDFORD, R.W. (1965), *J. Am. Chem. Soc.* 87, 5001.
151. REKKER, R.F. and NAUTA, W. Th. (1956), *Recueil* 75, 279.
152. RICARD, J., SANTIMONE, M. and VOGT, G. (1968), *C.R. Acad. Sci., Paris, Ser. D* 267, 1414.
153. RICARD, J., MAZZA, G. and WILLIAMS, R.J.P. (1972), *Eur. J. Biochem.* 28, 566.
154. ROMAN, R. (1972), Ph.D. Thesis, University of Alberta.
155. ROMAN, R. and DUNFORD, H.B. (1972), *Biochemistry* 11, 2076.
156. ROMAN, R. and DUNFORD, H.B. (1973), *Can. J. Chem.*, (in press).
157. ROMAN, R., DUNFORD, H.B. and EVETT (1971), *Can. J. Chem.* 49, 3059.
158. ROMBAUTS, W.A., SCHROEDER, W.A. and MORRISON, M. (1967), *Biochemistry* 6, 2965.
159. SAUNDERS, B.C. and STARK, B.P. (1967), *Tetrahedron* 23, 1867.
160. SAUNDERS, B.C., HOLMES-SIEDLE, A.G. and STARK, B.P. (1964), *Peroxidase*, Butterworths, London, p 10.
161. SCHONBAUM, G.R. and LO, S. (1972), *J. Biol. Chem.* 247, 3353.

162. SCHONBAUM, G.R., WELINDER, K. and SMILLIE, L.B. (1971), in *Probes of Structure and Function of Macromolecules and Membranes 2*, Acad. Press, New York and London, 533.
163. SCHONBEIN, C.F. (1855), *Verf. Naturf. Ges. Basel* 1, 339.
164. SCHMITZ, K.S. and SCHURR, J.M. (1972), *J. Phys. Chem.* 76, 534.
165. SCHULTZ, J., GORDON, A. and SHAY, H.J. (1957), *J. Am. Chem. Soc.* 79, 1632.
166. SHANNON, L.M., KAY, E. and LEW, J.Y. (1968), *J. Biol. Chem.* 241, 2166.
167. SIGEL, H. (1969), *Angew. Chem. Int. Ed.* 8, 167.
168. SIMMONS, N.S., COHEN, C., SZENT-GYORGYI, A.G., WETLAUFER, D.B., and BLOUT, E.R. (1961), *J. Am. Chem. Soc.* 83, 4766.
169. SMITH, D.W. and WILLIAMS, R.J.P. (1969), in *Structure and Bonding 7*, Springer-Verlag, N.Y., 1.
170. STRICKLAND, E.H., KAY, E. SHANNON, L.M., and HORWITZ, J. (1968), *J. Biol. Chem.* 243, 3560.
171. SUMNER, J.B. and HAWELL, S.F. (1936), *Enzymologia* 1, 133.
172. SWEDIN, B. and THEORELL, H. (1940), *Nature* 145, 71.
173. SWERN, D. (1971), *Organic Peroxides* Vol. 1, New York, N.Y., Wiley-Interscience, Chapter 6.

174. TAMURA, M. (1971a), *Biochim. Biophys. Acta* 243, 239.
175. TAMURA, M. (1971b), *Biochim. Biophys. Acta* 243, 249.
176. TAMURA, M. and HORI, H. (1972), *Biochim. Biophys. Acta* 284, 20.
177. TAMURA, M., ASAKURA, T. and YONETANI, T. (1972), *Biochim. Biophys. Acta* 268, 292.
178. TAUROG, A. (1970), *Recent Prog. Horm. Res.* 26, 189.
179. TAUROG, A. (1971), *Arch. Biochem. Biophys.* 139, 221.
180. THEORELL, H. (1941), *Enzymologia* 10, 250.
181. THEORELL, H. (1943), *Arkiv. Kemi. Mineral. Geol.* 16A, No. 2.
182. THEORELL, H. and AKESSON, A. (1943), *Arkiv. Kemi. Mineral. Geol.* 16A, No. 8.
183. THEORELL, H., BERGSTROM, S. and AKESSON, A. (1943), *Arkiv. Kemi. Mineral. Geol.* 16A, No. 13.
184. THEORELL, H. and EHRENBERG, A. (1951), *Acta Chem. Scand.* 5, 823.
185. THEORELL, H. and EHRENBERG, A. (1952), *Arch. Biochem. Biophys.* 41, 442.
186. THEORELL, H. and PAUL, K.G. (1944), *Ark. Mineral. Geol.* 18A, 12.
187. THEORELL, H. and SWEDIN, B. (1939), *Naturwiss.* 27, 95.
188. TOHJO, M., NAKAMURA, Y., KURIHARA, K., SAMEJIMA, T., HACHIMORI, Y. and SHIBATA, K. (1962), *Arch. Biochem. Biophys.* 102, 222.

189. VOLKOV, M.S. (1971), *Vop. Med. Khim.* 17, 193.
190. WACHHOLDER, K. (1942), *Biochem. Z.* 312, 394.
191. WANG, J.H. (1970), *Acc. of Chem. Res.* 3, 90.
192. WATERS, W.A. (1958), *Quarterly Reviews* 12, 277.
193. WATSON, H.C. (1968), in *Progress in Stereochemistry* 4, Butterworths, London, 299.
194. WELINDER, K.G. SMILLIE, L.B. and SCHONBAUM, G.R. (1972), *Can. J. Biochem.* 50, 44.
195. WELINDER, K.G. and SMILLIE, L.B. (1972), *Can. J. Biochem.* 50, 63.
196. WILDER, C.J. (1962), *J. Food Sci.* 27, 567.
197. WILLICK, G.E., SCHONBAUM, G.R. and KAY, C.M. (1969), *Biochemistry* 8, 3729.
198. WILLSTATTER, R. and POLLINGER, A. (1923), *Liebigs. Ann.* 430, 269.
199. WILLSTATTER, R. and POLLINGER, A. (1932), *Z. Physiol. Chem.* 130, 281.
200. WITTENBERG, J.B., NOBLE, R.W., WITTENBERG, B.A., ANTONINI, A., BRUNORI, M. and WYMAN, J. (1967), *J. Biol. Chem.* 242, 626.
201. YAMAZAKI, I., MASON, H.S. and PIETTE, L. (1960), *J. Biol. Chem.* 235, 2444.
202. YAMAZAKI, I. and YOKOTA, K. (1965), *Biochem. Biophys. Res. Commun.* 19, 249.
203. YONETANI, T. (1970), *Advances in Enzymology* 33, 309.

204. YONETANI, T., CHANCE, B. and KAJIWARA, S. (1966),
J. Biol. Chem. 241, 2981.
205. YONETANI, T. and EHRENBERG, A. (1967), in *Magnetic Resonance in Biological Systems 9*, Pergamon Press, London, 155.
206. YONETANI, T. and RAY, G.S. (1965), *J. Biol. Chem.* 240, 4503.
207. YAMAZAKI, I., NAKAJIMA, R., MIYOSHI, K., MAKINO, R. and TAMURA, M. (1971), in *Oxidases and Related Redox Systems*. Proc. 2nd Int. Symp., Editors: King, T.E., Mason, H.S. and Morrison, M.; University Park Press, Baltimore, Md. (in press).
208. ROBINSON, R.A. and BIGGS, A.I. (1957), *Australian J. Chem.* 10, 128.

Appendix 1.

The Analysis of Stopped-Flow Kinetic Data

The direct kinetic measurements of this study were all investigated under experimental conditions where the changing concentrations of the intermediate compound of the enzyme were first-order. In other words, the concentration of the HRP compound was always changing exponentially with time as described by the first-order differential equation:

$$-\frac{d[C]}{dt} = k_{obs}[C] \quad (A1.1)$$

where $[C]$ refers to the concentration of the compound HRP-I or HRP-II, k_{obs} is the first-order rate constant and t is the time. Of course, $[C]$ may also refer to some properties of the system which is proportional to the intermediate's concentration. Integration of Eq. A1.1 gives:

$$\ln \frac{([C]_0 - [C]_\infty)}{([C]_0 - [C]_t)} = k_{obs} t \quad (A1.2)$$

where $[C]_0$, $[C]_\infty$ and $[C]$ refer to the concentrations of the compounds at time 0, ∞ and t respectively. The half-time, that is, the time required for the concentration to decay to 50% of its original magnitude, $t_{1/2}$, is given by:

$$\ln \frac{([C]_0 - [C]_\infty)}{1/2([C]_0 - [C]_\infty)} = k_{obs} t_{1/2} = \ln 2 \quad (A1.3)$$

Therefore, the k_{obs} may be obtained without knowing the intermediate's initial concentration. This is of great practical significance when studying fast reactions of inherently unstable compounds. Under such circumstances the absolute starting concentrations are not known with any degree of precision. A plot of $\ln ([C] - [C]_\infty)$ against time will be linear with a slope of $-k_{obs}$. The y-intercept will provide a measure of the concentration of the HRP compound at a time which the experimentalist has chosen to begin monitoring the exponential change.

For the reaction of HRP-I or HRP-II with a reducing substrate S, the overall second-order rate expression is:

$$-\frac{d[C]}{dt} = k_{app}[C][S] \quad (\text{A1.4})$$

In this equation k_{app} is an apparent second-order rate constant. Because of its dependence on pH, it must contain a term in hydrogen ion concentration. If $[S] \gg [C]$, then, the change in [S] during the reaction may be considered to be very small and can be ignored. Under such conditions the reaction behaves as a first-order rate law would predict. The reaction is said to be overall pseudo-first-order and the rate constants k_{app} and k_{obs} are related by:

$$k_{obs} = k_{app}[S] \quad (\text{A1.5})$$

For the investigations of this thesis, the k_{obs} were obtained from nonlinear least-squares analyses of the exponential traces. Graphical analysis of the form $\ln ([C] - [C]_\infty)$ vs. time were performed occasionally to give a visual interpretation of the errors in the experimental values and to ensure that both graphical and computer analysis gave essentially the same result. The analyses by computer was well-suited to efficient organization and calculation of large volumes of repetitious data. It also provided the facility to weight the initial data most heavily where the largest change in concentration was occurring and the relation was most accurately defined. Variation of selected parameters also allowed one to optimize the fit to the experimental results. However, a nonlinear computer analysis must be used with caution. Graphical methods must be used in conjunction with nonlinear analysis to establish that the first-order rate law described the data satisfactorily.

In the stopped-flow apparatus, the reactions were observed as a function of a voltage change. The voltage was proportional to the intensity of the light reaching the photomultiplier and the relation is:

$$\frac{V}{V_0} = \frac{I}{I_0} \quad (\text{Al.6})$$

where I and I_0 refer to the light intensity through the

sample and vacuum, respectively, and V , V_o are the corresponding voltages. Since absorbance, A , and the intensity are related by:

$$\log \left(\frac{I_o}{I} \right) = A \quad (\text{A1.7})$$

voltage and absorbance may be related through a series expansion and shown to be related in a directly proportional fashion for sufficiently small absorbance changes ($\Delta A < 0.06$) (Maguire, unpublished results). The equation used for the first-order nonlinear analysis was:

$$V_t = (V_o - V_\infty) e^{-k_{\text{obs}} t} + V_\infty \quad (\text{A1.8})$$

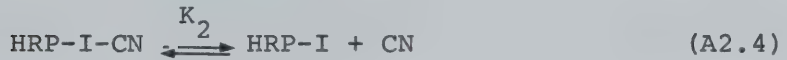
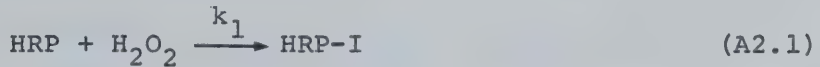
where V_t , V_∞ and V_o refer to the voltages at times t , infinity and zero, respectively. The variable parameters V_o , V and k_{obs} were adjusted to give the best fit to the experimental values V_t and t . It was for this reason that an *a priori* test for a first-order relation was necessary.

Appendix 2

Derivation of Expressions for the Steady-State HRP

Catalyzed Ferrocyanide Oxidation in the Presence of Cyanide

The ferrocyanide oxidation with cyanide present may be described by the reactions of Fig. 4.1:



where $\text{S} = \text{Fe}(\text{CN})_6^{-4}$ and $\text{P} = \text{Fe}(\text{CN})_6^{-3}$. One may apply the following conservation relation:

$$\begin{aligned} [\text{HRP}]_0 &= [\text{HRP}] + [\text{HRP-CN}] + [\text{HRP-I}] + [\text{HRP-I-CN}] + [\text{HRP-II}] \\ &\quad + [\text{HRP-II-CN}] \end{aligned} \quad (\text{A2.7})$$

The concentrations with subscript zeros are always with reference to initial concentrations. The initial concentration of HRP is then:

$$[\text{HRP}]_o = (1 + \frac{[\text{CN}]}{K_1}) [\text{HRP}] + (1 + \frac{[\text{CN}]}{K_2}) [\text{HRP-I}] + (1 + \frac{[\text{CN}]}{K_3}) [\text{HRP-II}] \quad (\text{A2.8})$$

From the steady-state assumption:

$$\frac{d[\text{HRP-I}]}{dt} = k_1 [\text{HRP}] [\text{H}_2\text{O}_2] - k_2 [\text{HRP-I}] [\text{S}] = 0 \quad (\text{A2.9})$$

$$\frac{d[\text{HRP-II}]}{dt} = k_2 [\text{HRP-I}] [\text{S}] - k_3 [\text{HRP}] [\text{S}] = 0 \quad (\text{A2.10})$$

Therefore from Eq. A2.9 and Eq. A2.10:

$$[\text{HRP}] = \frac{k_2 [\text{S}] [\text{HRP-I}]}{k_1 [\text{H}_2\text{O}_2]} \quad (\text{A2.11})$$

$$[\text{HRP-II}] = \frac{k_2 [\text{HRP-I}]}{k_3} \quad (\text{A2.12})$$

Substitution of Eq. A2.11 and Eq. A2.12 into Eq. A2.08 and rearrangement gives:

$$[\text{HRP-I}] =$$

$$\frac{[\text{HRP}]_o}{(k_2 [\text{S}] / k_1 [\text{H}_2\text{O}_2]) (1 + [\text{CN}] / K_1) + (1 + [\text{CN}] / K_2) + k_2 / k_3 (1 + [\text{CN}] / K_3)} \quad (\text{A2.13})$$

Following the reaction by monitoring the increase in product concentration, the velocity may be expressed as:

$$\frac{d[P]}{dt} = k_2 [S] [\text{HRP-I}] + k_3 [S] [\text{HRP-II}] \quad (\text{A2.14})$$

Substituting Eq. A2.12 into Eq. A2.14 gives:

$$\frac{d[P]}{dt} = 2k_2 [S] [\text{HRP-I}] \quad (\text{A2.15})$$

Substituting Eq. A2.13 into Eq. 2.15 and expressing the system in terms of the initial velocity v :

$$v =$$

$$\frac{2k_2 [S]_o [\text{HRP}]_o}{(k_2 [S]_o / k_1 [\text{H}_2\text{O}_2]) (1 + [\text{CN}]_o / K_1) + k_2 / k_3 (1 + [\text{CN}]_o / K_3) + (1 + [\text{CN}]_o / K_2)} \quad (\text{A2.16})$$

Putting Eq. A2.16 in the form of a Lineweaver-Burk double reciprocal relationship gives Eq. 4.7:

$$\frac{[\text{HRP}]_o}{v} = \frac{1}{2k_1 [\text{H}_2\text{O}_2]_o} \left(1 + \frac{[\text{CN}]_o}{K_1} \right) + \left[\frac{k_2 + k_3}{2k_2 k_3} + \left(\frac{1}{2k_2 K_2} + \frac{1}{2k_3 K_3} \right) [\text{CN}]_o \right] \frac{1}{[\text{S}]_o} \quad (\text{A2.17})$$

Since $k_2 \gg k_3$ this expression may be further simplified to:

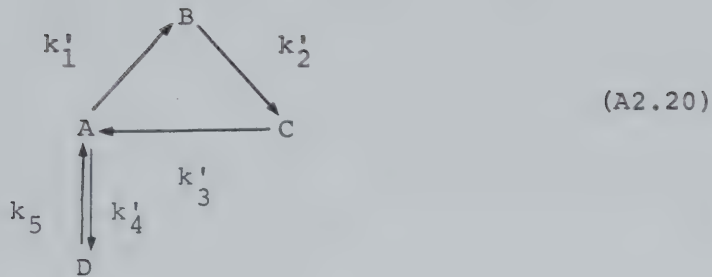
$$\frac{[\text{HRP}]_o}{v} = \frac{1}{2k_1 [\text{H}_2\text{O}_2]_o} \left(1 + \frac{[\text{CN}]_o}{K_1} \right) + \left[\frac{1}{2k_3} + \left(\frac{1}{2k_2 K_2} + \frac{1}{2k_3 K_3} \right) [\text{CN}]_o \right] \frac{1}{[\text{S}]_o} \quad (\text{A2.18})$$

The slope of $[HRP]_o/v$ plotted against $1/[S]_o$ will be $1/2k_3 + (1/2k_2K_2 + 1/2k_3K_3)[CN]_o$ and the intercept $1/2k_1[H_2O_2]_o(1 + [CN]_o/K_1)$. If binding to either intermediate compound occurs then a plot of these slopes against $[CN]_o$ should result in a linear correlation with a positive slope. However, in order to observe the effect of $[CN]_o$ conditions must be used such that the term in $[H_2O_2]_o$ of Eq. A2.18 is not dominant.

If the $[CN]_o = 0$ then the terms in $[CN]_o$ are no longer significant and the Eq. A2.18 reverts to the simple steady-state case published elsewhere (Hasinoff and Dunford, 1970) :

$$\frac{[HRP]_o}{v} = \frac{1}{2k_1[H_2O_2]_o} + \frac{1}{2k_3} \frac{1}{[S]_o} \quad (A2.19)$$

In order to establish whether the steady-state assumption is valid, the time required to attain the steady-state must be estimated. This is done by calculating the change in concentrations of the components in the pre-steady-state phase. The HRP reaction cycle shown in Eq. A2.1 through Eq. A2.6 with cyanide binding only to the native HRP may be represented by:



where k'_1 , k'_2 and k'_3 are defined in Fig. 4.1, $k'_4 = k_4[\text{CN}]$, A = HRP, B = HRP-I, C = HRP-II and D = HRP-CN. A published value of k_1 has been found to be pH independent over the region of interest (Chance *et al.*, 1967). Values of k_2 , k_3 , k_4 and k_5 as a function of pH are listed elsewhere (Hasinoff and Dunford, 1970; Ellis and Dunford, 1968).

The following equations were derived, using the method outlined by Matsen and Franklin (1950). In the absence of cyanide, the system is characterized by two relaxations τ_1 and τ_2 :

$$\frac{1}{\tau_1} = 1/2(p + q) \quad (\text{A2.21})$$

$$\frac{1}{\tau_2} = 1/2(p - q) \quad (\text{A2.22})$$

where

$$p = k'_1 + k'_2 + k'_3 \quad (\text{A2.23})$$

$$q = [p^2 - 4(k'_1k'_2 + k'_1k'_3 + k'_2k'_3)]^{1/2} \quad (\text{A2.24})$$

The rigorous equations for [A], [B] and [C] as a function of time are:

$$[A] = [A]_0 \left[k_2' \tau_1 \tau_2 \left(\frac{1}{\tau_1} + \frac{1}{\tau_2} - k_1' - k_2' \right) + \frac{\left(k_1' + k_2' - \frac{1}{\tau_2} \right) \left(k_2' - \frac{1}{\tau_1} \right)}{\frac{1}{\tau_1} \left(\frac{1}{\tau_2} - \frac{1}{\tau_1} \right)} e^{-t/\tau_1} \right.$$

$$\left. + \frac{\left(\frac{1}{\tau_1} - k_1' - k_2' \right) \left(k_2' - \frac{1}{\tau_2} \right)}{\frac{1}{\tau_2} \left(\frac{1}{\tau_2} - \frac{1}{\tau_1} \right)} e^{-t/\tau_2} \right]$$

(A2.25)

$$[B] = [B]_0 \left[k_1' \tau_1 \tau_2 \left(\frac{1}{\tau_1} + \frac{1}{\tau_2} - k_1' - k_2' \right) + \frac{k_1' \left(k_1' + k_2' + \frac{1}{\tau_2} \right)}{\frac{1}{\tau_1} \left(\frac{1}{\tau_2} - \frac{1}{\tau_1} \right)} e^{-t/\tau_1} \right.$$

$$\left. + \frac{k_1' \left(\frac{1}{\tau_1} - k_1' - k_2' \right)}{\frac{1}{\tau_2} \left(\frac{1}{\tau_2} - \frac{1}{\tau_1} \right)} e^{-t/\tau_2} \right]$$

(A2.26)

$$\begin{aligned}
 [C] = & [A]_0 \left[\frac{k'_1 k'_2}{k'_3} \tau_1 \tau_2 \left(\frac{1}{\tau_1} + \frac{1}{\tau_2} - k'_1 - k'_2 \right) + \frac{\left(k'_1 - \frac{1}{\tau_1} \right) \left(k'_1 + k'_2 - \frac{1}{\tau_2} \right) \left(k'_2 - \frac{1}{\tau_1} \right)}{k'_3 \frac{1}{\tau_1} \left(\frac{1}{\tau_2} - \frac{1}{\tau_1} \right)} e^{-t/\tau_1} \right. \\
 & + \left. \frac{k'_1 - \left(\frac{1}{\tau_2} \right) \left(\frac{1}{\tau_1} - k'_1 - k'_2 \right) \left(k'_2 - \frac{1}{\tau_2} \right)}{k'_3 \frac{1}{\tau_2} \left(\frac{1}{\tau_2} - \frac{1}{\tau_1} \right)} e^{-t/\tau_2} \right] \quad (\text{A2.27})
 \end{aligned}$$

Thus for $k'_1 = 1.6 \times 10^3$, $k'_2 = 3.2 \times 10^2$, and $k'_3 = 4.3$, all in s^{-1} , the concentration of B reaches 95 percent of its steady-state value in 20 ms.

When cyanide is present, one obtains from Eq.

A2.20 a cubic equation:

$$\frac{1}{\tau^3} + p\frac{1}{\tau^2} + q\frac{1}{\tau} + r = 0 \quad (\text{A2.28})$$

where

$$p = -(k'_1 + k'_2 + k'_3 + k'_4 + k'_5) \quad (\text{A2.29})$$

$$q = k'_1 k'_2 + k'_1 k'_3 + k'_1 k'_5 + k'_2 k'_3 + k'_2 k'_4 + k'_2 k'_5 + k'_3 k'_4 + k'_3 k'_5 \quad (\text{A2.30})$$

$$r = -(k'_1 k'_2 k'_5 + k'_1 k'_3 k'_5 + k'_2 k'_3 k'_4 + k'_2 k'_3 k'_5) \quad (\text{A2.31})$$

A computer program was used to generate a table of concentrations of the four enzyme species present at equal time intervals prior to the attainment of the steady-state. A listing of the program is to be found on the final pages of this Appendix. Numerical values for the three relaxation times were obtained by the solution of Eq. A2.28. Having four differential equations in four dependent variables a general solution for an enzyme intermediate E may be expressed as:

$$[E]_i = \sum_{n=1}^t s_{i,n} y_n e^{-t/\tau_n} \quad (\text{A2.32})$$

The coefficients y_n were obtained by solving the corresponding coefficient matrix at zero time. The constants x_i were calculated from the particular solutions and had the values:

$$x_1 = 1 \quad (\text{A2.33})$$

$$x_2 = k'_1 / (k'_2 - 1/\tau_1) \quad (\text{A2.34})$$

$$x_3 = k'_1 k'_2 / (k'_2 + k/\tau_2) (k'_3 + 1/\tau_3) \quad (\text{A2.35})$$

$$x_4 = k'_4 / (k'_3 + 1/\tau_3) \quad (\text{A2.36})$$

Under the experimental conditions used, calculated changes in concentration indicated that the steady-state assumption was valid.


```

> 1      C CALCULATION OF STEADY-STATE HRP CYCLE WITH CYANIDE
> 2      C DATA INPUT: RATE CONSTANTS
> 3          INITIAL HRP CONCENTRATION
> 4          HRP RATE PARAMETERS
> 5          COEFFICIENT MATRIX AND RHS VECTOR
> 6      C
> 7          REAL K1,K2,K3,K4,K5,A0,T11,T12,T13,D1,D2,D3,D4,D5,Q1,Q2,Q3,Q4,TE1,
> 8          TE2,TE3,INT,STD,RSTR,RT,HRP(500),HRP1(500),HRP2(500),HRPCN(500),
> 9          2T(500)
> 10         REAL BB(4,4),RR(4),A(4,4),B(4),X(4),EVR(4),EVI(4),
> 11         $VECR(4,4),VECI(4,4),DG(4,4)
> 12         REAL*8 OPR(50),OPI(50),EPS,ZEROR(50),ZEROI(50),FBND(50)
> 13         INTEGER DEGREE,NODIST,MULT(50)
> 14         INTEGER PIVOT(4),INDIC(4)
> 15         LOGICAL RLDPOLY,FLAG(50),TRYIMP,FAIL
> 16      C
> 17         STD=0.01
> 18         A0=1
> 19         DEGREE=3
> 20         NC=DEGREE+1
> 21         N=4
> 22         READ(5,200)K1,K2,K3,K4,K5,INT
> 23         IF(INT.EQ.999.)GO TO 104
> 24         OPR(1)=1.
> 25         OPR(2)=-(K1 + K2 + K3 + K4 + K5)
> 26         OPR(3)=K1*(K2 + K3 + K5) + K2*(K3 + K4 + K5) + K3*(K4 + K5)
> 27         OPR(4)=-(K1*K5*(K2 + K3) + K2*K3*(K4 + K5))
> 28         CALL CS281A(OPR,DEGREE,ZEROR,ZEROI,FAIL)
> 29         IF(FAIL) GO TO 10
> 30         T11=ZEROR(1)
> 31         T12=ZFROR(2)
> 32         T13=ZEROR(3)
> 33         A(1,1)=1.
> 34         A(1,2)=1.
> 35         A(1,3)=1.
> 36         A(1,4)=1.
> 37         A(2,1)=K1/K2
> 38         A(2,2)=K1/(K2-T11)
> 39         A(2,3)=K1/(K2-T12)
> 40         A(2,4)=K1/(K2-T13)
> 41         A(3,1)=K1/K3
> 42         A(3,2)=((K1+K4-T11)-K4*K5/(K5-T11))/K3
> 43         A(3,3)=((K1+K4-T12)-K4*K5/(K5-T12))/K3
> 44         A(3,4)=((K1+K4-T13)-K4*K5/(K5-T13))/K3
> 45         A(4,1)=K4/K5
> 46         A(4,2)=K4/(K5-T11)
> 47         A(4,3)=K4/(K5-T12)
> 48         A(4,4)=K4/(K5-T13)
> 49         B(1)=A0
> 50         B(2)=0.
> 51         B(3)=0.
> 52         B(4)=1. - A0
> 53         CALL CS009A(A,B,X,N,BB,RR,PIVOT)
> 54         Q1=X(1)
> 55         Q2=X(2)
> 56         Q3=X(3)
> 57         Q4=X(4)
> 58      C INITIAL CONDITIONS
> 59         N=450
> 60         T(1)=0.
> 61         HRP(1)=B(1)
> 62

```



```

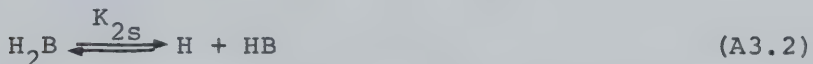
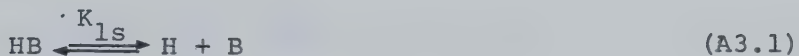
> 63      HRP1(1)=B(2)
> 64      HRP2(1)=B(3)
> 65      HRPCN(1)=B(4)
> 66      C GENERATE TABLE OF CONCENTRATIONS
> 67      DO 11 I=2,N
> 68      T(I)=T(I-1) + INT
> 69      TE1=EXP(-T(I)*T11)
> 70      TE2=EXP(-T(I)*T12)
> 71      TE3=EXP(-T(I)*T13)
> 72      C
> 73      HRP(I)=Q1 + Q2*TE1 + Q3*TE2 + Q4*TE3
> 74      C
> 75      HRP1(I)=Q1*K1/K2 + Q2*K1*TE1/(K2 - T11) + Q3*K1*TE2/(K2 - T12) +
> 76      1Q4*K1*TE3/(K2 - T13)
> 77      C
> 78      HRP2(I)=Q1*K1/K3 +
> 79      1Q2*TE1*((K1 + K4 - T11)/K3 - K4*K5/(K3*(K5-T11))) +
> 80      2Q3*TE2*((K1 + K4 - T12)/K3 - K4*K5/(K3*(K5 - T12))) +
> 81      3Q4*TE3*((K1 + K4 - T13)/K3 - K4*K5/(K3*(K5 - T13)))
> 82      C
> 83      HRPCN(I)=Q1*K4/K5 + Q2*K4*TE1/(K5 - T11) + Q3*K4*TE2/(K5 - T12) +
> 84      1Q4*K4*TE3/(K5 - T13)
> 85      C
> 86      IF((I + 50).GT.N)GO TO 11
> 87      IF(ABS((HRPCN(I) - HRPCN(I-1))/(HRPCN(I) - HRPCN(1))).LT.STD)N=
> 88      $I + 50
> 89      11 CONTINUE
> 90      RSTD=100.-STD*100.
> 91      RT= T(I-50)*1000.
> 92      XRSTD=100. - RSTD
> 93      L=I-51
> 94      M=I-50
> 95      WRITE(6,201)K1,K2,K3,K4,K5,RSTD,RT,L,M,XRSTD,INT
> 96      WRITE(6,204)T11,T12,T13
> 97      WRITE(6,205)Q1,Q2,Q3,Q4
> 98      WRITE(6,202)
> 99      DO 12 L=1,II
> 100     M=-1
> 101     12 WRITE(6,203)M,HRP(L),HRP1(L),HRP2(L),HRPCN(L)
> 102
> 103     C FORMAT STATEMENTS
> 104     99 FORMAT(' -COLUMNS ARE ZEROS(REAL, IMAGINARY),BOUNDS,MULTIPLICITY,
> 105        OVERLAP FLAGS//')
> 106     200 FORMAT(6F10.1)
> 107     201 FORMAT('1','THE HRP REACTION CYCLE WITH CYANIDE BINDING TO HRP'/
> 108       '15X/5X/'RATE CONSTANTS GIVEN FOR THE REACTION SCHEME ARE: K1=',E12.
> 109       '2G/51X,'K2=',E12.6/51X,'K3=',E12.6/51X,'K4=',E12.6/51X,'K5=',E12.5/
> 110       '3'THE TIME REQUIRED TO REACH',F6.2,1X,'PERCENT OF THE STEADY-STATE
> 111       '4EQUILIBRIUM IS:',F7.2,1X,'MILLISECONDS.')
> 112       '5'THAT IS, THE PERCENT CONCENTRATION CHANGE OF HRPCN BETWEEN ',13,
> 113       '61X,'AND',13,1X,'IS LESS THAN',F5.2,1X,'PERCENT RELATIVE TO ITS'/
> 114       '7'TOTAL CONCENTRATION CHANGE FROM ZERO TIME.'/
> 115       '8'CYANIDE HAS BEEN ADDED WITH PEROXIDE TO THE SYSTEM.'/
> 116       '9'INTERVAL=',F5.3,1X,'SECONDS.')
> 117     202 FORMAT(' -',5X/5X/38X,'TABLE OF CONCENTRATIONS OF SPECIES PRESENT'/
> 118       '15X/5X/34X,'IIRP',12X,'HRP1',11X,'HRP2',10X,'HRPCN'/5X)
> 119     203 FORMAT(' -',18X,13,5X,5E15.4)
> 120     204 FORMAT(' -','THE RELAXATION CONSTANTS ARE:',3E15.7)
> 121     205 FORMAT(' -','THE COEFFICIENTS Q ARF:',4E15.7)
> 122     GO TO 10
> 123     104 STOP
> 124     END

```


Appendix 3

The Derivation of an Expression for the Dependence of Absorbance on pH for Two Spectrophotometrically Observable pK_a Values

Consider the two independent ionizations occurring on a molecular species having three states of protonation B , HB , and H_2B :



where the two acid dissociation constants K_{1s} and K_{2s} are defined by:

$$K_{1s} = \frac{[H][B]}{[HB]} \quad (A3.3)$$

$$K_{2s} = \frac{[H][HB]}{[H_2B]} \quad (A3.4)$$

The total concentration of all the different states of protonation $[B]_o$ is given by:

$$[B]_o = [B] + [HB] + [H_2B] \quad (A3.5)$$

and the total absorbance due to all the various species in solution, A , at a given pH is:

$$A = \epsilon_B[B] + \epsilon_{HB}[HB] + \epsilon_{H_2B}[H_2B] \quad (A3.6)$$

where ϵ_B , ϵ_{HB} and ϵ_{H_2B} are the molar absorptivities of B, HB and H_2B , respectively. Substitution of Eq. A3.3 and Eq. A3.4 into Eq. A3.5 and rearrangement gives:

$$[B] = \frac{[B]_o}{(1 + [H]/K_{1s} + [H]^2/K_{1s}K_{2s})} \quad (A3.7)$$

Similarly, substitution into Eq. A3.6 gives:

$$A = \left(\frac{\epsilon_{H_2B}}{K_1 K_2} [H]^2 + \frac{\epsilon_{HB}}{K_1} [H] + \epsilon_B \right) [B] \quad (A3.8)$$

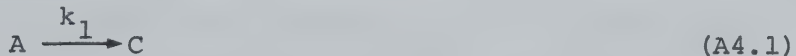
Therefore, the final expression becomes upon combining Eq. A3.7 and Eq. A3.8:

$$A = \left[\frac{\frac{\epsilon_{H_2B}}{K_1 K_2} [H]^2 + \frac{\epsilon_{HB}}{K_1} [H] + \epsilon_B}{1 + \frac{[H]}{K_{1s}} + \frac{[H]^2}{K_{1s}K_{2s}}} \right] [B]_o \quad (A3.9)$$

Appendix 4

Concerning the Observed Deviations from First-Order Kinetics for the Aromatic Amine, p-Aminobenzoic Acid

First, consider the case of two parallel first-order reactions producing a common product:



where A and B may represent two reactive forms of either HRP-II or the substrate PABA, and C represents the native enzyme. In the presence of either A or B but not both:

$$[A] = [A]_0 e^{-k_1 t} \quad (A4.3)$$

$$[B] = [B]_0 e^{-k_2 t} \quad (A4.4)$$

but $[C] = [A]_0 + [B]_0 - ([A] + [B]) \quad (A4.5)$

since $[C]_\infty = [A]_0 + [B]_0 \quad (A4.6)$

$$[C]_\infty - [C] = [A]_0 e^{-k_1 t} + [B]_0 e^{-k_2 t} \quad (A4.7)$$

In this expression $[C]_\infty - [C]$ may be related to the absorbance change ΔA for HRP-II reduction:

$$\Delta A = [A]_0 e^{-k_1 t} + [B]_0 e^{-k_2 t} \quad (A4.8)$$

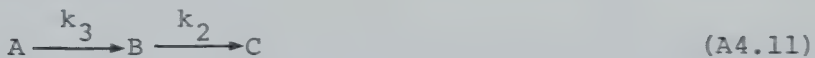
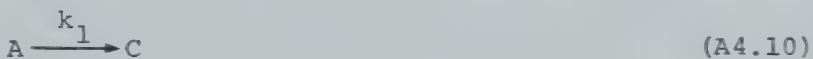
A plot of $\log \Delta A$ vs. time t gives a linear correlation only if $k_1 = k_2$, $[A]_0 = 0$ or $[B]_0 = 0$. If HRP-II reduction is

accurately described in terms of two reactive forms of HRP-II or of PABA, then, the system may be readily resolved into two first-order reactions if one of the reactive forms (say A) has a smaller concentration than the other form (B). The final linear portion of the trace shown in Fig. 3.3 may be analyzed as a simple first-order reaction to yield the slope of $-k_2/2.303$ and intercept $[B]_0$. From this information [A] may be calculated from the initial curvature by difference:

$$[A] = [C]_{\infty} - [C] - [B] \quad (\text{A4.9})$$

and the resulting data for [A] analyzed also by first-order kinetics.

This is in contrast to alternative possibility which is not likely to occur if the two reactive forms are substrate related or a result of HRP isoenzymes:



In this case an additional step has been introduced in which B is formed from A rather than being present initially. This reaction sequence may be described also by Eq. A4.8. However, because $[B]_0 = 0$ the value of k_1 may be estimated from the initial slope of the correlation (Fig. 3.3). The coefficient [B] in Eq. A4.8 now represents $[A]_0$ minus the

amount of A which forms C directly rather than by way of the intermediate B. The final linear portion defines a regime in which A has been totally converted to B. Again, first-order kinetics will allow the estimation of k_2 .

Appendix 5

Concerning the Characterization of HRP

The enzyme preparation obtained from Boehringer-Mannheim has been isolated in electrophoretically purified quantities by the classical preparation technique of Shannon *et al.* (1968). It has been shown by many workers (Phelps and Antonini, 1969; Yamazaki *et al.*, 1971) that such a technique isolated efficiently isoenzymes B and C (Shannon *et al.*, 1968) from crude horseradish extracts. That the procedures used to purify the commercially available sample are consistent with the presence of only isoenzymes B and C indicated by laboratory analysis (Roman, 1972) on a lot to lot basis has been established (M. Iqbal, Oxford Enzyme Group, preparation laboratory, personal communication to H.B. Dunford). Separation of these two isoenzymes would necessarily involve a tedious five column procedure (Biozymes Inc., Buckingham-Shire, England). Such high purity enzyme preparations are only available at considerable expense.

The consistency of the preparation was monitored for lot to lot variations by insuring that the P.N., defined as the ratio of absorbance at 403 nm to that at 280 nm, was never less than 3.1. This is a good test for an intact heme-protein system with a minimum amount of denatured protein present. The kinetic reproducibility indicates good lot to lot consistency. Such experimental evidence for

enzyme characterization is analogous to data obtained from assay methods for activity.

B30053